UCL Université catholique de Louvain

École polytechnique de Louvain (EPL)

epl

Carbon nanotubes morphology and dispersion in nanocomposites

Dissertation presented by
Anna Sangregorio

for obtaining the Master's degree in
Chemical and Materials Engineering

Supervisors
Prof. Christian BAILLY , Dr. Michael CLAES

Readers
Dr. Alicia RUL, Prof. Arnaud DELCORTE

Academic year 2015-2016

Acknowledgments

I would first like to thank my thesis supervisors, Prof. C. Bailly and Dr. M. Claes, for giving me the opportunity to work on this interesting project.

I would like to thank A. Rul and M. Houllé, for their daily advice and they enthusiasm and willing to spend time to suggest me and to discuss with me about the topic.

Furthermore, I would also like to thanks all the people working in Nanocyl S.A., for being available for help any time I needed, and for making a pleasure to work in the team.

Finally, a special thanks to my parents, who supported me during my studies and who made everything possible.

Abstract

The unique properties of carbon nanotubes (CNTs) offer great opportunities for nanocomposites with applications in many different sectors. Carbon nanotubes can be found in electronic devices, in application related with transportation, as well as energy and biotechnologies. Currently, the most popular use for carbon nanotubes is as reinforcement for polymer nanocomposites both for electrical and structural applications. CNTs are more efficient compared with other traditional fillers, primarily thanks to the large aspect ratio and surface area which increases the stress transfer and promote the formation of percolation network in the matrix. At the same time, the particular structure of the nanotubes also promotes the aggregation of the nanotubes due to strong Van der Waals attraction between the nanotubes, limiting the final properties of the nanocomposites. The ability to tailor electrical and mechanical properties and to totally employ the potential of CNTs widely depends on the ability to obtain a homogeneous dispersion of the fillers in the polymeric matrix. The influence of the morphology of the CNTs on the dispersion and on the rheological, electrical, mechanical and thermal properties of PC/CNTs and HDPE/CNTs were studied. Different synthesis conditions and different catalysts were tested in order to produce CNTs with different morphology. From the TEM analysis of the samples it was clear that particles produced at high temperature are characterized by larger diameters. Rheology measurements were performed on the samples in order to evaluate the level of dispersion of the nanotubes, showing significant differences between samples produced by different catalysts. Various nanocomposites were produced by micro compounding experiments in order to study the electrical properties of the samples and to discriminate the best ones. Finally, a study concerning the electrical and mechanical properties of specimens produced by injection molding was performed.

Contents

1 Introduction **1**

2 State of art **5**
2.1 Carbon nanotube synthesis 5
2.1.1 CNT precursors 9
2.1.2 CNT catalyst 9
2.1.3 CVD process conditions 15
2.2 Carbon nanotube nanocomposites 20
2.2.1 Effect of CNTs morphology and agglomeration on mechanical properties of polymer nanocomposites 24
2.2.2 Effect of CNTs morphology and agglomeration on electrical properties of polymer nanocomposites 28
2.2.3 Effect of CNTs morphology and agglomeration on rheological properties of polymer nanocomposites 36

3 Experimental process and method **45**
3.1 CNT synthesis method: Catalytic chemical vapor deposition . . . 45
3.2 Nanocomposite processing method 47
3.2.1 DSM twin screw microcompounder 47
3.2.2 Twin screw extruder and injection molding 48
3.3 Characterization methods 50
3.3.1 Scanning electron microscopy 50
3.3.2 Transmission electron microscopy 50
3.3.3 Electrical measurements 51
3.4 Mechanical measurements 54
3.4.1 Rheological measurements 55

4 Experimental results and discussion **56**
4.0.1 CNTs synthesis and characterization 56
4.1 Study of the variation of the carbon nanotubes diameter by TEM 60
4.2 Density measurement 60
4.3 Study of the level of dispersion: rheological measurement 62
4.4 Study of the level of dispersion: SEM analysis 67
4.5 DSM microcompouding experiments 70
4.6 Injection molding experiments 78

5 Conclusions and prospective **84**

List of Figures

1.1 Two different types of CNTs. (a)SWNT (b)MWNT 1
1.2 Number of published articles and issued patents on carbon nanotubes as a function of year 2
1.3 CNTs aggregation 3

2.1 Electron micrographs of MWCNTs with different diameters 5
2.2 Schematic representation of electric arc apparatus and laser-vaporization apparatus 6
2.3 Schematic representation of CVD method 7
2.4 Growth mechanisms for CNTs 8
2.5 Variation of yield of reaction with hydrocarbon partial pressure . 10
2.6 SEM micrographs for vertically aligned CNTs grown on different catalysts 11
2.7 Effective mass of obtained multi-walled carbon nanotubes after purification as a function of the catalyst composition 11
2.8 TEM images of carbon nanotubes grown over catalysts with different compositions 12
2.9 TEM images of iron nanoclusters of different diameters 13
2.10 TEM images of carbon nanotubes grown using different average diameters iron nanoclusters 14
2.11 Cross section FESEM images of CNTs at different growth temperature 16
2.12 TEM images of CNTs deposited at different growth temperature . 17
2.13 SEM images of vertically well aligned CNTs on Fe deposited SiO_2 substrate 17
2.14 Effect of growth time on C amount and growth rate in CNTs . . . 18
2.15 SEM images of MWNTs grown over $Tb_{90}Fe_{10}$-coated Si substrate 19
2.16 Yield as a function of time from CO over Mo particles and C_2C_4 over Fe:Mo particles 20
2.17 Global Carbon Nanotubes Market Estimates and Forecast, by Application 21
2.18 Electronic microscope images of different CNTs 22
2.19 TEM micrographs of PC-MWNT composites 23
2.20 Tensile testing data as a function of nanotube concentration for the PC/MWCNT composites 26
2.21 Tensile modulus of the neat epoxy and the various nanocomposite samples 27
2.22 Tensile strength of the neat epoxy and the various nanocomposite samples 27
2.23 Tensile strength and elastic modulus of CNT/polymer composites 28

2.24 Typical application of conductive composites and schematic representation of percolation phenomenon and conductive network in conductive composites 29
2.25 Comparison between experimental thresholds and theoretical threshold concentrations based on CNTs length prior to melt mixing . . 30
2.26 Comparative plot of nanocomposite (MWCNT/epoxy) conductivity as a function of the CNTs weight fraction 31
2.27 TEM images of CNT agglomerates dispersed with different techniques 32
2.28 Processing methods used to disperse CNTs and the corresponding percolation thresholds 33
2.29 Electrical conductivity of nanocomposites as a function of CNT content 33
2.30 Volume resistivity versus mixing speed at different mixing temperatures 34
2.31 Specific mixing energy in dependence on mixing speed at different temperatures 35
2.32 Optical micrographs showing dispersion of MWNT in polycarbonate at different mixing conditions 36
2.33 TEM images of composites based on different polymer types and matrix viscosity 37
2.34 complex viscosity of CNTs filled polycarbonate at 260℃ and complex viscosity versus CNTs content at different frequencies 38
2.35 Storage modulus G' and Loss modulus G" of CNTs filled polycarbonate at 260℃ 39
2.36 Frequency dependence of the shear storage modulus G' at 170℃and 280℃ 41
2.37 Frequency dependence of complex viscosity at 170℃ and 280℃ . . 41
2.38 Effect of temperature on the rheological percolation threshold of polycarbonate/MWCNT nanocomposites 42
2.39 Variation of the storage modulus G' and loss modulus G" for two different suspensions 43
2.40 Variation of the storage modulus G' and loss modulus G" for two different suspensions with different aspect ration 44
2.41 Steady shear viscosity μ of 0.5 wt% MWNT/epoxy for three different suspensions 44

3.1 Schema of the CVD apparatus used for the synthesis of MWCNTs at Nanocyl S.A. 46
3.2 Images of twin-screw DSM Xplore microcompounder 47
3.3 Images of twin-screw DSM Xplore microcompounder 48
3.4 Pellets of HDPE/CNTs obtained after mixing with twin screw extruder 49
3.5 Images of an injection molding machine 49
3.6 Images of an SEM principles and apparatus 51
3.7 Images of an TEM principles and apparatus 52
3.8 Preparation of the samples for electrical measurement 52

3.9 Comparison between the percolation threshold of two nanocomposites with different matrix 53
3.10 Curves obtained from the mechanical tests 54
3.11 Dimension of the samples used for impact test, according to the norm ISO 180. 55
3.12 Rheometer used for measuring rheological properties 55

4.1 TGA analysis of a sample 85% carbon purity 59
4.2 TGA analysis of a CNTs sample with 90% carbon purity 59
4.3 TEM images of sample CatA1 taken at different magnifications in order to measure the value of the diameters. 61
4.4 Variation of the density for the 18 samples produced. On the x-axis the synthesis conditions are indicated. Red diamonds indicate samples synthesized by catalyst A; Green squares indicate samples synthesized by catalyst C; Yellow triangles indicate samples synthesized by catalyst C. 62
4.5 (a) complex viscosity of a mixture 2wt% CNTs/epoxy versus temperature. (b) complex viscosity of a mixture 2wt% CNTs/epoxy versus frequency (measurement taken at 25°). 64
4.6 (A) Storage modulus G' of a mixture 2wt% CNTs/epoxy versus frequency (measurement taken at 25°). (B) Loss modulus G" of a mixture 2wt% CNTs/epoxy versus frequency (measurement taken at 25°) 65
4.7 (A) Comparison of complex viscosity between three samples 0.5wt% CNTs/epoxy and 2wt% CNTs/epoxy (measurement taken at 25°) (B) Comparison of storage modulus G' between three samples 0.5wt% CNTs/epoxy and 2wt% CNTs/epoxy (measurement taken at 25°) 66
4.8 SEM analysis of samples CatA1 (a), CatB1 (b), CatC1 (c) at different magnifications. 68
4.9 SEM analysis of CatA4 (a), CatB4 (b), CatC4 (c) at different magnifications. 69
4.10 Percolation curves of the PC/CNTs produced with the nanotubes previously synthesized 71
4.11 Optical images of (A)CatA5, (B) CatB4, (C) CatC3. The scale bar is $50\mu m$ 72
4.12 Percolation curves of the HDPE/CNTs produced with the CNTs previously synthesized 73
4.13 Electrical resistivity of nanocomposites PC/CNTs at different mixing speed for (A) 1,5wt% CNTs and (B) 1,0wt% CNTs. 75
4.14 Electrical resistivity of nanocomposites PC/CNTs at different processing temperature for (A) 1,5wt% CNTs and (B) 1,0wt% CNTs. 76
4.15 Electrical resistivity of nanocomposites PC/1,5wt%CNTs at different processing time 77
4.16 Electrical resistivity of nanocomposites HDPE/CNTs (top) and PC/CNTs (bottom) produced by injection molding at different conditions. 79

4.17 Elastic modulus of nanocomposites HDPE/CNTs produced by injection molding in different conditions. 81
4.18 (A) Stress at yield and (B) Elongation at yield of nanocomposites HDPE/CNTs produced by injection molding at different conditions. 82
4.19 Notched impact of nanocomposites HDPE/CNTs produced by injection molding at different conditions 83

List of Tables

3.1 Specifications of the standard product NC7000 produced at Nanocyl S.A.. 46

4.1 Synthesis parameters for producing 18 samples that will be used for the study of this Master's thesis. 57
4.2 Values of the diameters of all the CNTs samples. 60
4.3 Value of the slope of the curve $G'vsf^{\alpha}$ in a mixture 0,5wt% CNTs/epoxy 67
4.4 Processing conditions used in different experiments in order to verify the effect of the parameters on CNTs produced by different catalyst. 74
4.5 Process conditions used for producing the CNTs series used for injection molding experiments 78

Chapter 1

Introduction

Carbon nanotube (CNT) is an allotrope of carbon consisting of a sheet of graphene rolled seamlessly to form a cylinder, having a diameter on the nanometer scale. Carbon nanotubes can have different length, thickness, number of layers as well as different structures, depending on how the graphene sheet has rolled up to form the tube. Figure 1.1 shows the atomic structure of two different types of carbon nanotubes, single walled nanotubes (SWNT) (figure 1.1a) and multi walled nanotubes (MWNT) (figure 1.1b). SWNT consists of a single sheet of graphene while a MWNT is made of multiple concentric graphite layers.The particular nanostructure of CNTs endow them with high surface area, large aspect ratio and unique and remarkable physical and chemical properties.

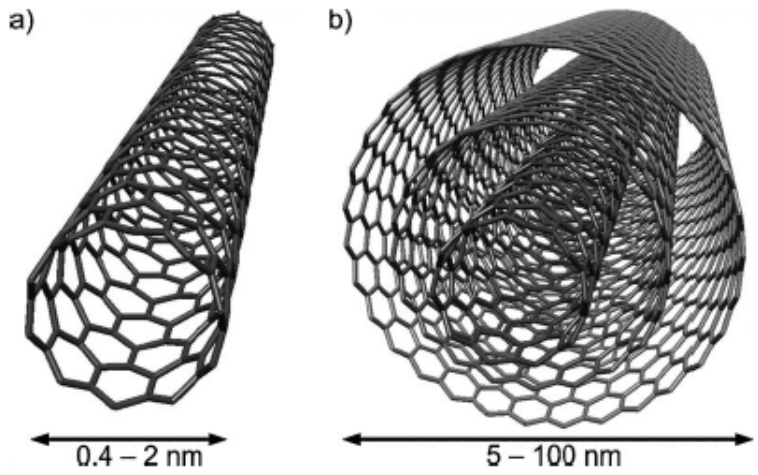


Figure 1.1: Two different types of CNTs. (a)SWNT (b)MWNT[1]

Carbon nanotubes were described for the first time by Iijima in 1991 [2]. From this moment, carbon nanotubes generated huge interest in many sectors of science and engineering thanks to their unprecedented properties. Carbon nanotubes can find applications in devices for electronics, for example for electronic packaging, sensors and EMI shielding, in the filed of transportation, in structural parts or as filler for tires, or either they can be used in devices for energetic applications, as for fuel cell or Li-ion batteries, as well as in biotechnologies. Thanks to its extraordinary potential in all these different applications, the interest in carbon nanotubes keeps on increasing and plenty of researches are focusing every year on this subject. Figure 1.2 highlights the importance of studies concerning carbon

nanotubes showing the increasing number of published articles and patents about carbon nanotubes.

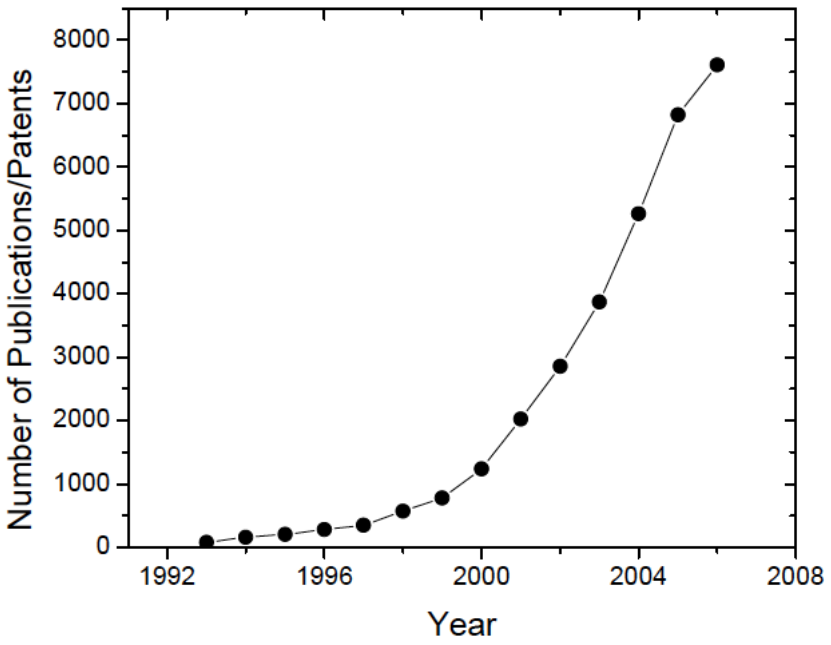


Figure 1.2: Number of published articles and issued patents on carbon nanotubes as a function of year[3].

Lack in control of the synthesis and chemical processing of the CNTs is still one of the long-standing problem in the carbon nanotube research area. Of great interest is to improve the ability to control the chirality of the product, which determines whether a CNTs is metallic or semiconducting, the diameter of the carbon nanotube, determining the bandgap of a semiconducting SWNT, and the placement and orientation on large substrates. Nowadays, the most interesting challenges in the study of carbon nanotubes are: (i) mass production, i.e., the development of cost effective, large scale process for the synthesis of high quality nanotubes, including SWNTs. (ii) Selective production, i.e., control over the structure and the electronic properties of the produced CNTs. (iii) Organization, i.e., control over the location and orientation of the produced nanotubes on a flat substrate. (iv) Mechanism, i.e., the development of a thorough understanding of the processes of nanotubes growth [4].
Currently, the most popular use for carbon nanotubes is as reinforcement and conductive additive in polymer nanocomposites for structural and electronic applications. CNTs are more effective compared with other traditional fillers, primarily thanks to the large aspect ratio which increase the stress transfer and promotes the formation of percolation networks in the matrix, allowing to use a significantly lower content of nanoparticles compared with the main competitor, carbon blacks. Nonetheless, the particular structure of CNTs also increases Van der Waals attractions between CNTs and decreases their solubility in polymeric matrix. This phenomena leads the nanoparticles to aggregate easily and hinders

an optimal dispersion in the matrix. Figure 1.3 shows carbon nanotubes tightly aggregated in agglomerates of diameter up to $500\mu m$.

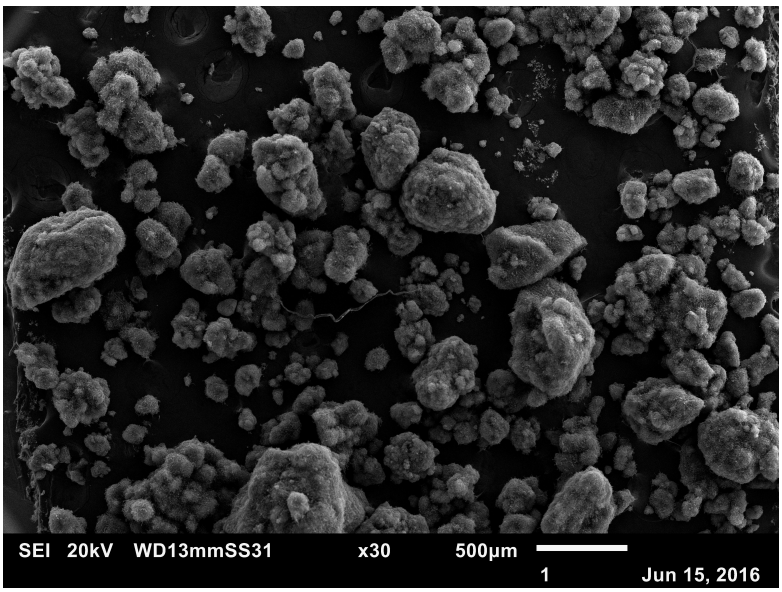


Figure 1.3: Van der Waals forces between CNTs lead to the formation of big aggregations. SEM picture of a sample produced at Nanocyl S.A.

The ability to tailor electrical and mechanical properties and totally employ the potential of CNTs widely depends on the ability to obtain an homogeneous dispersion of the fillers in the polymeric matrix. This is an important first step towards many potential applications that harness the unique properties of CNTs. Dispersion of CNTs in the matrix has a major role in the final properties of the composite, in particular electrical and mechanical. A better understanding of the relationship between processing, CNTs dispersion and final properties of CNTs nanocomposites is one of the most interesting challenges in the field of nanotubes, which may lead to obtaining materials with unprecedented characteristics.
At present, most of the researches focused on studying mechanical or functionalization techniques which demonstrated to be helpful in increasing the dispersion of the CNTs in the matrix. Mechanical techniques rely on imposing a high shear stress on the CNTS polymer mixture. Functionalization techniques are based on improving the stability of the CNTs polymer solution and prevent their reagglomeration. Both these techniques present some advantages as well as many drawbacks.
In the work of this master's thesis, a completely different approach to this issue is adopted. The goal of this research project is to study the link between the morphology of the CNTs, their distribution in the polymeric matrix and the final properties of the nanocomposite. The objective is to define how different synthesis routes induce different morphologies and how different nanotubes morphologies can affect the dispersion and the final properties of the nanocomposites. As a first step, we focused on the synthesis of CNTs with different process parameters and catalysts, which were then characterized with electron microscopes in order to study their morphologies and level of aggregation. The samples were

then used as filler in polycarbonate (PC) and high density polyethylene (HDPE) matrices, in order to study the differences in their electrical and mechanical properties.

The next paragraph deals with the state of the art concerning the influence of the synthesis on the final morphology of the CNTs and reports how a good level of dispersion affects the final properties of nanocomposites. The ensuing chapter is dedicated to the description of the methods and techniques used for the experiments done for this master's thesis. An analysis of the results obtained will be then described, organized in two different sessions. As a first step, the study concerning CNTs synthesis and characterization will be discussed, followed by the analysis of the results concerning the properties of the nanocomposites produced either at small scale, by micro compounding and at larger scale, by injection molding. The final chapter is dedicated to conclusions highlighting the role that this master's thesis may have on future researches.

Chapter 2

State of art

The state of the art concerning the influence of the synthesis on the final morphology of the carbon nanotubes and the importance of the dispersion of the CNTs on the final properties of nanocomposites is described in the following paragraphs.

2.1 Carbon nanotube synthesis

CNTs were observed for the first time by Sumio Iijima in 1991 [2]. CNTs with different diameters were grown in the soot of an arc discharge apparatus (figure 2.1).

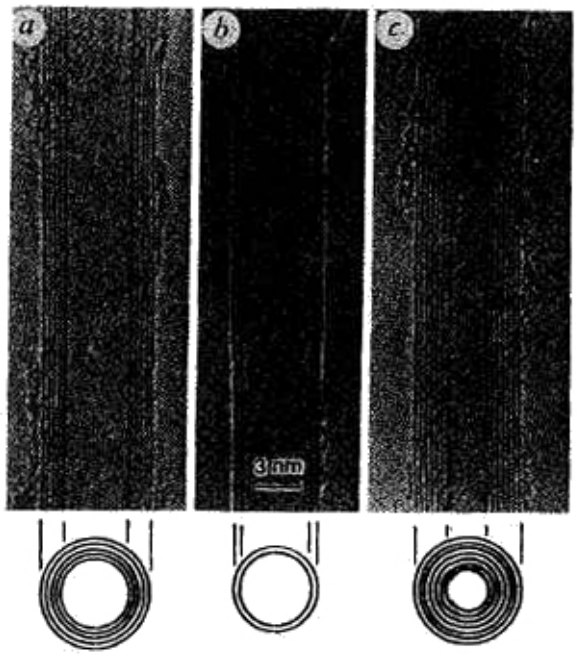


Figure 2.1: Electron micrographs of MWCNTs with different diameters [2].

The principle of arc discharge is based on an electrical arc discharge generated between two graphite electrodes under an inert atmosphere (figure 2.2a). The high temperature employed during the process leads to the sublimation of carbon. After the first synthesis of CNTs, other different techniques have been devised to produce carbon nanotube. A very powerful method used for producing carbon nanotubes is laser ablation technique (figure 2.2b). During this process, a piece of graphite is vaporized by laser irradiation under inert atmosphere [5, 4].

Laser ablation and arc discharge were the primarily approaches used for CNTs production. Both methods involve the condensation of carbon atoms generated from evaporation of solid carbon sources. The working temperature reaches 3000-4000℃, melting temperature of graphite. Both synthesis ways are able to produce MWNTs and SWNTs, and both these methods are still widely used by researchers [6, 7]. For a long time these approaches have been the most used to produce CNTs. Nonetheless, there are several issues concerning these methods. In order to evaporate the carbon atoms from solid carbon, the synthesis are carried out at temperature higher than 3000℃, the chambers have to be under vacuum, and continuous graphite target replacement are needed, posing difficulties to the large-scale production of CNTs, leading to low yield synthesis and poor selection towards CNTs. Moreover, CNTs synthesized by evaporation methods are in tangled forms and thus difficult to purify, manipulate and assemble [7, 8, 9].

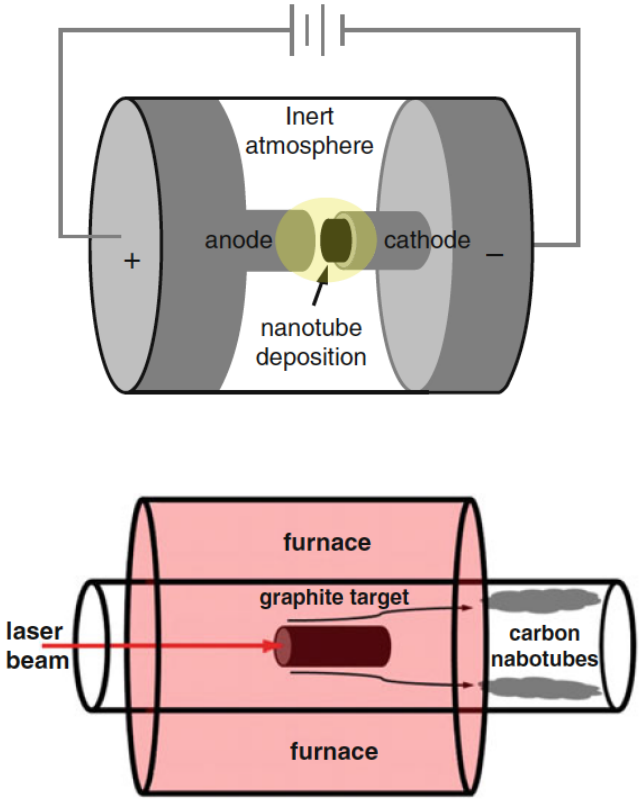


Figure 2.2: (a) Schematic representation of electric arc apparatus. (b) Schematic representation of laser-vaporization apparatus [9].

In recent years Chemical Vapor Deposition (CVD), either called Catalytic Chemical Vapor Deposition (CCVD), demonstrated to be a valid substitute to these methods to obtain very good quality CNTs. Nowadays, CVD is the most popular method for producing CNTs. This method is a simple and economic way for synthesizing CNTs at a relatively low temperature and ambient pressure

thus is the solution for achieving the goal of mass production with an acceptable price. CVD technique allows to control the structure of CNTs and is a very versatile method. CVD offers the possibility to use many different precursors or catalysts, permits to growth CNTs in many forms, such as powder or thin or thick films, and allows to obtain desired architectures of CNTs [10]. Figure 2.3 shows a simple schematic diagram of the experimental set up used for CNT growth by CVD method.

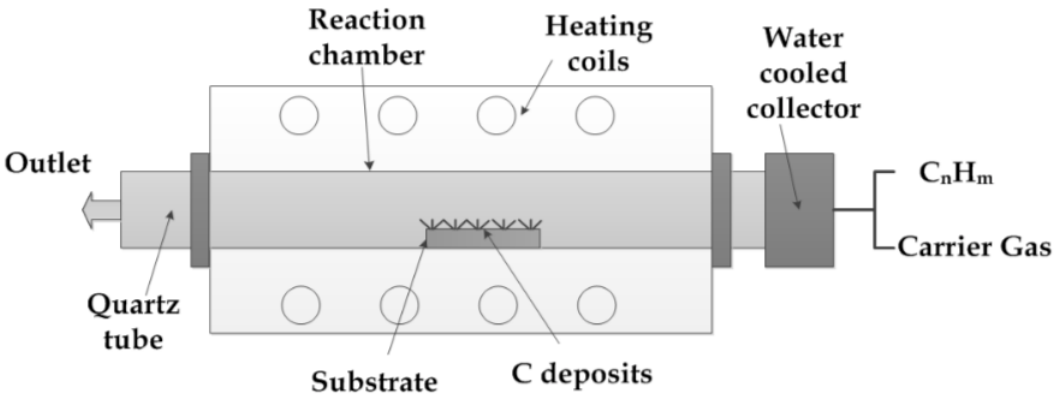


Figure 2.3: Schematic representation of CVD method [11].

The working principle is based on the decomposition of the hydrocarbon in presence of a catalyst. In this process, lasting typically 15-60 min, a mixture of hydrocarbons and inert gas is flow in the reactor heated at around 600-1200℃, where a catalyst is set. CNTs grow on the active site of the catalyst and hydrogen is released [6, 12, 13, 14, 7, 15, 16, 10, 17]. Methane CVD was developed by Dai's group at Stanford [18]; they first reported the synthesis of bulk amounts of SWNTs by CVD from methane at 900 ℃[18, 19, 20]. This process is particularly interesting because it offers the main advantage of a relative easy and economical apparatus. For this reason, from the discovery of CNTs growth by CVD method, several groups studied this technique proposing different reaction conditions and suggesting optimal process parameters, often contradicting each other. Many different variations in the synthesis routes have been tested in order to obtain products with different properties. Another advantage of CVD is the possibility to control numerous parameters during the synthesis, leading to many possible variations of the final product [10]. Anyway, the relationship between process parameters and properties of the final product is still not clear. Despite the growth mechanism of CNTs has been widely studied, this topic is still controversial. Various mechanism have been proposed for CNTs nucleation and growth from nanometric metals [21, 22, 23]. At present, the basic growth mechanism of carbon nanotube in CVD approach has been established. CNTs growth is based on the dissociation of carbon precursor into carbon atoms, dissolution and

saturation of these atoms in the catalyst metal particles. Super saturation of the metal results in solid carbon precipitation with subsequent formation of the carbon nanotube structure. The growth temperature, the type of catalyst and the particle size are the main factors determining the limit of solubility in the metal particles.
Two different growth mechanisms, illustrated in Figure 2.4, can occur depending on the catalyst support interaction. The tip growth model takes place when the catalyst-substrate interaction is weak. The hydrocarbon decomposes on the top surface of the metal, carbon diffuses down through the metal and the catalyst is lifted off the support while CNTs grow. Once the metal is fully covered with excess of carbon, the catalyst is not active anymore and the CNT growth is stopped (figure 2.4a). When the catalyst-substrate interaction is strong, the CNT precipitation fails to push the metal particle up and the metal-support contact is preserved; thus CNT grows up with the catalyst particle rooted on its base. This latter growth mechanism is called base-growth model (figure 2.4b) [24, 15, 10, 22].

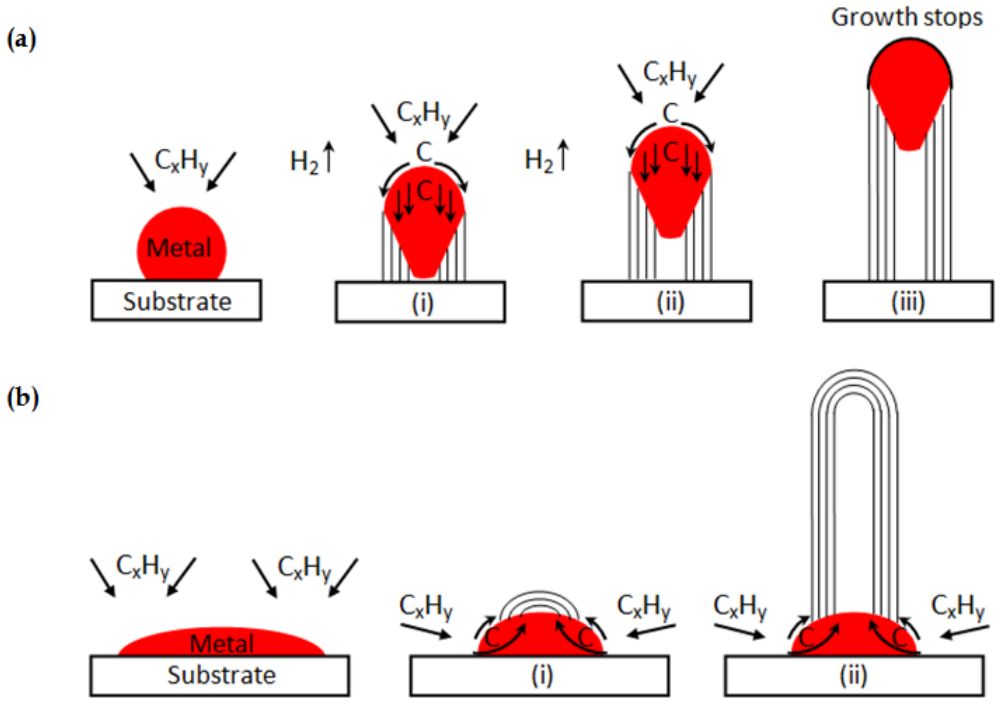


Figure 2.4: Growth mechanisms for CNTs: (a) tip-growth model, (b) base-growth model [15].

The type and the concentration of the carbon precursor, the growth temperature, the nature and size of the catalyst and the time of the experiment are all parameters that can be adjusted in order to obtain different products [7, 25, 24, 16].
In the following paragraphs, the effect of the synthesis parameters on the final carbon nanotubes properties will be discussed.

2.1.1 CNT precursors

The precursor used for synthesizing carbon nanotube in CVD method is an hydrocarbon, typically fed into the system in the gaseous state. The nature of the hydrocarbon, together with the nature of the metal-support interface, play an important role in the CVD process, determining the final yield. The degree of supersaturation is generally determined by the affinity for carbon formation of the gas phase. The nature of the support interface mainly determines the rejection or precipitation of carbon at this interface. During the production process, oxygen is typically removed with a continuous flow of nitrogen or argon, in order to avoid oxidation of the carbon.
Different studies have been done on the choice of the carbon precursors. Most commonly used carbon gaseous source are methane, ethylene, acetylene, benzene, xylene and carbon monoxide [25, 15, 26, 27, 10, 22]. The gas flow can also be a mixture of hydrocarbon and hydrogen (H_2), which was shown to play an important role in the synthesis of CNTs. H_2 can help preventing the catalytic sites from being encapsulated by graphite and thus to avoid deactivation during synthesis of long duration [26]. Nonetheless, an high content of hydrogen in the reactor feeding could lead to negative effects. A large volume of hydrogen reduces considerably the hydrocarbon conversion during the process, contributing to reduce the number of active carbon atoms on the catalyst surface and consequently the amount of grown CNTs [28].
In order to understand how the carbon nanotube formation is influenced by the features of carbon precursors, the CVD products of different carbon precursors have been investigated [25, 15].The possibility of selective synthesis of SWNTs and MWNTs by changing carbon precursor was demonstrated. The molecular structure of the precursor play a key role on the morphology of the CNTs grown. Aromatic molecules favors the growth of SWNTs, while aliphatic molecules generally tends to form MWNTs or non tubular carbon structure [25, 15]. Not only the nature of the precursor demonstrated to be important, but also the concentration and the partial pressure of the hydrocarbons influence the final product. The effect of the precursor concentration, in particular of CH_4, during CVD process were studied [29]. It was observed that the carbon yield increased by increasing the gas concentration, but no effect on the final morphology of the CNTs was found. Some experiments on the carbon partial pressure in the feed were also carried out [30, 31]. It was shown that changing the carbon partial pressure in the feed affected the formation of co-generated amorphous carbon [30]. The influence of the partial pressure of the precursor on the final yield of SWNTs was also studied. As shown in Figure 2.5, the product mass increase when increasing the partial pressure of acetylene (C_2H_2) up to 5 Torr. Anyway, when the partial pressure is increased above 5 Torr, thermal decomposition of the carbon occurs, making the catalyst particles inactive and decreasing the production of carbon nanotubes [31].

2.1.2 CNT catalyst

One of the most important parameters controlling the final properties of the CNTs is the choice of the catalyst and the nature of the catalyst-substrate inter-

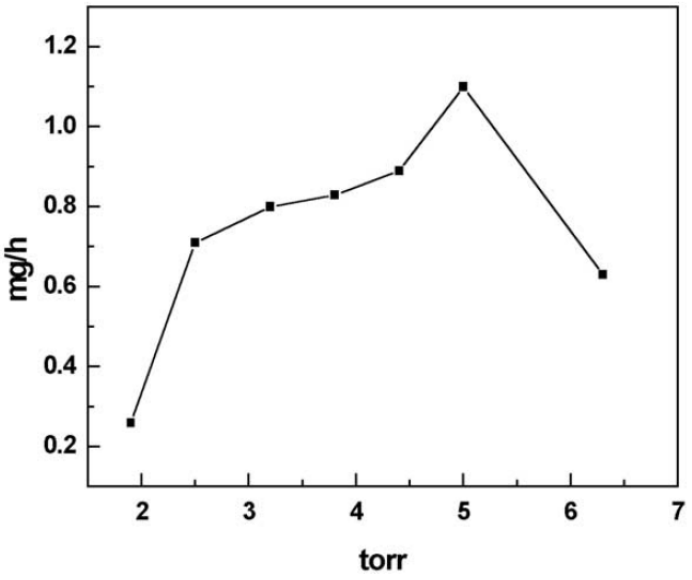


Figure 2.5: Partial pressure of C_2H_2 vs the yield of SWNT. The reaction temperature is 900℃[31].

action. Nanosized transition metal particles are typically used in CCVD process, either in oxide or metallic forms or as mixtures. The most common metals are Iron (Fe), Cobalt (Co) and Nickel (Ni). The high solubility of carbon at high temperature and the high carbon diffusion rate in these metals make them the most efficient catalysts. Moreover, the high melting point and the low equilibrium-vapor pressure of these metals offer a wide temperature window of CVD for many different carbon precursors.
Carbon nanotube formation strongly depends on the ability to catalytically decompose gaseous carbon-containing molecules. Many different composition, size and preparation methods have been studied, showing that the precise catalytic composition, as well as its chemical state and the particle size, have a great influence on the final product [24, 15, 16, 32, 30, 20, 33, 34]. A comparison concerning the efficiency of the three most used catalysts, Fe, Co and Ni, was reported [33]. The final length of vertically aligned CNTs as well as the average diameter was observed to significantly vary with the different catalysts. As shown in Figure 2.6, the length of the carbon nanotubes grow with Fe, Co and Ni was respectively 10, 17 and 20 μm. Also the average diameters was observed to change, being 130 nm in case of Fe catalyst, 110 nm when using Co and 100 nm for synthesis with Ni. The average growth rate was also observed to change with different catalysts. The possibility to manipulate the growth rate, the diameter and the crystallinity by selecting the catalyst was demonstrated.

Other studies focused on the possibility to control the carbon nanotube morphology using binary mixtures of cobalt with other transition metals [34]. Again, it was shown that depending on the catalyst used, it is possible to control some characteristics of carbon nanotubes, especially the outer diameter distributions and the carbon deposit. $Fe_{1-x}Co_x$ alloys demonstrated to be among the most efficient catalysts for the synthesis of MWNTs. The resulting yield and the CNTs

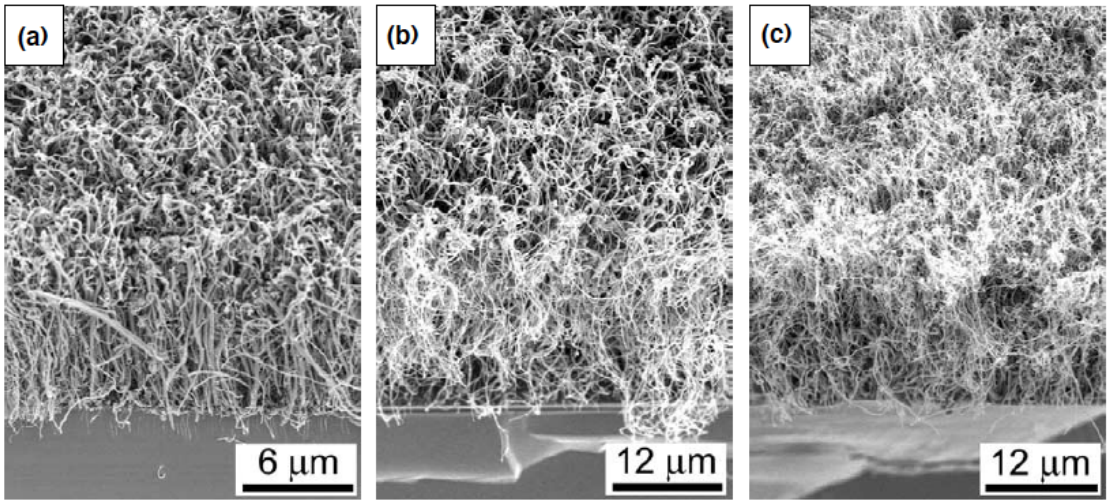


Figure 2.6: SEM micrographs for the vertically aligned CNTs grown on (a) Fe, (b) Co and (c) Ni catalyst particles deposited SiO_2 substrate, under the condition that C_2H_2 flows with a rate of 30 sccm for 10 min at 950℃ [33].

morphology strongly depend on the concentration x.
Magrez *et al.* [24] studied the variation of the yield with the variation of the parameter x, highlighting also the effect on the final carbon nanotube diameter, as well as on the amount of catalyst particles present in the product.

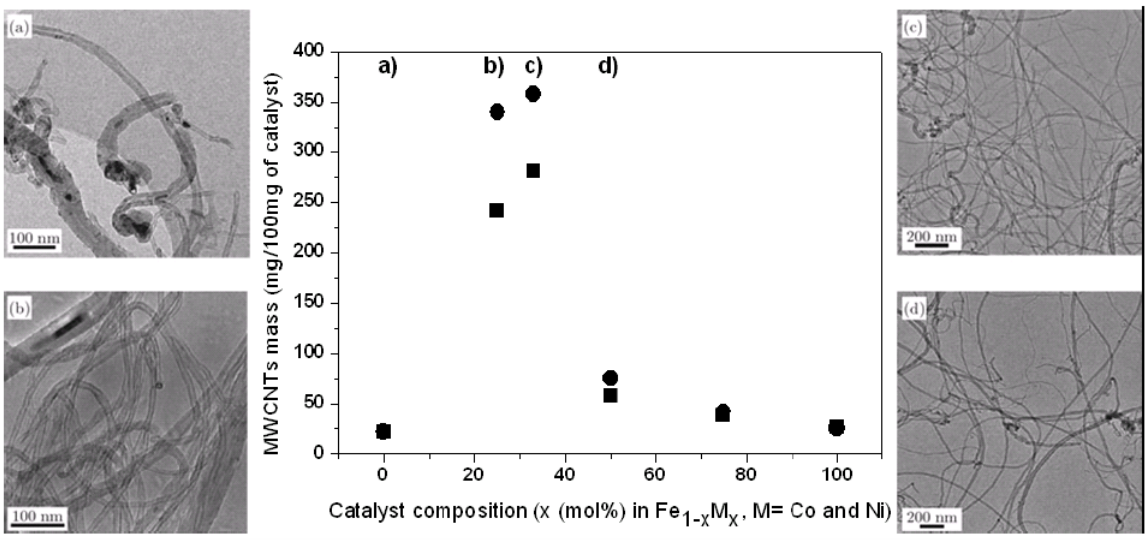


Figure 2.7: Effective mass of the obtained multi-walled carbon nanotubes after purification as a function of the catalyst composition $Fe_{1-x}M_x$ with M = Co (square) and Ni (•). The TEM images show representative carbon nanotubes obtained for (a) x = 0 mol%, (b) x = 25 mol%, (c) x = 33 mol% and (d) x = 50 mol% $Fe_{1-x}M_x$ catalyst. [24].

As shown in figure 2.7, the catalyst efficiency increases almost 100 times by increasing x up to 25 mol% for growth temperature at 700℃, followed by a drop in yield for exceeding 33 mol%. This result shows that the most active cata-

lyst in the $Fe_{1-x}Co_x$ compound is metallic alloy Fe_2Co. Transmission Electron Microscopy (TEM) images in figure 2.7 highlights that for composition strongly deviating from x= 33 %mol, an high diameter distribution with diameters ranging from 10 nm to 50 nm and the presence of many catalyst particles as embedded particles is observed. In case of x=33%mol, no enclosed catalyst particles are found and carbon nanotubes with diameter of 15 ±2 mm are produced.
The effect of the chemistry of the catalyst can be also observed by studying the diameter distribution of the carbon nanotubes. Ago *et al.* [29] studied the effect of the metal concentration in the catalyst on the growth of SWNTs, analyzing their diameter distribution (figure 2.8). The carbon nanotubes were grown on Fe particles supported on porous MgO. It was observed that the low concentration of Fe gives only SWNTs. Figure 2.8e shows that SWNTs have small diameters with a narrow distribution. By increasing the Fe concentration, double walled nanotubes (DWNTs) were observed together with SWNTs (figure 2.8d), as well as an increase of the average diameter and the broadened diameter distribution (figure 2.8f).

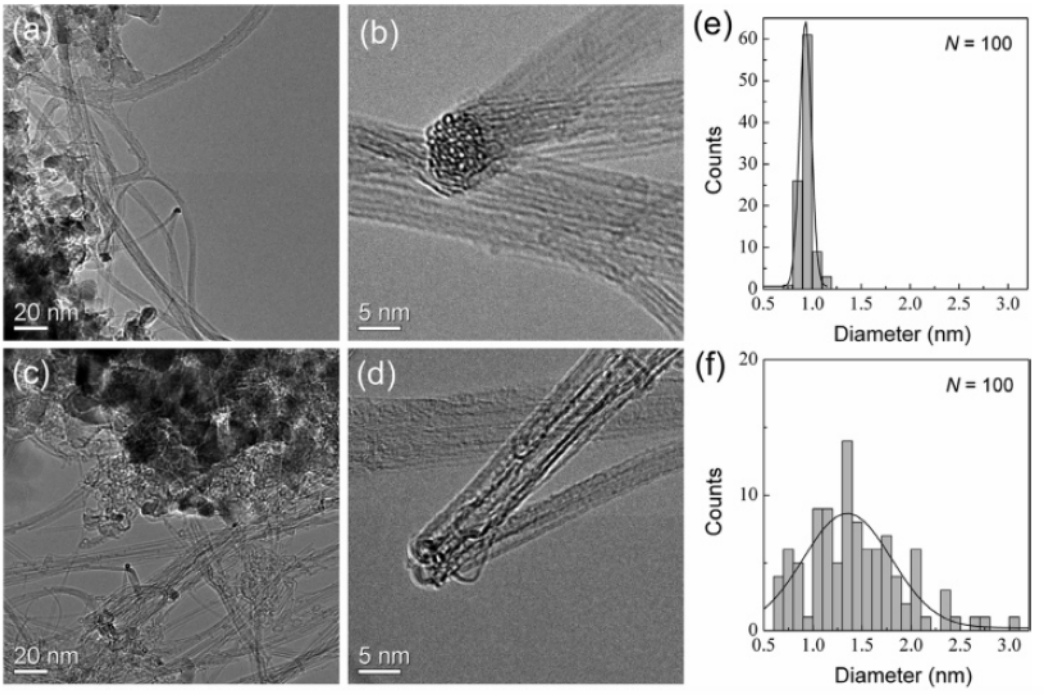


Figure 2.8: TEM images of carbon nanotubes grown over Fe 0,6wt% (a,b) and 3wt% supported on the porous MgO. The histogram of the outer diameter of carbon nanotubes determined from TEM images are plotted respectively in (e) and (f). [29].

The size of the nanocluster catalysts is also a powerful parameter that can be used to control the diameters and structure of CVD-grown CNTs [35]. Iron nanoclusters with three different nearly monodisperse average diameters were prepared and used to grow carbon nanotubes (figure 2.9).

Carbon nanotubes were grown by CVD at 800°C with ethylene reactant using 3, 9 and 13 nm average diameter iron nanoclusters as catalyst. A close correlation between diameters of the nanocluster catalyst and of the carbon nanotubes was

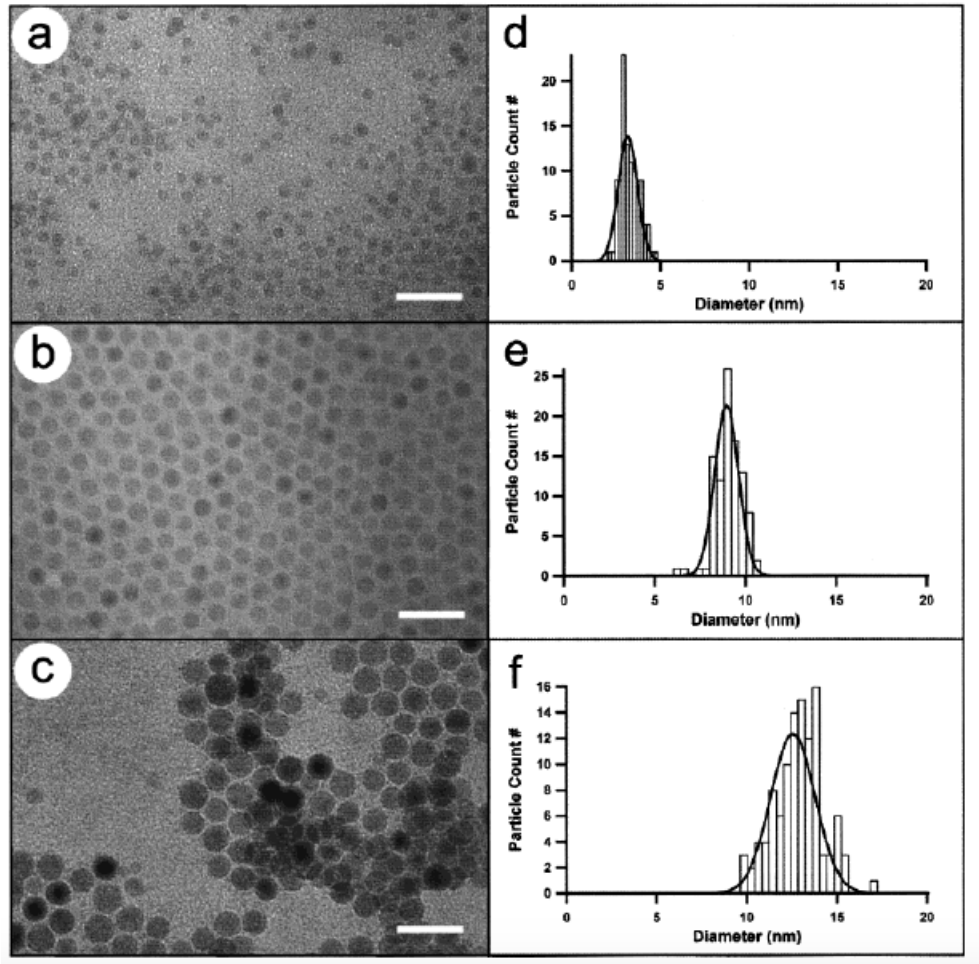


Figure 2.9: (a,b,c) TEM images of iron nanoclusters of different diameters. The scale bars are 30 nm. (d,e,f) Corresponding histograms of the nanocluster diameters distribution [35].

observed (Figure 2.10).

TEM images shows that increasing the diameter of the nanocluster catalyst is possible to obtain reproducible growth of larger diameter carbon nanotubes (Figure 2.10a,b,c). The CNTs diameters increase proportionally with the catalyst diameter. The influence of the catalyst in defining the CNTs diameters is highlighted from the variation of the diameter distribution (Figure 2.10d,e,f). It is possible to define a close correlation between the diameter distribution of the catalyst particles and the carbon nanotubes. For the largest diameter nanotubes, there is some broadening relative to the nanocluster catalyst distribution, due to the greater difficulty in achieving uniform nucleation at the largest diameters.
Also the effect of the growth temperature and carbon reactant species on the different nanoclusters were explored. Synthesis carried out at 900℃ using 9 nm diameter iron nanoclusters produces large diameter, thin-walled MWNTs with typically only 2 or 3 walls with substantially fewer defects compared to similar diameter nanotubes grown at 800℃. However, high-temperature growth from ethylene was observed to lead to substantial amorphous carbon on CNTs due to homogeneous decomposition of ethylene in the gas phase. Thus, in order to

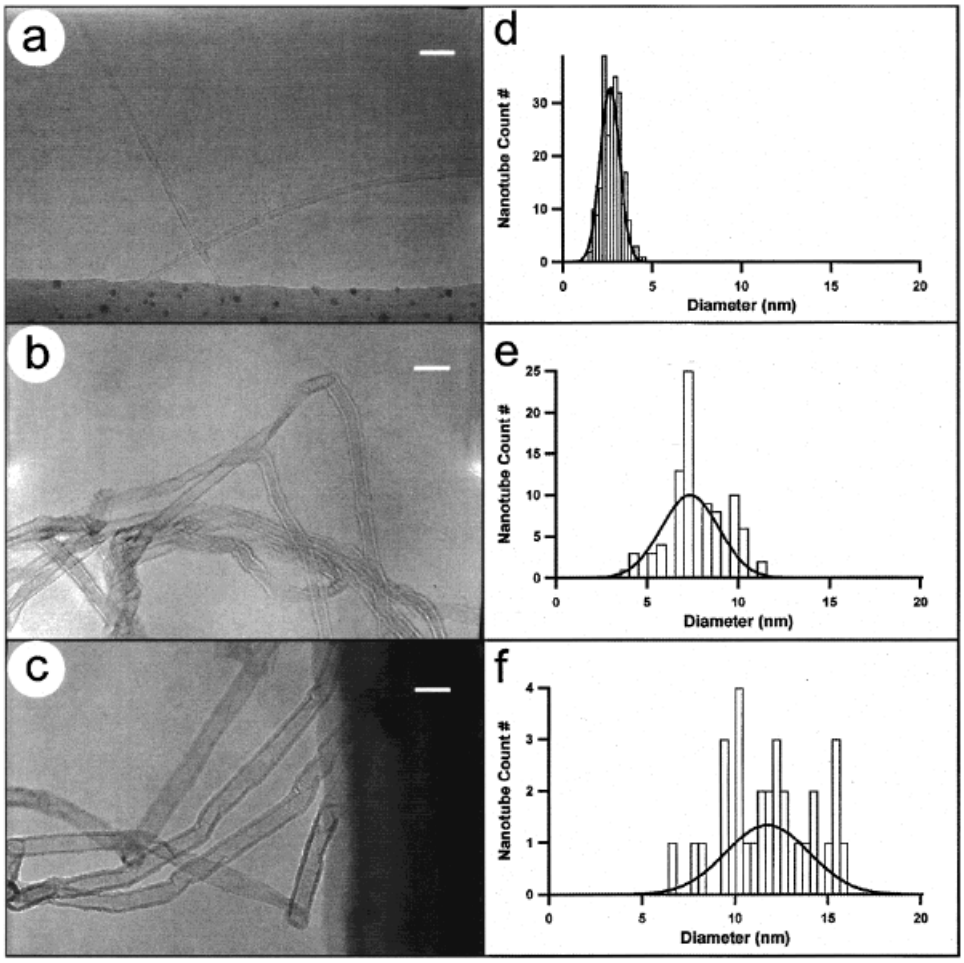


Figure 2.10: TEM images of carbon nanotubes grown using (a) 3, (b) 9, and (c) 13 nm average diameters iron nanoclusters. Scale bars are 20 nm. Corresponding histograms of the carbon nanotube diameters are plotted in (d), (e), and (f), respectively. [35].

obtain high-quality large diameter nanotubes free from amorphous carbon coatings, synthesis using methane was also investigated. Significantly, methane-based growth from 9 nm average diameter nanoclusters yields relatively clean SWNTs and Double Walled Carbon Nanotubes (DWNTs).

Another crucial aspect in the synthesis process is the substrate material. In particular the choice of the catalyst-support material pair is crucial. Commonly used substrate in CVD are silicon, silicon carbide, silica, alumina and aluminiosilicate. The catalytic properties of the catalytic-support material combination mainly depends on the affinity between catalyst and the support material. The nature of the substrate, its surface morphology and textural properties contribute to determine the yield and the quality of the final CNTs. By varying the support, the resulting morphology of the metal cluster is affected, and as a result, the chiral angle of the CNTs produced and its properties [4, 36]. Several studies concerning the effect of substrate on the growth of carbon nanotubes were carried out in order to determine the most efficient combination. One of the best performance were found in synthesis carried out with alumina as supporting material and

iron catalyst. The strong metal-support interaction established between this two materials allows high metal dispersion and thus a high density of catalytic sites [16, 37, 10].

2.1.3 CVD process conditions

The choice of the catalyst is of primary importance in order to control the final product, but the process conditions employed during the synthesis have a crucial effect as well. The temperature of synthesis was demonstrated to be of great importance in order to tailor the final diameters of the CNTs and the diameter distribution, the final length as well as the yield of reaction. The temperature effect may still vary based on the type of carbon source and catalyst employed during the synthesis, thus it is possible to find controversial and very different results in the literature. In general, synthesis carried out at higher temperature lead to an increase of the diameter of the final CNTs. This effect is explained as an increase of the diameter of the catalyst particles as a consequence of the acceleration of thermal sintering of the metal nanoparticles [29, 30, 38, 36, 39].

The effect of the temperature on the final properties of the carbon nanotubes was deeply investigated by many researchers. Temperature showed to have an effect also on the final length of the CNTs. Low temperature synthesis (650℃) carried out with benzene (C_6H_6) were reported to lead shorter and more entangled tube, with more defects in the graphite layers. Increasing the process temperature about 100℃ was found to produce longer tubes, rather straight than curved and with a better degree of graphitization [40].
The effect of the reaction conditions on the synthesis of CNTs through catalytic decomposition of acetylene was also studied [36, 27]. The percentage of carbon deposited under acetylene flow was shown to increase with the reaction time. Increasing the flow rate of N_2 demonstrated to decrease the carbon deposit. Concerning the time and the flow rate of acetylene, an increase of these parameters led to a significant increase of carbon deposit [36].
Cui *et Al.* [27] studied in detail the growth behavior under acetylene gas flow of carbon nanotubes in chemical vapor deposition under different temperature conditions, ranging from 500 to 1100℃. Figure 2.11 shows the cross section FESEM images of CNTs after 20 min growth at different temperatures.

At 600℃ it was already possible to grow MWNTs. The majority of MWNTs were vertically aligned with a length of about 1 μm, with some longer tubes up to 3 μm (Figure 2.11a). A big difference in length can be observed increasing the temperature up to 700℃. In this case the CNTs were able to reach a length of about 54 μm, as shown in Figure 2.11b. At 800℃ the length of the nanotubes decreases (Figure 2.11c), losing the characteristic alignment observed in the previous images and some bundles with an estimated length of about 10 μm are observed. The variation in the organization of the CNTs is due to the decrease of the density and thus absence of crowding. More bundles are observed at 900℃ (figure 2.11d), suggesting the presence of CNTs with quite small diameters. Bundles with large diameters can be observed to extend upward from the surface, and other appear to form close to the substrate with random direction. Increasing the temperature up to 1000℃, less surface coverage and consequently

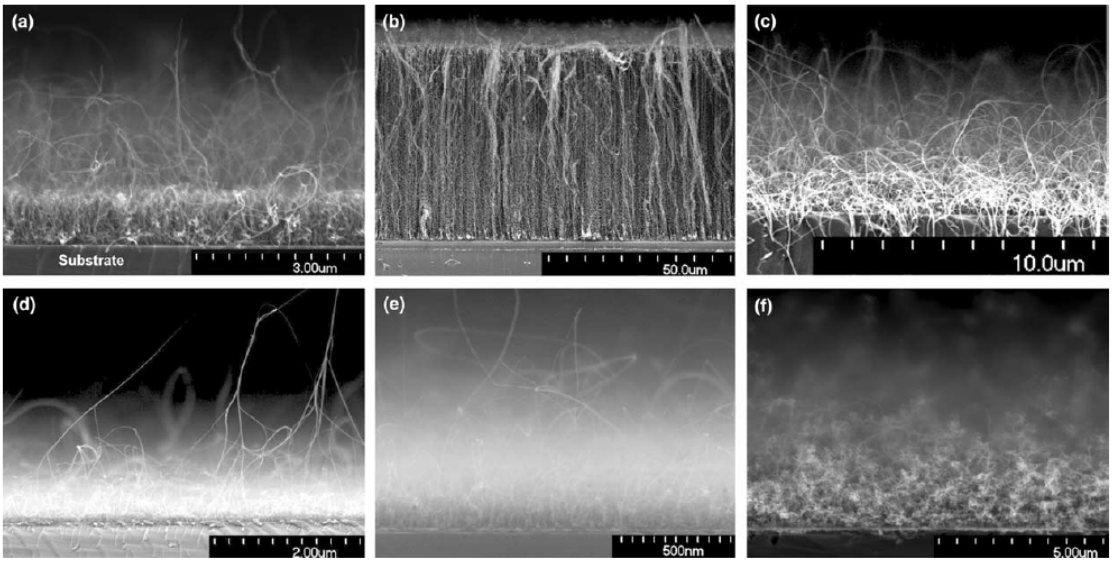


Figure 2.11: Cross section FESEM images of CNTs at different growth temperature: (a)600℃(b)700℃(c)800℃(d)900℃(e)1000℃(f)1100℃[27].

less crowding and vertical alignment is observed. Figure 2.11e shows that both the CNT length and nucleation density were reduced at 1000℃. Then, when synthesis were carried out at 1100℃, the substrate surface was found to be densely occupied by curly carbon structure (figure 2.11f). CNTs morphology was also studied using TEM as shown in figure 2.12.

Figure 2.12a shows that at low temperature (600℃), CNTs are multi walled and highly defective. When the temperature is increased to 700℃ CNTs are also observed but with smaller diameters and fewer graphitic layers (figure 2.12b). DWNTs have an amorphous graphitic layer on their outer wall, but their existence is spare. At 800℃ a mixture of DWNTs, MWNTs and the appearance of some SWNTs is observed (figure 2.12c) and a similar result was found at 900℃, with an increase in DWNTs which are much more abundant than SWNTs (figure 2.12d). Increasing the temperature up to 1000℃, carbon fibers with larger diameters are found among smaller CNTs, as observed in figure 2.12e. Compared with CNTs, the fibers have no distinct wall structure and hollow cavities, thus showing their high defective nature. In case of synthesis at 1100℃, carbon fibers appear to be the only product (figure 2.12f).

A similar study concerning acetylene CVD synthesis on a different catalyst was carried out by Lee *et Al.* [41]. CNTs grown at 750℃, 850℃ and 950℃ were analyzed. At all three temperatures it was possible to grow vertically well aligned CNTs. As observed in Figure 2.13, the length as well as the diameter of the carbon nanotubes were shown to increase with the process temperature. The density of the CNTs decreased by increasing the temperature.

These studies demonstrated that CNTs with larger diameter and lower density were demonstrated to be possibly grown by selecting the process temperature. The relationship between the degree of crystallinity and the process temperature was also verified by studying the loss of weight by TGA, highlighting that the

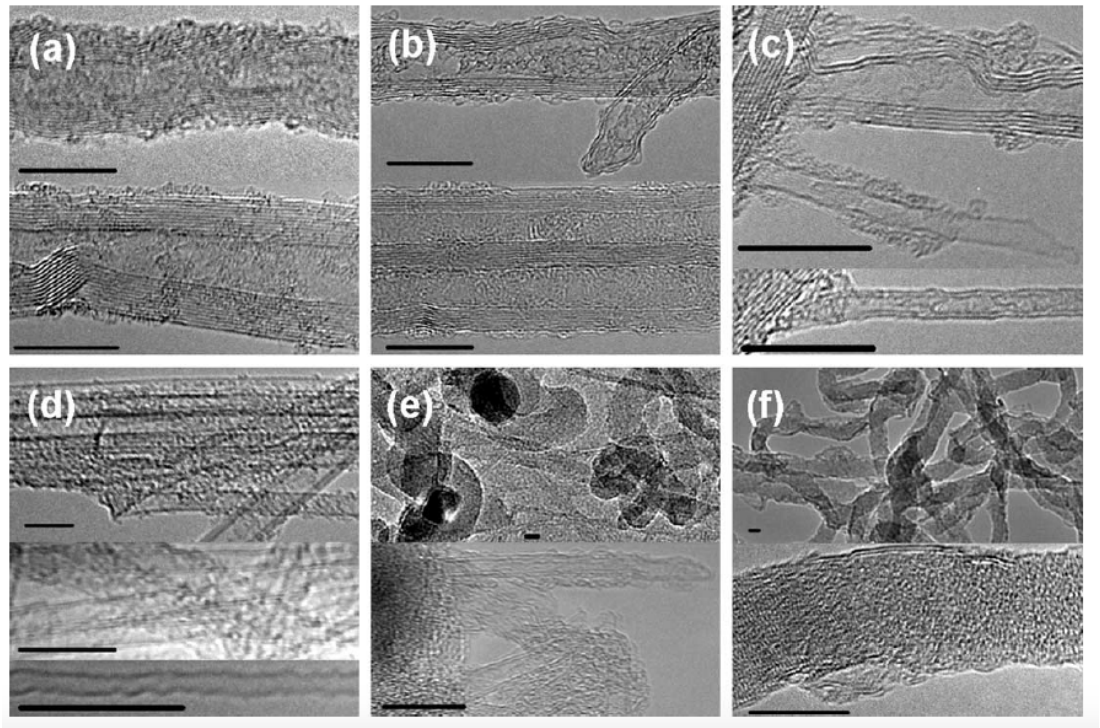


Figure 2.12: TEM images of CNTs deposited at different growth temperature: (a)600℃(b)700℃(c)800℃(d)900℃(e)1000℃(f)1100℃. The scale bar is 10 nm [27].

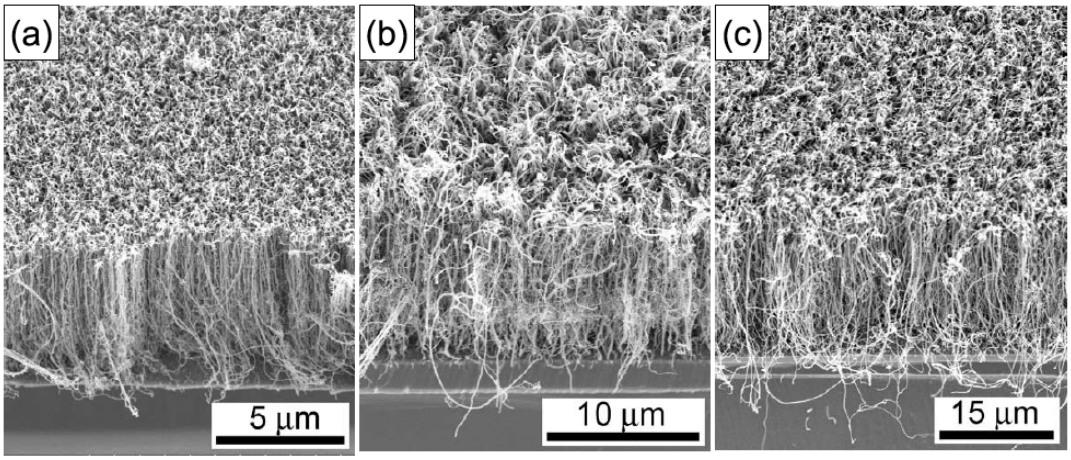


Figure 2.13: SEM images of vertically well aligned CNTs on Fe deposited SiO_2 substrate. (a) 5μm long CNTs grown at 750℃(b) 10μm long CNTs grown at 850℃(c) 20 μm long CNTs grown at 950℃[41].

cristallinity becomes better as the growth temperature increases [41].
Other papers report the link between the CNTs morphology and the synthesis parameter in methane CVD synthesis [28]. The process parameters on CNT features, amount and growth rate were described. The effect of the temperate on the amount of C formed was studied. The experimental data showed a maximum C rate production at 600℃ (Figure 2.14a). The amount of carbonaceous product

C (including CNT) formed during the reaction was observed to increase with the increase of growth time. The growth rate rapidly decreased after the first 30 min of reaction, then for long reaction times tended to flatten (Figure 2.14b).

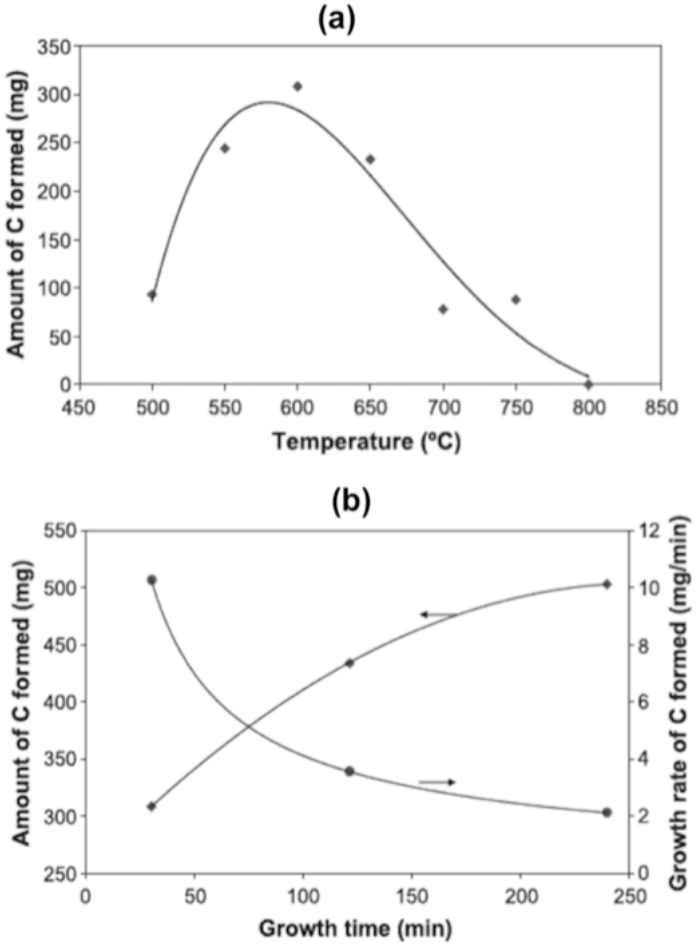


Figure 2.14: (a) Effect of temperature on C amount formed at constant growth time (30 min), pressure (100 mbar) and H_2/CH_4=10/70 ratio.(b) Effect of growth time on C amount and growth rate formed at constant temperature (600℃), pressure (100 mbar) and H_2/CH_4=10/70 ratio [28].

The effect of the temperature could also be observed on CNT morphology. The comparison of CNTs grown at 600℃ with those grown at 500 and 700 ℃ indicated that a low temperature corresponded to thicker, shorter and less curved CNT, probably due to the reduced reaction rate, while a high temperature was responsible for thinner diameter and greater length CNT thanks to the faster reaction rate [28].

The growth of MWNTs with xylene, over silicon and alumina substrate using various thin film catalyst coating was found to be strongly related with (i) the reaction chamber temperature (ii) the reaction time (iii) the type of substrate [42]. Microscopy analysis revealed that for temperature lower then 700℃ the density of MWNTs mats significantly decrease, with no tube grown below 550℃. Moreover, even increasing the temperature above 700℃, the MWNTs density

could not increase beyond that achieved at 700℃. Studying the effect of the reaction time, it was observed very dense mats of MWNTs after 120 min; reducing the reaction time to 60 min, the MWNTs yield was found to radically decrease. Figure 2.15 shows the difference in density after 120 min and 60 min.

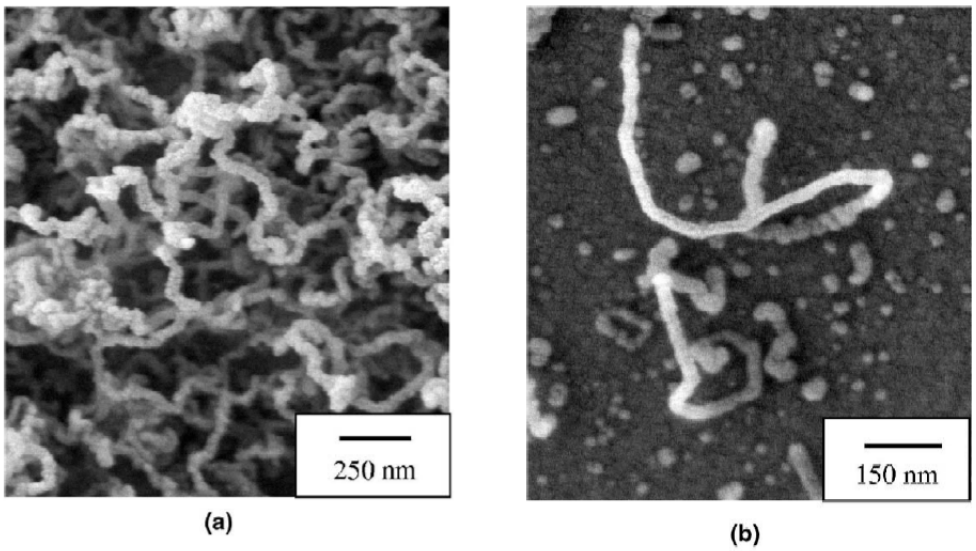


Figure 2.15: SEM images of MWNTs grown over $Tb_{90}Fe_{10}$-coated Si substrate. The pyrolysis was carried out at 700℃ for (a) 120 min, (b) 60 min [42].

Some more experiments were done for longer time, showing that increasing to 180 min the synthesis time had no effect on the length of the MWNTs could be observed. Nonetheless, an increase in the MWNTs diameters attributed to the coarsening of the carbon nanotubes by continuous pyrolysis of xylene was reported.
Hafner *et Al.* [43] reported the study of the production of carbon nanotubes by disproportionation of CO and C_2H_4 over alumina-supported Mo particles under different conditions. In the case of CO the resulting product is SWNTs very monodispersed in diameters. In case of C_2H_4, nanotubes bundles containing SWNTs and DWNTs. The amount of DWNTs increase from 30% at 700℃ to 70% at 850℃. Outer diameter of the individual tubes in a bundle range from 0,5 to 3 nm. From this study, no correlation between outer diameter and number of walls was observed, other than that the smaller CNTs, <1nm diameter, are never double walled. The yield was shown to increase with the reaction temperature and the time. In case of synthesis with CO, the yield increased even for very long reaction times, as observed in figure 2.16.

Other studies were undertaken in order to relate the time of synthesis with the morphology of the final product. It was found that longer reaction time resulted in the wide SWNT diameter distribution[29]. Different researches demonstrated that increasing the reaction time leads to an enhanced appearance of amorphous soot covering the graphitic nanostructures [40].

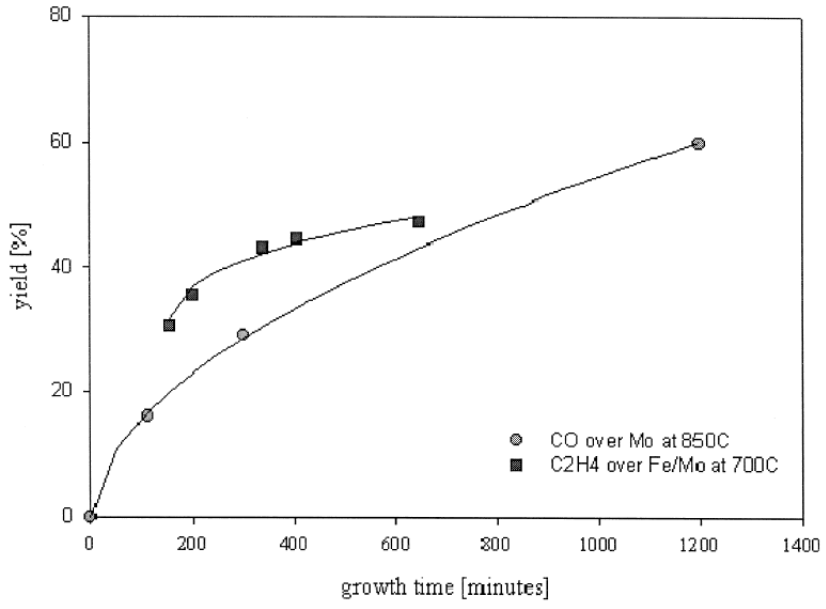


Figure 2.16: Yield as a function of time from CO over Mo particles and C_2C_4 over Fe:Mo particles. [43].

2.2 Carbon nanotube nanocomposites

Since their discovery, CNTs have been of great interest for many different fields. CNTs are characterized by the peculiarity of having high flexibility, low mass density and high aspect ratio. At the nanoscale, CNTs show extraordinary mechanical and physical properties, with predicted elastic moduli of about 1 TPa, strength in the range of 30 GPa, and exceptional resilience, showing large, nonlinear deformation before fracture. Carbon nanotubes also possess exceptionally high axial thermal conductivity as well as electrical conductivity that can be metallic or semi-conducting depending on the atomic structure. Thanks to this combination of mechanical and electrical properties of the individual carbon nanotubes, this nanoparticles are considered one of the most interesting reinforcing agent in a number of applications. Global carbon nanotubes market is anticipated to witness growth due to growing application scope of nanomaterials in electronics, plastics and energy storage applications, as shown in Figure 2.17.

The first time the first carbon nanotube-polymer nanocomposite was reported, was in 1994 by Ajayan *et Al.* [45]. After this moment, many papers concerning different processing methods and the study of the mechanical and electrical properties of this new nanocomposite started being published.
The properties of polymer nanocomposites containing CNTs depends on several factor in addition to the matrix used. The syntheses processes used to produce CNTs, the CNTs purification (if any), the amount and type of impurities in the carbon nanotubes, the diameter, the length, the aspect ratio, the arrangement of the CNTs in the matrix (isolated, ropes, bundles) and the CNTs orientation in the polymer matrix, are all parameters affecting the final properties. All known preparation of CNTs used as reinforcement gives a mixture of various chiralities,

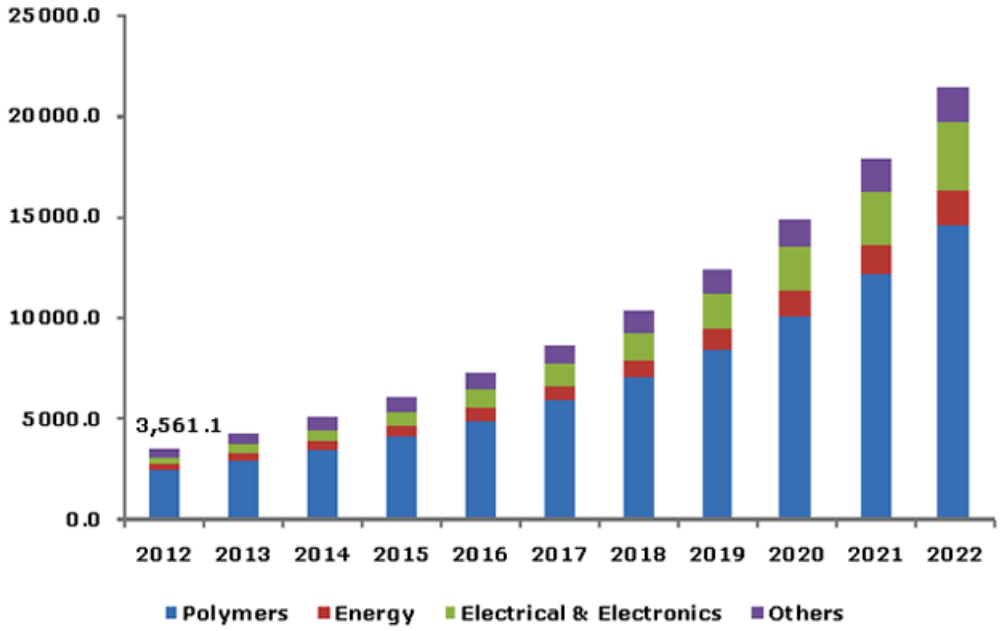


Figure 2.17: Global Carbon Nanotubes Market Estimates and Forecast, by Application, 2012 - 2022 (Tons) [44].

diameters, and length, with a different amount of impurities and defects. These parameters significantly changes both between carbon nanotubes of the same sample and between samples produced in different batches and laboratories.

In nanocomposites, three different networks can be expected, determining the properties of the product: (i) the temporary polymer network formed by entanglements, (ii) the carbon nanotube network and (iii) a combined carbon nanotube-polymer network. Noteworthy, the CNTs in the polymer matrix do not always really touch or "overlap geometrically". Nonetheless, the distance between the carbon nanotubes is small enough in order to allow a good stress transfer and to allow hopping and/or tunnelling processes [46, 47, 48, 49, 50, 51, 52, 53].

There has been an immense effort to understand the best conditions in order to optimize the transfer of the mechanical and electrical properties of the individual carbon nanotubes through the polymeric matrix. Significant insights have been achieved so far but there are still many unsolved issues which need to be further investigated in order to completely benefit from the extraordinary properties of CNTs.
One of the most debated topic is the difficulties associated with dispersion and alignment of CNT. Due to the poor interfacial interaction between CNTs and polymer matrix CNTs are easy to agglomerate, bundle together and entangle, leading to many defect sites in the composites. Any aggregation of CNTs in polymer composites results in a significant decrease of the properties, as it prevents efficient stress transfer to individual carbon nanotubes [47, 46, 48, 54, 55, 56]. The nature of the dispersion problem of CNTs is different from the one of other

fillers, due to its peculiar shape. CNTs possess diameters in the nanometer scale with high aspect ratio, thus extremely high surface area being on the range rom 250 to 1200 m^2/g. Moreover, most of the commercialized CNTs are supplied in the form of heavily entangled bundles, increasing the difficulties in the dispersion. In addition to the problems linked with the particular morphology of the carbon nanotubes, also the physical nature of the carbon nanotubes contribute to the final arrangement in the matrix. Once produced, CNTs are observed as stuck in bundles or entanglements of 50 to a few hundreds individual CNTs, hold together by Van der Waals forces [55, 57]. Figure 2.18 shows an examples of SWNTs and MWNTs bundles.

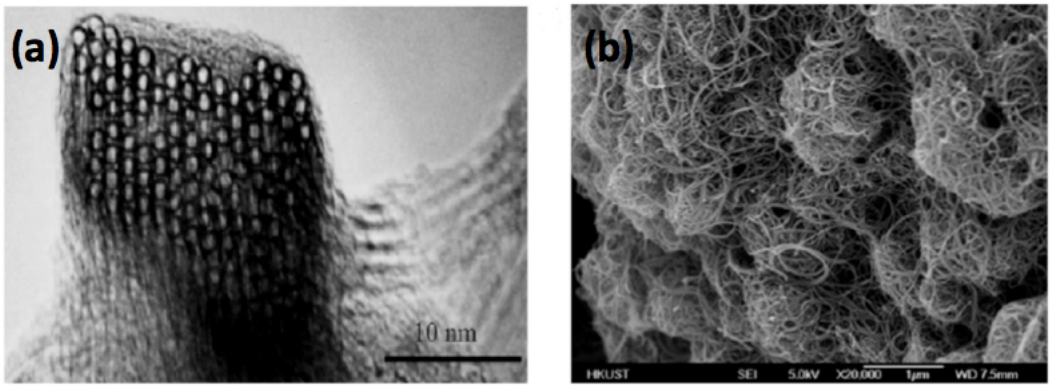


Figure 2.18: Electronic microscope images of different CNTs (A) TEM image of SWNTs bundle; (B) SEM image of entangles MWNTs agglomerates [55].

Many different techniques have been employed in order to increase CNTs dispersion, including mechanical techniques and functionalization of the polymers. Various methods of chemical modification have been studied and proved to be a valid solution in order to increase the dispersion of the carbon nanotubes in the matrix. Researches focused both on covalent and non covalent surface modifications, able to improve the chemical affinity of CNTs to polymer matrices, achieved very good results. Anyways, all these techniques present also numerous disadvantages [46].

Several processing methods are available for producing polymer/CNT composites based on either thermoplastics or thermosets. All the used techniques are inherently different from each other but they all aim at breaking agglomeration of bundles and ropes, increase and optimize the dispersion and alignment and optimize interfacial bonding. A big issue in processing CNTs is to be able to improve CNTs dispersion without destroying their integrity or reducing their aspect ratio [58].

Melt-mixing of CNTs into thermoplastic polymers using conventional processing techniques, such as extrusion, internal mixing, injection molding and blow molding, are particularly interesting, because of the speed, simplicity and availability of these processes in the plastics industry. Fiber breakage rarely occurs, allowing to preserve an high aspect ratio and without compromising the final properties.

High-shear mixing and long processing times can be utilized and offer the great advantage of enhancing dispersion; moreover, when coupled with elongational flow, aligned carbon nanotubes can be further obtained [58, 59].

Potschke *et Al.* [60] studied the distribution of carbon nanotubes at different dilution after mixing in a twin screw microcompounder. A masterbatch of PC-MWNT (15 wt%) was diluted with different amounts of PC, either below the percolation threshold (1wt%) and above (2 wt%, 5 wt%). The state of dispersion was studied in order to obtain better information concerning the polymer network inside the polymeric matrix at different concentrations. At 15 wt% MWNT, the structure consists of highly entangled and 'percolating' nanotubes in the PC matrix which are all wetted by the polymer matrix. By adding PC into the network like structure, the MWNT structure expand and gradually incorporate PC chains between the tube. The percolation state is preserved until a very high amount of PC is added, and the percolation network no longer exist since MWNT are distributed uniformly, as fine dispersion, without touching each other. Figure 2.19 a-d shows the TEM micrographs with varying concentrations of MWNT.

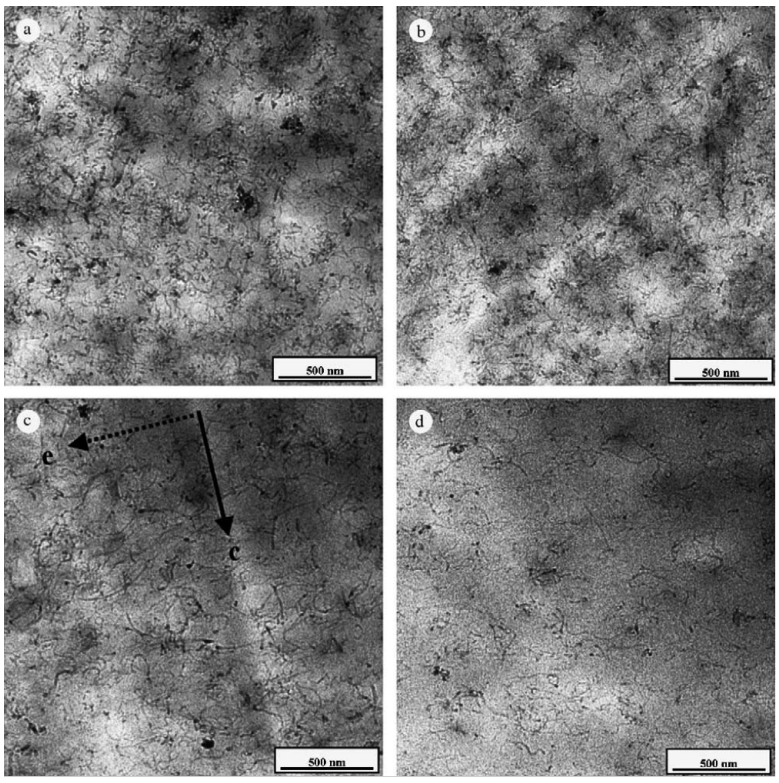


Figure 2.19: TEM micrographs of PC-MWNT composites: (a) 5 wt% MWNT cut perpendicular to extrusion direction, (b)-(d) cut along extrusion direction: (b) 5 wt% MWNT, (c) 2 wt% MWNT (arrow 'c' indicates cut direction, arrow 'e' indicates extrusion direction), (d) 1 wt% MWNT [60].

Figure 2.19a shows a sample which is cut perpendicular to the extrusion direction containing 5 wt% MWNT. All other samples in figure 2.19 were cut in the extrusion (flow) plane. Very small areas of enhanced carbon density can be observed, explained as amorphous carbon parts or catalytic impurities in the

nanotube material. Further dispersion of the CNTs can be easily observed when diluting the masterbatch to 2wt% and 1wt% (Figure 2.19c and d). Due to the lower concentration they are better visible as individual tubes or, parts of tubes which have at least lengths of about 500 nm. Carbon nanotubes are distributed homogeneously over the entire matrix. From this micrographs, it is possible to distinguish the percolated MWNT structure starting at 2 wt%. At 1 wt% level (Figure 2.19d) the tubes visible in the thin section do not appear to touch one another and thus fail to form a pathway of connected CNTs, which can be easily observed at higher MWNT contents.

The specific structure of the CNTs and the level of dispersion of the CNTs are among the most important parameters determining the final properties of the nanocomposite.

In the following chapter, researches focused on the influence of the carbon nanotubes morphology and dispersion on the mechanical, electrical and rheological properties will be discussed.

2.2.1 Effect of CNTs morphology and agglomeration on mechanical properties of polymer nanocomposites

Carbon nanotubes and polymer matrix composite materials are used in an increasing number of structural applications. Some of the reason behind the interest on this nanocomposites are their high durability, high strength, light weight, design, process flexibility, etc. Polymers such as thermosets, thermoplastics and gels have all been used as matrix. Unlike the microscopic particulate composites, in addition to the properties of the filler and the matrix, the mechanical properties of carbon nanotubes nanocomposites depend strongly on the dispersion state of nanofillers. The reinforcement potential of the CNTs can only be exploited if there is an effective load transfer from the surrounding matrix into the CNTs. The structural strength characteristics of composites greatly depends on the nature of bonding at the interface, the mechanical load transfer from the matrix to the carbon nanotube and the yielding of the interface [55, 61, 62, 50]. An high aspect ratio is required in order to maximize the load transfer between the CNTs and matrix material and thus to achieve enhanced mechanical properties. However, the larger the provided interface, the more difficult it is to efficiently disperse the reinforcing phase. The composite properties are strongly influenced by the mechanics that govern the carbon nanotube-polymer interface, which is crucial for the dispersion state as well. In nanocomposite materials, the constituents do not dissolve or merge completely. Thus, they often exhibit an interface between one another, which can be considered as a different material with different mechanical properties, decreasing the final properties of the nanocomposites. A strong interfacial adhesion corresponds to high mechanical properties of composites through enhance load transfer from matrix to CNT. Thus, chemical and physical functionalization is often used in order to enhance interfacial adhesion [50, 55, 61]. Van der Waals interactions are created between the layers of the tube, leading to a transfer of the load to the carbon nanotube via shear stress at the CNTs/matrix interface. Due to this effect, the effective

stiffness of multi walled nanotubes in a polymer matrix is reduced [63].

A good dispersion is fundamental for increasing the mechanical properties for many reasons. A good dispersion makes more fillers surface area available for bonding with the polymer matrix, and also prevent the aggregated fillers from acting as stress concentration, dramatically reducing the final mechanical properties of the composites. Many parameters have to be controlled in order to optimize and homogenize the dispersion, such as the CNT content in composites, length and entanglement of CNTs as well as viscosity of matrix [55]. Also the CNTs diameter, together with the CNT content, were demonstrated to play a key role in the degree of CNT alignment in the composite. On one side, the degree of CNT alignment can be enhanced by small diameter CNTs due to the greater extensional flow; on the other side, a higher CNT content decreases their alignment because of the CNT aggregation and restriction in motion from neighboring CNTs [50].

Characterization and structure/property nanomechanics modeling research has shown that properties of multiwalled nanotube composites are strongly diameter dependent [64]. The potential of CNTs to improve strength and stiffness can be correlated to the specific mechanical properties, the aspect ratio and the specific surface area. Thus, the exploitation of the provided interface is playing a major role concerning the improvement of mechanical properties [53].

A comparative study concerning the variation of the mechanical properties with the aspect ratio was carried out by Guo *et Al.* [65]. Young's moduli, tensile strengths, and strains at break for the PC/MWCNT composites were studied (Figure 2.20).

Young's modulus for the composites having high aspect ratio nanotubes slightly increases with increasing MWNT content for all the samples [66]. On the contrary, for samples characterized by low aspect ratio, the nanocomposite shows no changes in Young's modulus as a function of nanotube concentration, as shown in Figure 2.20a. As observed in the data collected in figure 2.20, the tensile strengths are independent on the CNTs concentration up to 1 wt %, as it was also observed in studies concerning lower aspect ratio [66]. The strain at break decreases with increasing the CNTs contents as shown in Figure 2.20c. Comparing high aspect ratio (313, 474) and low aspect ratio (94) CNTs, it was observed that the Young's modulus is slightly higher in the first case and the strain at break decreases more in the case of high aspect ratio with increasing CNTs content. The more significant decrease in strain at break with the longer CNTs is attributed to the more severe degradation of the polymer during melt mixing [65].

In order to better investigate the effect of the dispersion of the CNTs in the matrix, CNTs dispersed in epoxy by mixing the solution with different sonication time were studied [61]. Ultrasonication employs ultrasound energy to agitate particles in a solution, which results in an effective way to disperse carbon nanotubes. Depending on the sonication condition, an enhancement in the tensile strength can be observed in the modified systems compared to the neat resin suggesting that the sonication parameters highly affect the dispersion of CNTs in the epoxy resin. Figure 2.21 presents the effect of CNT addition and sonication duration on the tensile modulus of the neat and CNT modified epoxy systems.

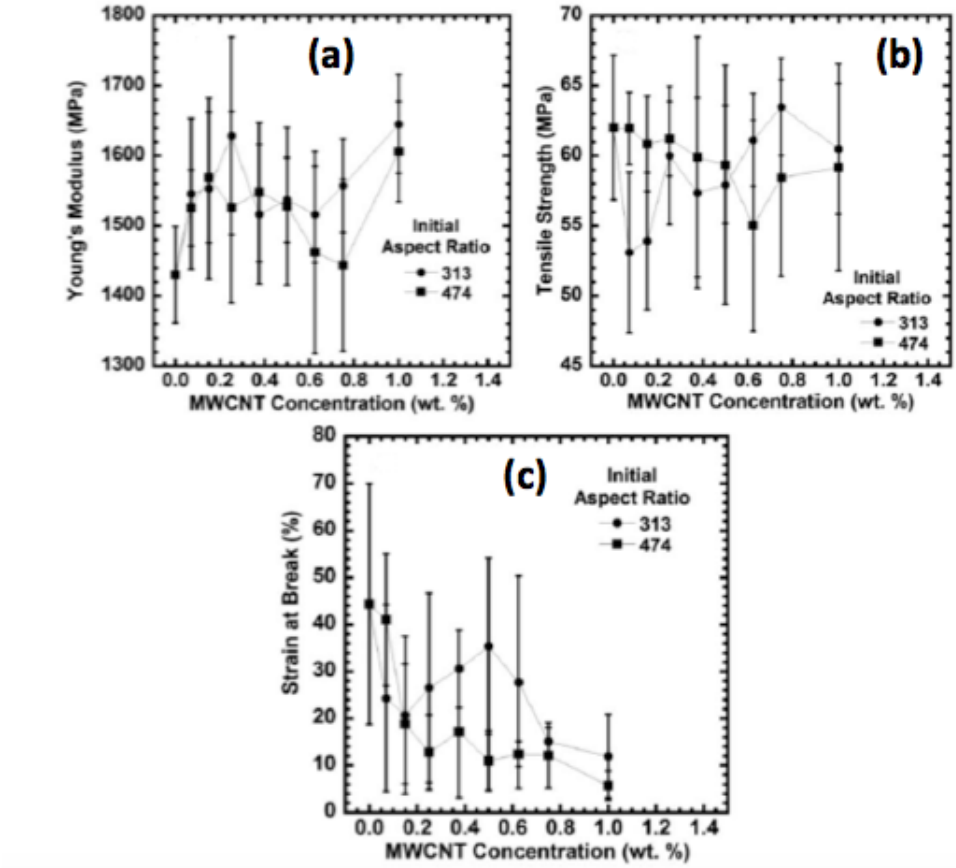


Figure 2.20: Tensile testing data as a function of nanotube concentration for the PC/MWCNT composites having nanotubes with different aspect ratios before melt-mixing: (a), Young's modulus; (b), tensile strength; (c), strain at break. The results are for those composites melt mixed at 200 rpm for 5 min only[65].

As can be seen from the obtained results the addition of a small amount of CNTs did not significantly influence the tensile modulus. The average value of the tensile modulus of the modified systems remained almost unaffected being close to that of the neat resin.

The influence of the sonication process and the CNTs loading is highlighted studying the variation of the tensile strength (Figure 2.22). Intermediate levels of sonication duration (between 1 and 2 h of sonication) lead to better mechanical properties. Small mixing time is not sufficient for good CNT dispersion, while very high mixing time may lead to breakage of the CNTs. These two conflicting mechanisms may also explain the quite big scatter that can be observed between specimens with the same CNT loading and sonication duration.

Alignment of carbon nanotube also widely affect the final mechanical properties, compared to randomly oriented CNT/polymer composites, being higher efficient as reinforcement. In Figure 2.23, the tensile strength (Figure 2.23a) and elastic modulus (Figure 2.23) of randomly oriented and aligned CNT/polymer composites are compared.

In most cases, both tensile strength and elastic modulus of aligned CNT/polymer

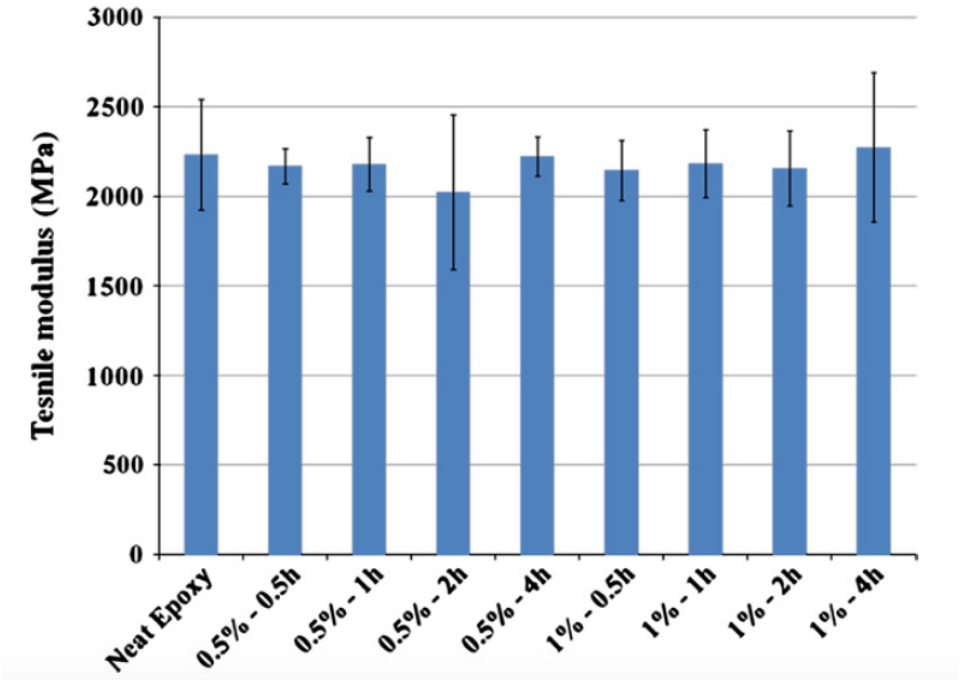


Figure 2.21: Tensile modulus of the neat epoxy and the various nanocomposite samples as a function of the CNT loading and the sonication duration. [61].

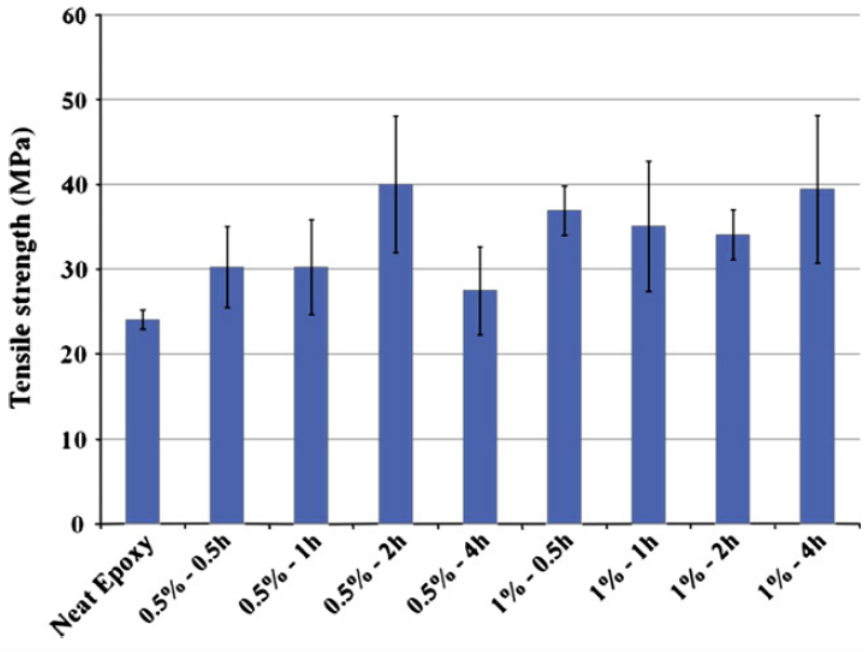


Figure 2.22: Tensile strength of the neat epoxy and the various nanocomposite samples as a function of the CNT loading and the sonication duration. [61].

composites are significantly improved. Tensile strength and elastic modulus of aligned CNTs/polymer composites reach up to 3600 MPa and 80 GPa, re-

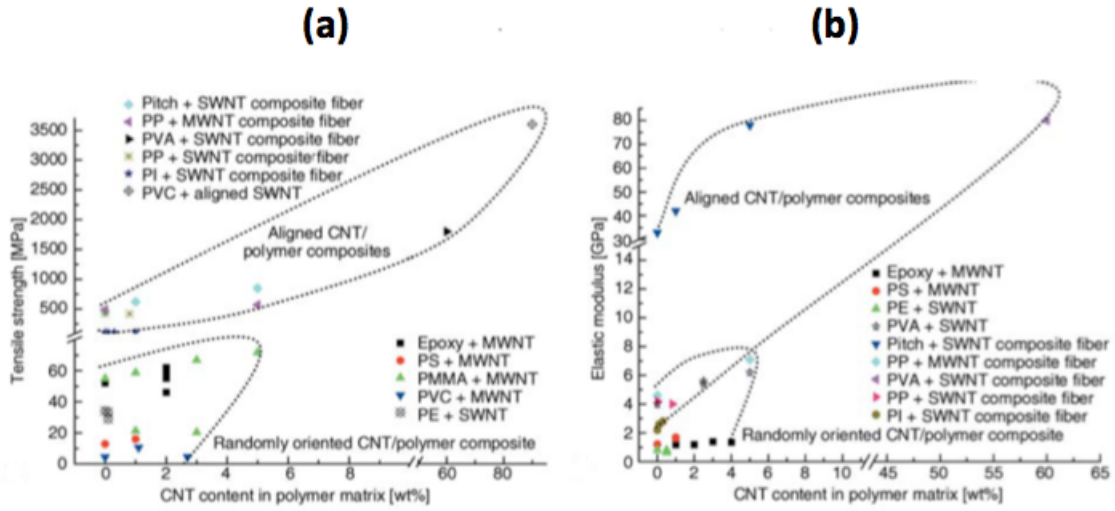


Figure 2.23: Tensile strength (a) and elastic modulus (b) of CNT/polymer composites [67].

spectively. On the other side, in case of randomly orientated nanotube, tensile strength and elastic modulus are generally less than 100 MPa and 6 GPa, respectively. Moreover, the tensile strength and elastic modulus are always higher for aligned CNT/polymer composites containing higher CNT content, while this is not the case for randomly oriented CNT/polymer composites. A critical CNT content in matrix has been identified for many CNT/polymer composites. Below this content, the strengthening effect for randomly oriented CNT/polymer composites increases with increasing CNT content. Above this content, the strength of CNT/polymer composites decreases, sometimes even below that of the polymer matrix. The reason could be either an excess of CNTs, which increases too much the viscosity of polymers, and also the difficulties in completely covering the surface of all the fillers by polymer matrix, due to the large specific surface area of CNTs, which makes uniform dispersion and load transfer more difficult. Moreover, it is very difficult for high quantity of polymers to intercalate among CNTs when the CNT content becomes high.

2.2.2 Effect of CNTs morphology and agglomeration on electrical properties of polymer nanocomposites

Carbon nanotube nanocomposite is a great solution to obtain highly conductive materials that can be used for electronic devices. In order to explain the electrically conductive behavior of composites consisting of conducting fillers and insulating matrices, the percolation theory can be applied. Increasing the conducting filler content, the composites undergoes an insulator-to-conductive transition. The content at which the measured electrical conductivity of the composite sharply increase of several order of magnitude is referred to as percolation threshold. The percolation threshold is observed as a stepwise change in resistivity of several order of magnitude and is the result of a formation of

a interconnected structure of carbon nanotubes [55, 68]. This phenomenon is explained by the formation of continuous electron paths or conductive networks, as shown in Figure 2.24.

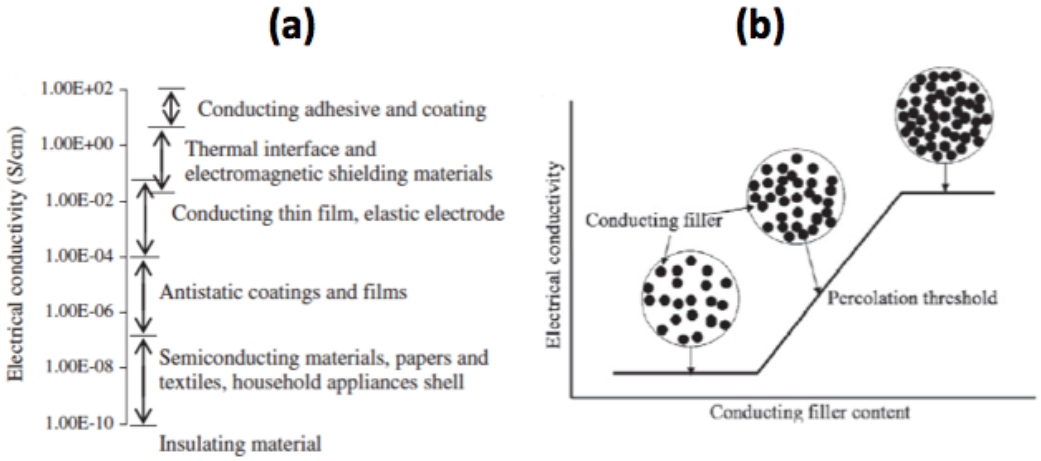


Figure 2.24: (a) Typical application of conductive composites (b) and schematic representation of percolation phenomenon and conductive network in conductive composites[55].

The use of CNTs as nanofillers offers the great advantage of minimizing the content of filler necessary to reach the percolation threshold. Compared with traditional conducting fillers, CNTs have the unique peculiarity of having an high aspect ratio and superior electrical conductivity, facilitating the formation of conductive network and thus transforming the insulating polymer in a conductive composite at a low CNT content, depending on the matrix used. Anyways, a common agreement concerning the value of the percolation threshold for each polymer matrix could not be reached, considering that this value may strongly vary from sample to sample. The nature of the polymer used, the intrinsic characteristics of the CNTss, the CNTs-CNTs and the CNTs-polymer interactions as well as the processing condition have an direct effect on the achievable dispersion and thus on the final properties of the nanocomposite [55, 66].
A good level of dispersion could lead up to 50 times higher values of conductivity compared with entangled CNTs [69]. The CNT dispersion was demonstrated to be the most important parameter to control in order to obtain an optimal percolation threshold value. The critical factor determining the percolation threshold were reported to be: (i) aspect ratio of CNTs (ii) disentanglement of CNT agglomerates on the nanoscopic scale (iii) uniform distribution of individual CNTs of CNT agglomerated on microscopic scale [70, 71]. Many different parameters were studied in order to determine their influence on the percolation threshold. The influence of the carbon nanotube aspect ratio on the final electrical properties was studied [65]. Low aspect ratio and high aspect ratio CNTs were compared as a function of the percolation threshold (figure 2.25).

In case of CNTs having aspect ratio lower than 313, the percolation thresh-

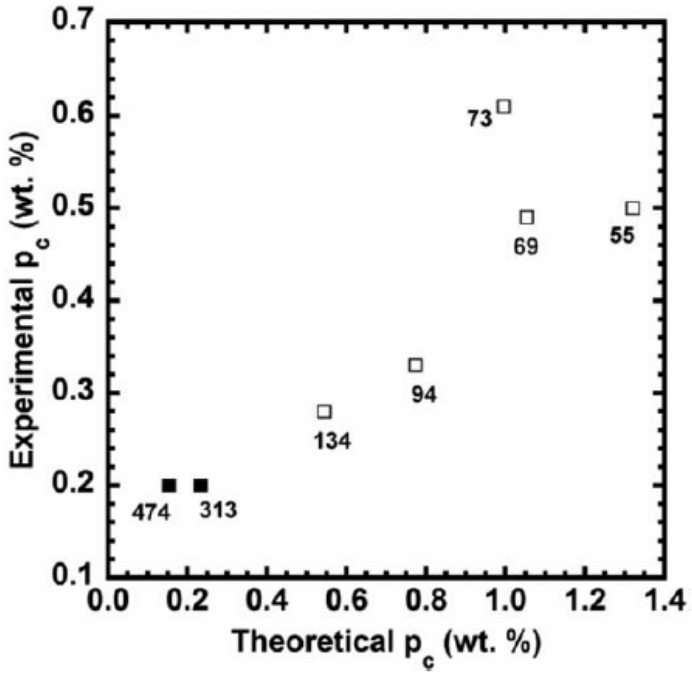


Figure 2.25: Comparison between experimental thresholds and theoretical threshold concentrations based on CNTs length prior to melt mixing. The numbers in the figure indicate the initial aspect ratio of the CNTs.[65].

old concentration increases with decreasing aspect ratio. This behavior can be explained by conductive network theory: the higher the aspect ratio, the lower concentration required to form a conducting network. However, for the aspect ratio equal to 313 and 474, the percolation threshold was not affected by this parameter. This behavior may be due to the fact that mixing process actually decrease the aspect ratio of long aspect ratio samples leading their average length to be nearly the same but nonetheless longer that the other samples analyzed [65].
In order to evaluate the effect of the dispersion process on the final percolation threshold different researches focused on studying the electrical properties of composites obtained with different dispersion method and condition [69, 70]. The variation of the percolation threshold after different stirring conditions is observed in figure 2.26.

Three different methods of sample preparation were studied: slow (50 rpm), medium (500 rpm), and fast (2000 rpm) stirring of a epoxy/MWNTs dispersion for 5 min at elevated temperature (80℃) prior to curing. Slow or medium stirring were observed to lead to percolation threshold at significantly lower filler concentrations. Fast stirring led to percolation near 0.1 wt%. Once the filler concentration approaches the percolation threshold, the effect of stirring and thereby the effect of particle movement vanishes and the three samples show the same value of conductivity. Also the effect of CNT alignment on percolation conductivity in SWNT/PMMA composites has been investigated [72]. Various

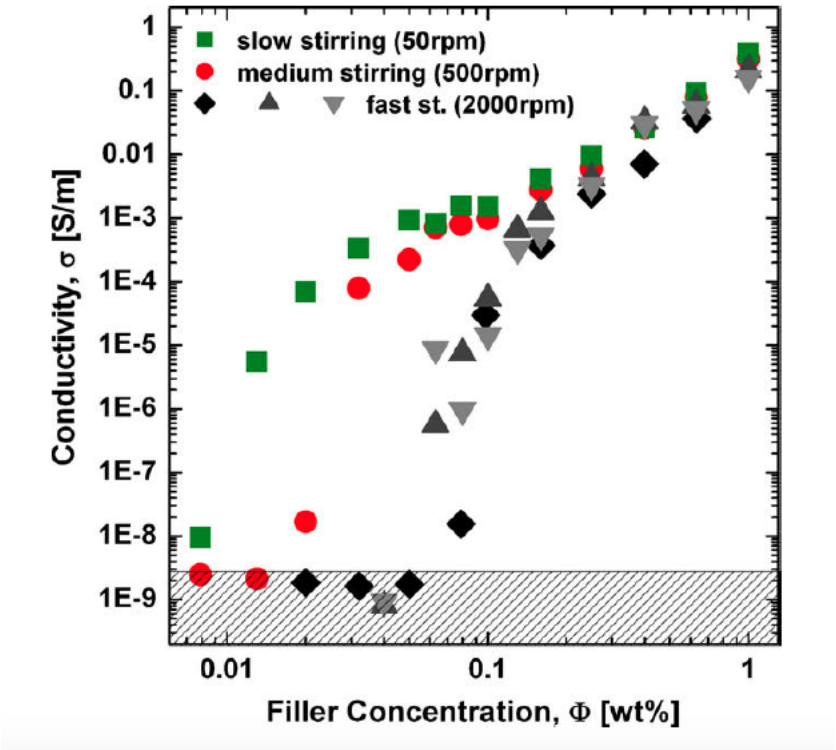


Figure 2.26: Comparative log-log plot of the nanocomposite (MWCNT/epoxy) conductivity as a function of the carbon nanotube weight fraction for three different sample preparation methods: slow (50 rpm), medium (500 rpm), and fast (2000 rpm) stirring of the dispersion for 5 minutes at elevated temperature (80 ℃) prior to curing.[69].

level of SWNT alignment were reached by melt fiber spinning. As a function of alignment the conductivity exhibits a power-law behavior. Conductivity was observed to increase in case of slightly aligned CNTs, rather than isotropic. A theoretical investigation also confirmed that minimum resistivity occurs for a partially aligned rather than a perfectly aligned CNTs film [73, 72].

Li *et Al.* [70] studied different processing methods in order to obtain 4 different levels of dispersion, as reported in Figure 2.27. All the dispersion methods used are reported in Figure 2.28.

Conditions A and B lead to large CNT agglomerates. In case of conditions C and D, these agglomerates were almost completely absent. For Condition C, entangled CNT bundles were not observed, the dispersion state was not as uniform as for Condition D. The electrical conductivity was studied in function of the different level of dispersion obtained by the different processing conditions. The results are summarized in Figure 2.29.

Sample prepared under condition A shows a quite high percolation threshold, 0.4 wt%, due to the large tightly entangled CNT agglomerates which hinder the formation of a conducting networks at low filler contents. The sample prepared by Condition B had the lowest percolation threshold, 0.1 wt%. This low value is due to the loosely entangled and uniformly distribution of CNT agglomerates in the matrix. Condition C presents a moderate percolation threshold value,

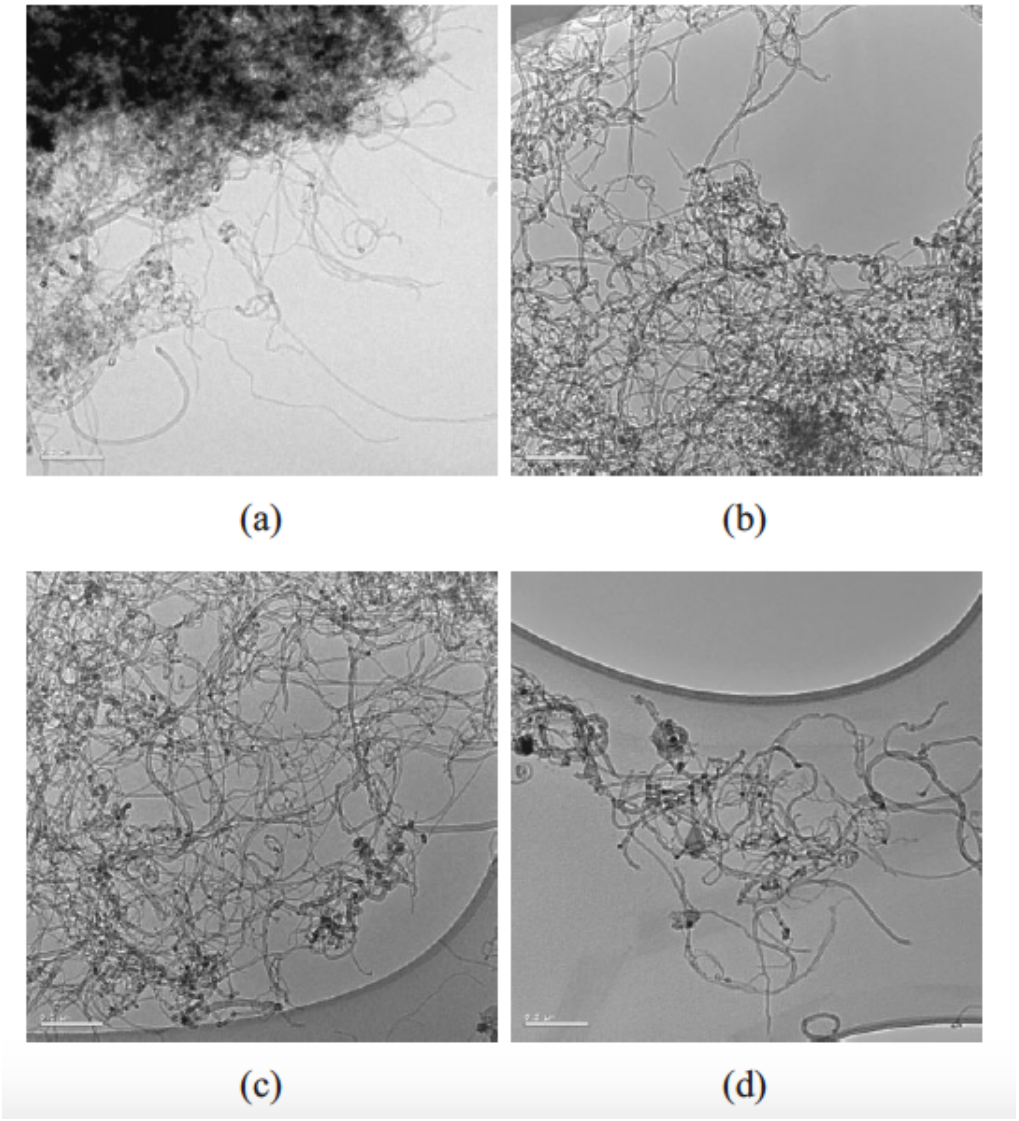


Figure 2.27: TEM images of CNT agglomerates dispersed according to conditions A,B,C,D (scale bar = 0.2 μm) [70].

around 0.25-0.30 wt%, explained by the not uniform microscopic distribution of CNTs. Although, CNTs from Condition D exhibited the best dispersion state at both the nano- and microscales, no apparent percolation threshold was observed. The insulating nature of the product is probably due to a severe damaging of the carbon nanotubes that were broken into very short particles during the process method, resulting in a large reduction in the CNT aspect ratio. This result suggests that when the CNT aspect ratio is too low, the formation of conduction networks requires a very high CNT content, no matter how the CNT dispersion state is.
Another important factor to be considered in order to evaluate the dispersion of the CNTs in the matrix is the mixing method and the processing conditions utilized for the nanocomposite production. For the production of polymer-MWNT

Condition	Dispersion method
A	As-received CNTs + epoxy Shear mixing for 30 min at 3000 rpm
B	CNTs dispersed by ultrasonication for 1 h in acetone + epoxy Ultrasonication for 2 h at 60 °C
C	UV/ O_3 treatment of CNT for 1 h and ultrasonication for 2 h in acetone + epoxy Shear mixing for 30 min at 3000 rpm
D	CNTs were ball milled for 2 h, ultrasonicated in toluene for 1 h, and UV/O_3 treated for 2 h, followed by silane treatment [13] + epoxy Ultrasonicated for 2 h at 60 °C

Figure 2.28: Processing methods (Conditions A, B, C, and D) used to disperse CNTs and the corresponding percolation thresholds [70].

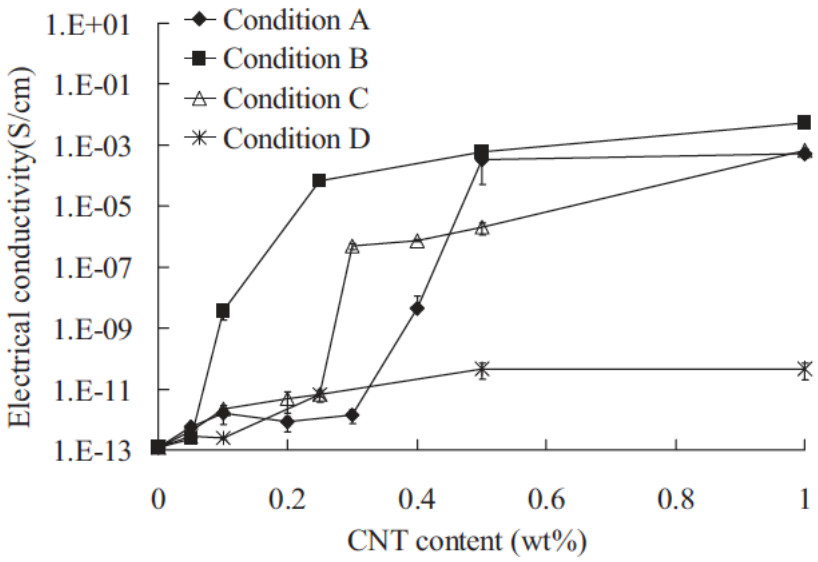


Figure 2.29: Electrical conductivity of nanocomposites as a function of CNT content.[70].

nanocomposites on industrial scale, melt processing represents an economically suitable method to produce large volumes of industrial and consumer products. For this reason, melt mixing process parameters have been widely investigated in order to optimize the dispersion of the CNTs in the matrix. One interest

parameter during the process is the shear forces applied during melt processing. Indeed, by changing shear force it is possible to influence the final properties by increasing the dispersion and distribution of the CNTs in the polymer matrix. Kasaliwal *et Al.* [74] focused on the electrical properties of PC/MWNTs samples produced by small-scale microcompounder under different mixing temperature and mixing speed at fixed mixing time. Volume resistivity was evaluated for composites produced at 260℃, 280℃ and 300℃, with speed varying from 50 rpm, 100 rpm and 200 rpm. The volume resistivity results are reported in figure 2.30.

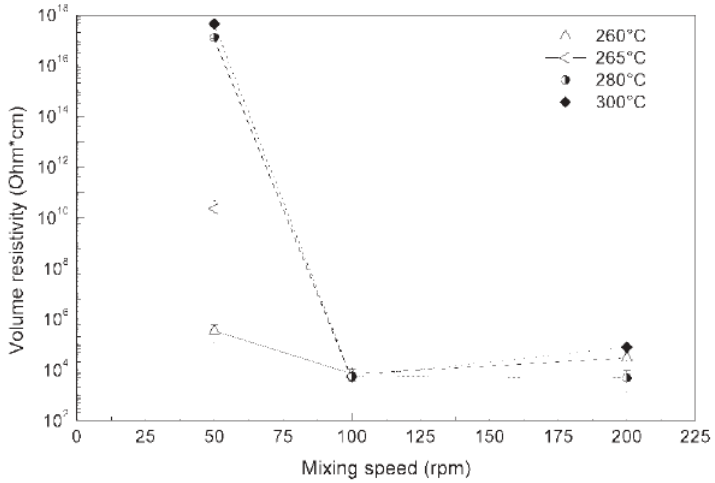


Figure 2.30: Volume resistivity versus mixing speed at different mixing temperatures of PC/MWNTs nanocomposite [74].

The difference in resistivity was found to change up to 14 orders of magnitude. The mixing energy was also evaluated in order to understand the influence of the shear force on the final dispersion and electrical properties (Figure 2.31). An increase in mixing speed and lowering of melt temperature result in higher torque values and thereby leads to increasing mixing energy.

Composites prepared at high mixing temperature and low mixing speed are electrically not percolating, showing resistivity values similar to neat PC. Processing the mixture at 265℃ and 50 rpm, the percolation threshold is reached and the samples are conductive. All the other samples are percolated and only small differences up to two decades are seen between different processing conditions. The results were explained by dissolution of primary agglomerates and variation of the dispersion of the CNTs in the matrix. Agglomerates not dispersed during the mixing procedure reduce the amount of individualized MWNT available for the network formation. The good level of dispersion in the matrix was explained by a combination of different step processes. During melt mixing, the molten polymer first wets all the available surface area of the MWNT agglomerates. Wetting quality depends on the interfacial energy between carbon nanotubes and the polymer melt. Good wetting is a prerequisite for polymer infiltration inside the primary agglomerates. MWNT agglomerated are broken due to the high shear force applied during compounding, creating new surface area, which

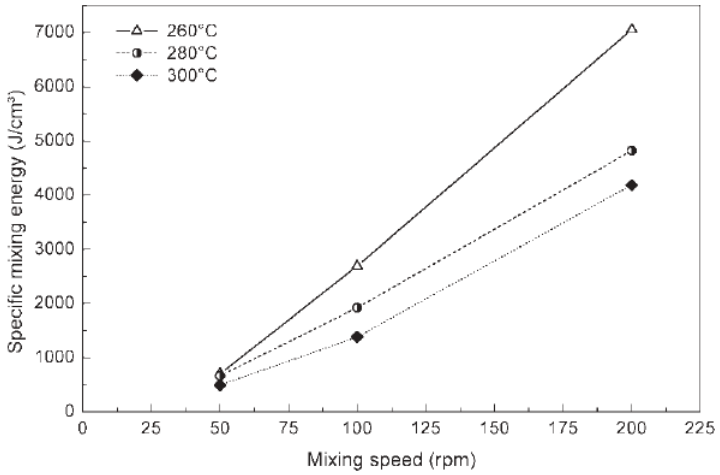


Figure 2.31: Specific mixing energy in dependence on mixing speed at different temperatures of PC/MWNTs nanocomposite. [74].

is again wetted by the polymer melt. In the mean time, MWNT aggregates start getting distributed in the polymer melt. Thus, depending on the shear forces acting on the aggregates, a certain minimum size can be achieved by shearing, and in parallel, the newly formed smaller aggregates get again infiltrated by the polymer chains. As a consequence, again smaller aggregated can be broken and clusters and individual MWNT can be obtained. The processes of wetting, infiltration, and erosion are strongly enhanced at lower polymer viscosity; therefore it is widely significant at high melt temperature and mixing speed. On the other hand, by having high melt viscosity combined with high shear rates, the shear stresses acting on agglomerates can be increased. In case of very high shear stress, also the possibility of carbon nanotube breakage has been considered. In this case, reducing the aspect ratio of the carbon nanotube the value of resistivity percolation would significantly increase. The level of macrodispersion in the matrix was evaluated by microscopic images. Figure 2.32 highlights that at high mixing temperatures (280℃ and 300℃) and low mixing speed (50 rpm), the shear stresses generated inside the compounder are too low to break the primary agglomerates efficiently and erosion is probably too weak to separate enough tubes for the formation of an electrical network.

As observed in Figure 2.32 a, b, at higher mixing temperature the dispersion is poor and the matrix is characterized by quite big MWNT aggregates, cluster, and only some individual MWNTs, resulting in very high electrical resistivity values.

To further investigate the real effect of the melt viscosity of the matrix, Socher *et Al.* [75] evaluated the level of dispersion and the relative percolation threshold for five different polymer matrices with different viscosities. Nanodispersion of MWNTs in the composites were evaluated by TEM characterization. The samples were prepared by twin screw microcompounder, from polyamide 12 (PA12), polibutylene terephtalate (PBT), polycarbonate PC, polyether ether ketone (PEEK), low density polyethylene (LDPE) matrices, with different vis-

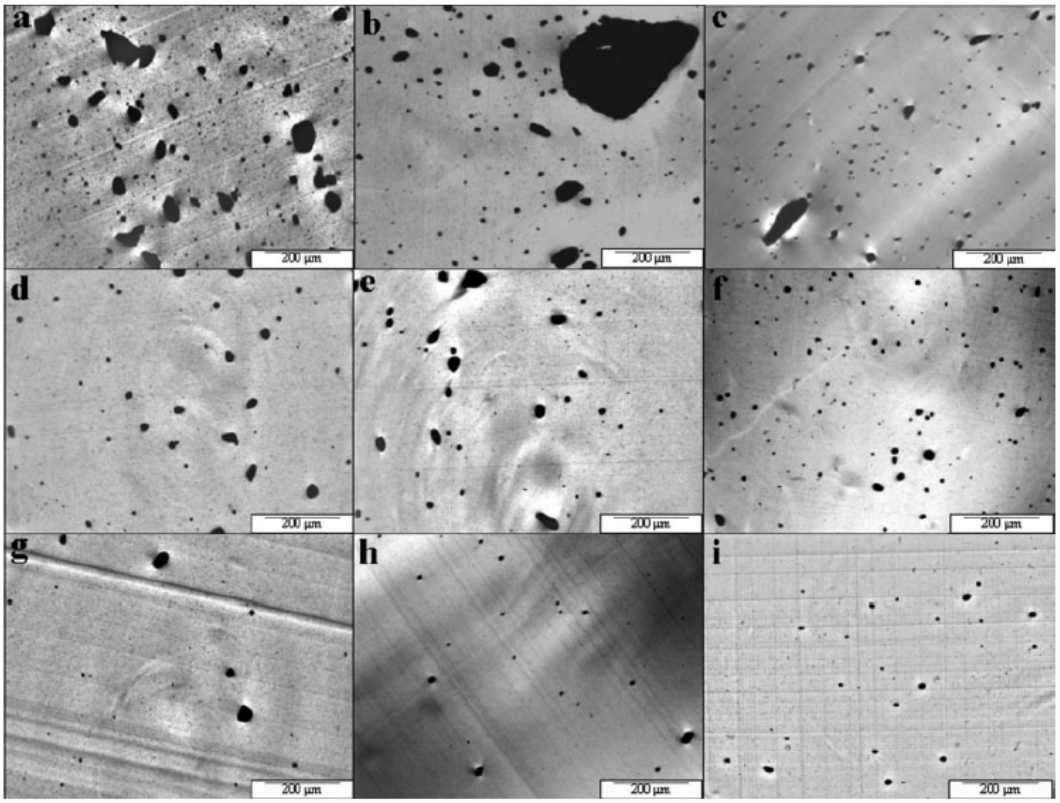


Figure 2.32: Optical micrographs showing dispersion of MWNT in polycarbonate at different mixing conditions: (a) 300℃,50 rpm; (b) 280℃, 50 rpm; (c) 260℃, 50 rpm; (d) 300℃, 100 rpm; (e) 280℃, 100 rpm; (f) 260℃, 100 rpm; (g) 300℃, 200 rpm; (h) 280℃, 200 rpm; and (i) 260℃, 200 rpm. [74].

cosities.

From TEM analyses shown in Figure 2.33, it is observed that a better level of dispersion is achieved in case of higher viscosity matrices. Nonetheless, the composites based on low viscosity matrices also show isolated CNTs between the observed primary and secondary agglomeration but in a lesser extent. A shortening in the nanotubes length was found in case of high viscosity samples, due to the increase of the shear stress, and a consequent increase of the value of the percolation threshold. This phenomenon was explained by a decreasing of the aspect ratio that could be significant for the final electrical properties.

2.2.3 Effect of CNTs morphology and agglomeration on rheological properties of polymer nanocomposites

The study of the rheological properties of CNTs/polymer nanocomposites is of great importance in order to obtain information concerning the effect of the nanocomposites processing, dynamics and microstructure. The rheological properties of CNT/polymer nanocomposites depend on many factors: the microstructure, as its network structure, CNT concentration, dispersion and orientation state, polymer molecular weight and the interfacial interaction between the poly-

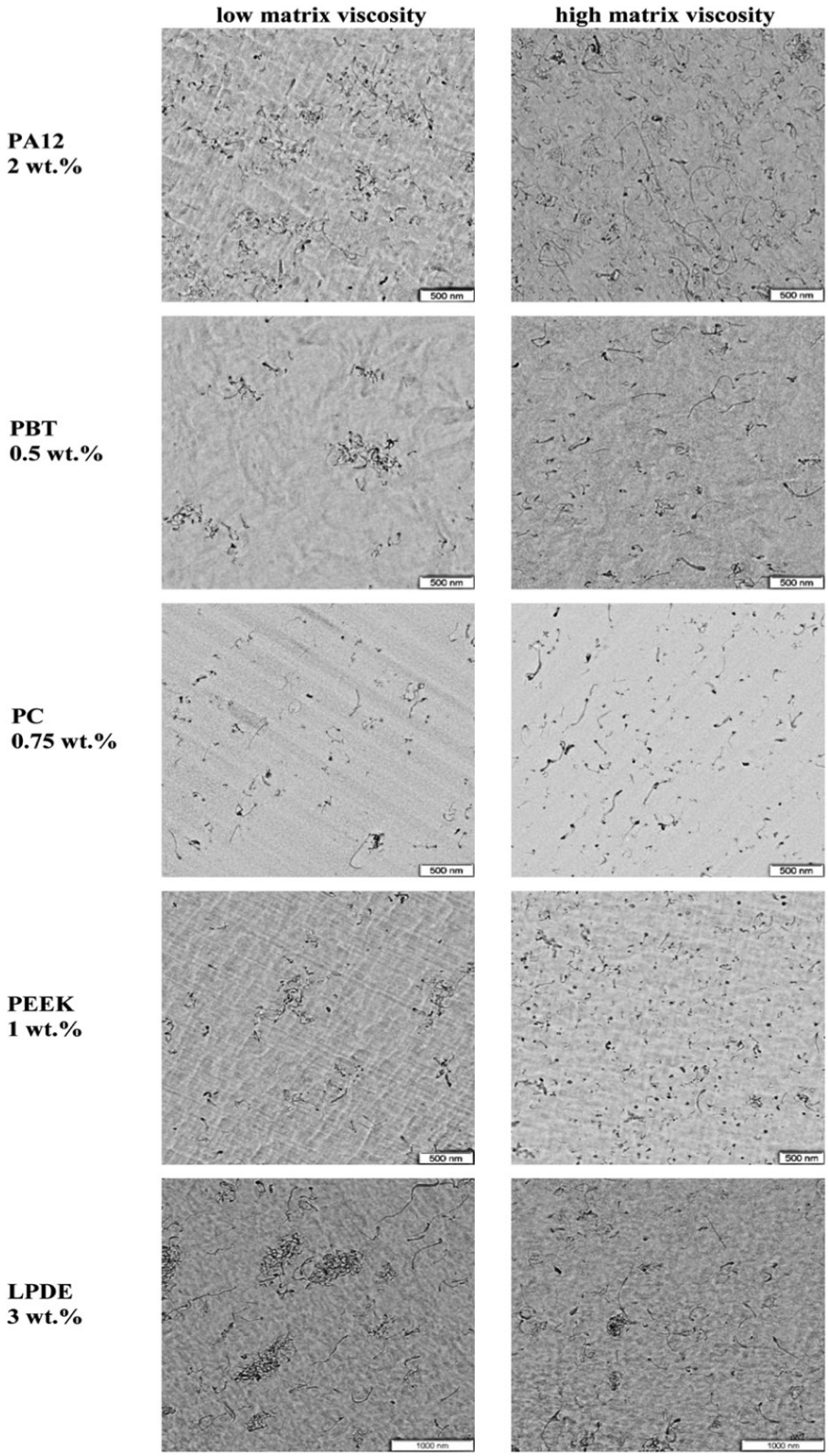


Figure 2.33: TEM images of composites based on different polymer types and matrix viscosity with Baytubes (MWCNT content as indicated in the figure). [75].

mer and filler. The variation of the viscosity and storage modulus of composites with the frequency and the temperature are used to characterize the rheological properties of CNT/polymer nanocomposites. Interconnected structures of anisometric fillers lead to qualitative changes in the spectra of dynamic moduli and viscosity [55, 68, 52, 76].
Both low frequency and high frequency behavior demonstrated to be of high importance in order to obtain information concerning the effect of the filler on the final properties. Low frequency behavior is affected by the structure of the composite and can be used to obtain information concerning the percolation state of the carbon nanotubes within the composite.
The rheological response of the sample is affected by the addition of carbon nanotube which generates an interconnected CNT-polymer structure in the matrix. Increasing the content of CNTs such interaction begin to dominate leading to the formation of a CNT-polymer network, corresponding to a liquid- to solid-like transition. Figure 2.34 shows a typical rheological response.

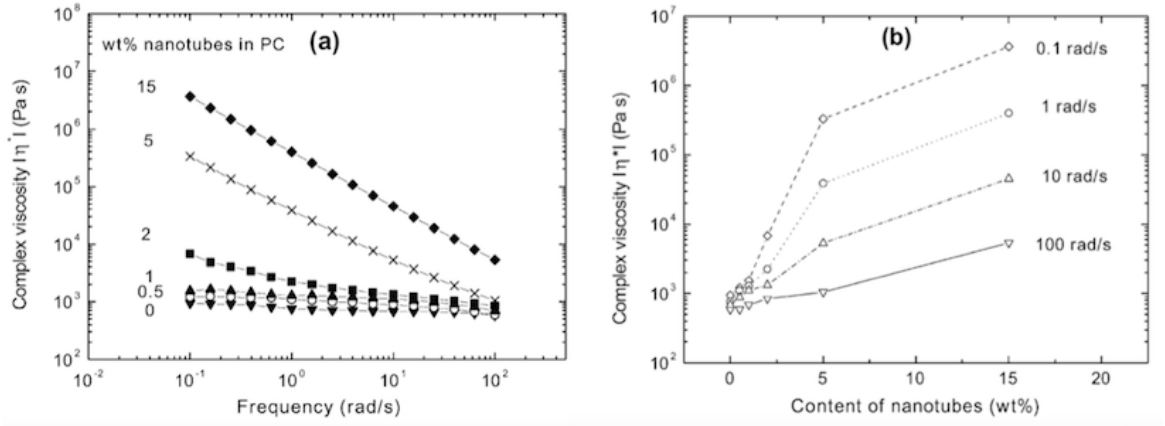


Figure 2.34: (a) Complex viscosity of nanotube filled polycarbonate at 260°C. (b) Complex viscosity versus CNTs content at different frequencies [68].

At low frequency the neat polymer is characterized by a typical Newtonian plateau due to fully relaxed polymer chain and a very small frequency dependence. The masterbatch, containing 15 wt% of MWNTs is orders of magnitude more viscous than neat polymer, even at high frequencies. At high content of CNTs, the material is characterized by a strong shear thinning effect. Increasing the content of CNTs, the low-frequency complex viscosity significantly increases, whereas the whole trend of complex viscosity drops with an increase of frequency at given CNT content, due to a shear thinning effect, as shown in figure 2.34A, indicating that the relaxation of polymer chains in the nanocomposites is effectively restrained by the presence of CNTs. Above 2 wt% CNTs, there is no Newtonian plateau within the frequencies studied and the viscosity curve has a much steeper slope at low frequencies. The rate at which the complex viscosity decreases at 5 wt% CNTs is almost the same as for 15 wt%, indicating that the viscosity curve is nearly linear over the viscosity range of frequencies shown. Figure 2.34B shows the complex viscosity versus CNT content at differ-

ent frequencies. At low frequencies the increase of viscosity is not linear with the content of CNTs. At low content of CNTs, from 1 wt% to 5 wt % , a sharp slope characterizes the viscosity in case of 0,1 and 1 rad/s, which is slower for composition ranging from 5 wt% to 15 wt%. This significant increase in complex viscosity at low CNT content is explained by the dramatic increase of storage modulus G', as shown in figure 2.35A. The corresponding increase in the loss modulus G" is much slower, as observed in figure 2.35B. The storage modulus G' that describes the elastic response was found to decreases with the alignment of CNTs. When CNTs are aligned in the polymer matrix, the probability of tube-tube contacts decreases, and the CNT network is less effective at impeding the polymer motion [52, 68, 77, 55]. Both moduli are shown to increase with frequency but the rate of increase become much slower with an increase of CNTs content indicating that the effect of carbon nanotubes is more significant at low frequencies than at high frequencies.

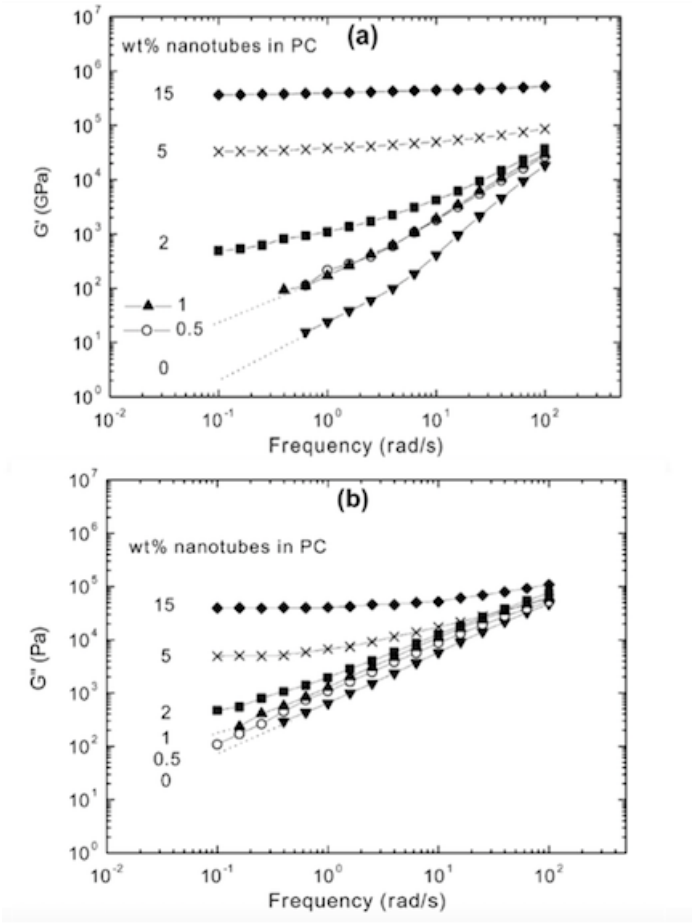


Figure 2.35: (A) Storage modulus G' of CNTs filled polycarbonate at 260°C. (B) Loss modulus G" of CNTs filed polycarbonate at 260°C[68].

Similar to the electrical percolation behavior, the rheology of CNTs/polymer nanocomposites also exhibit a transition from a rheology state to a solid like

behavior. The rheological state is referred to as the significant change of the viscosity or the storage modulus with the content of filler. The solid like behavior is observed when the viscosity or the storage modulus is insensitive or slightly sensitive to the increase of filler content. As it is observed in figure 2.35A above 5 wt% CNTs the material become almost independent from frequency [78, 55, 71, 68, 52].
The rheological behavior was explained by Potschke *et. Al* [52]. The low frequency plateau in G' is explained by assuming that the connection of polymer chains to the carbon nanotubes is much more stable than the entanglements of the polymer chains, i.e. its disentanglement time is larger than the characteristic time for polymer-polymer entanglements. At low content of carbon nanotubes, the main contribution to the mechanical properties is given by the polymer-polymer network and a flow zone is observed at low frequencies. Increasing the content of CNTs, the mechanical interaction between the nanotubes is mediated by polymer chains between the CNTs, forming a CNTs-polymer-CNTs structures. With increasing concentration of nanotubes, this nanotube-polymer-nanotube links lead to a rubber-elastic continuous network structure. The necessary concentration of fillers to form such a rubber-elastic active network is expected to be considerably lower than the geometrical percolation threshold for a CNTs-CNTs network (measured in the conductivity). Even at a low content of carbon nanotubes there may exist a continuous network of carbon nanotubes and polymer chains, but it would be weak, i.e. the plateau level of G' would be small. As the content of carbon nanotubes increases, the probability that a certain location along a CNT has a neighboring CNT increases dramatically, and much more polymer chains can contribute to the linkage of CNTs. This can be observed in low frequency measurement of high content nanocomposites. The level of G' of this rubber like plateau increases dramatically with increasing content of carbon nanotubes. At very high content of carbon nanotubes, the crosslink density of the combined carbon nanotube-polymer network is higher than that of the entangled polymer network, thus the contribution of the polymer-polymer entanglement network to the properties is hidden [52].
The rheological behavior is also dependent on temperature. Characteristic changes in the rheological behavior with increasing carbon nanotube content were found for temperatures well above the glass transition or melting temperature. The rheological response of nanocomposites is dominated by the networks formed by polymer chains and CNT-polymer interactions, and the mobility of these networks can be significantly enhanced by increasing the temperature. Figure 2.36 and 2.37 shows the variation of the storage modulus and the complex viscosity of a PC/MWNTs composites at two different temperatures, 170℃ and 280℃.

The increase of G' with the content of MWNTs is observed for all temperatures studied. However, the magnitude of enhancement and the shape of the G' vs ω curves are significantly different. At 170℃, G' changes over about 2 decades by adding 15 wt% MWNT, whereas at 280℃, G' changes over nearly 5 decades by adding 15 wt% MWNT. Moreover, at 170℃ no significant changes in the frequency dependence of the moduli and complex viscosity at low frequency can be detected up to 4 wt% MWNT. Starting from 5 wt% MWNT, the curves are characterized by a plateau at low frequencies in G' and a pronounced shear thin-

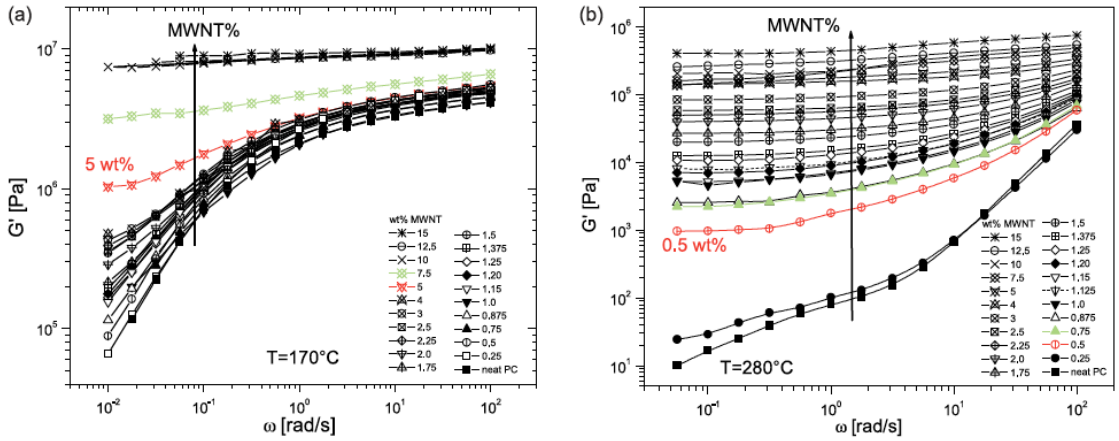


Figure 2.36: Frequency dependence of the shear storage modulus G' at 170°C(a) and 280°C(b) [52].

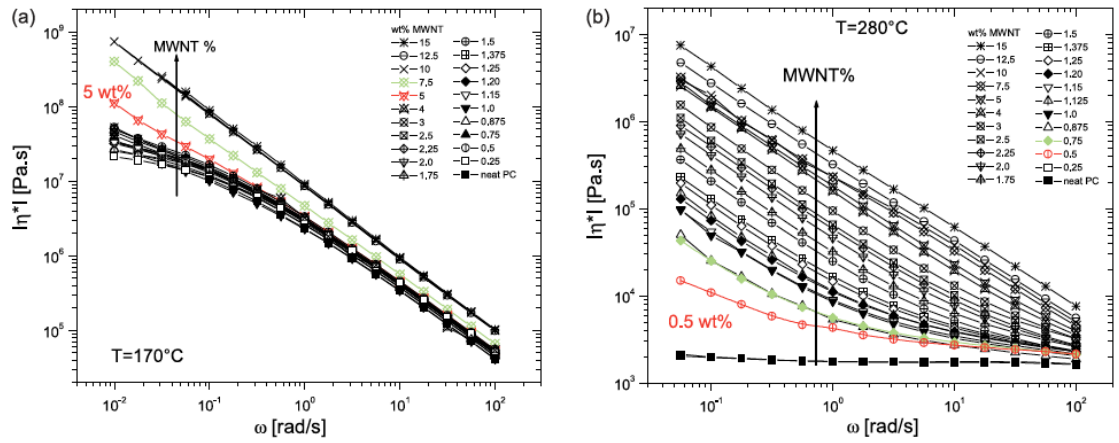


Figure 2.37: Frequency dependence of complex viscosity at 170°C (a) and 280°C(b) [52].

ning behavior is noticeable in complex viscosity. The transition from a liquid-like behavior to a solid-like behavior occurs at 5wt% MWNT at 170°C and at 0,5 wt% MWNT at 280°C, demonstrating its strongly temperature dependence [52].
To investigate the effect of temperature in more details, the rheological percolation thresholds of the nanocomposites were studied versus the measurement temperature. Figure 2.38 highlights the dependency of the percolation threshold with the temperature, decreasing considerably as the temperature rises. Once the measured temperature is high enough, the percolation threshold tends to reach a plateau [78].

The necessary content of CNTs to reach the rheological percolation threshold is smaller compared to the one needed for electrical percolation, which cannot be changed by increasing the temperature. Electrical percolation threshold requires contacts of CNTs to form solid conducting network, thus it is only slightly sensitive to the temperature effect. On the contrary, the rheological response

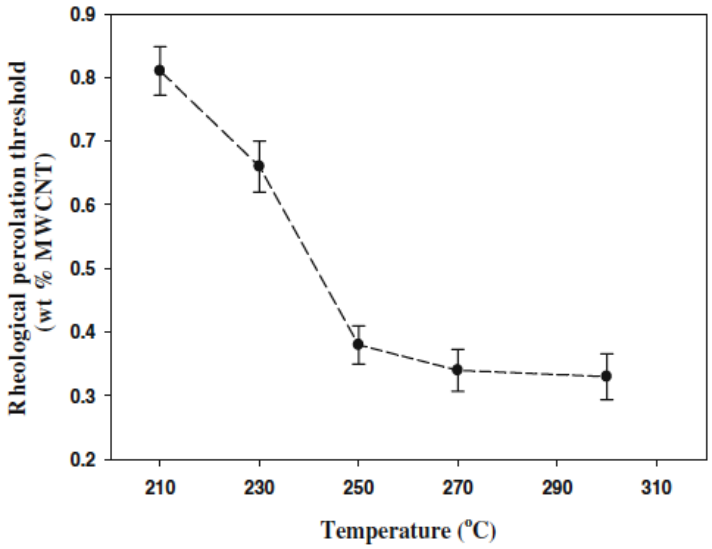


Figure 2.38: Effect of temperature on the rheological percolation threshold of polycarbonate/MWCNT nanocomposites [78].

significantly depends on the superposition of the entangled polymer network and the combined nanotubes-polymer network rather than the CNT network. Thus it depends on the mobility of the polymer chain, determining the temperature dependency of the rheological properties [55, 52].

Fan *et Al.* [76] investigated the effect of the degree of dispersion and of the aspect ratio on the final rheological properties. To evaluate the importance of the dispersion effect in a MWNT suspension, the storage and loss modulus behavior of two suspensions were compared. In suspension A, a magnetic stirrer method was used to mix the CNT. In Suspension B, ultrasonic agitation method was used to separate the CNT aggregates. Both the mixture contained the MWNTs from the same batch with high aspect ratios. The only difference between suspension A and suspension B was their dispersion quality: Suspension A had large aggregates or nonuniform dispersion; while Suspension B had uniform MWNTs dispersed aggregates of dimensions around 1-3 μm and some separated MWNTs. Figure 2.39 shows the frequency sweep of 0,5wt% MWNT/epoxy suspension A and suspension B. It can be observed that better MWNT dispersion did increase both the storage modulus G' and the loss modulus G". Noteworthy, the storage modulus of suspension B was over two orders of magnitude higher than that of suspension A at low frequencies.

Moreover, a rubbery plateau in the storage modulus G' appears at low frequency in case of suspension B. This means that suspension B behaved similar to a solid as compared to Suspension A and suggests the presence of an interconnecting MWNT network in Suspension B. This result is consistent with expectations, considering that the MWNTs in suspension B are more separated and have higher probability of getting entangled with each other, increasing the elastic component. Other interesting results were found studying the variation of the rheological properties with the aspect ratio. Indeed, it was expected that

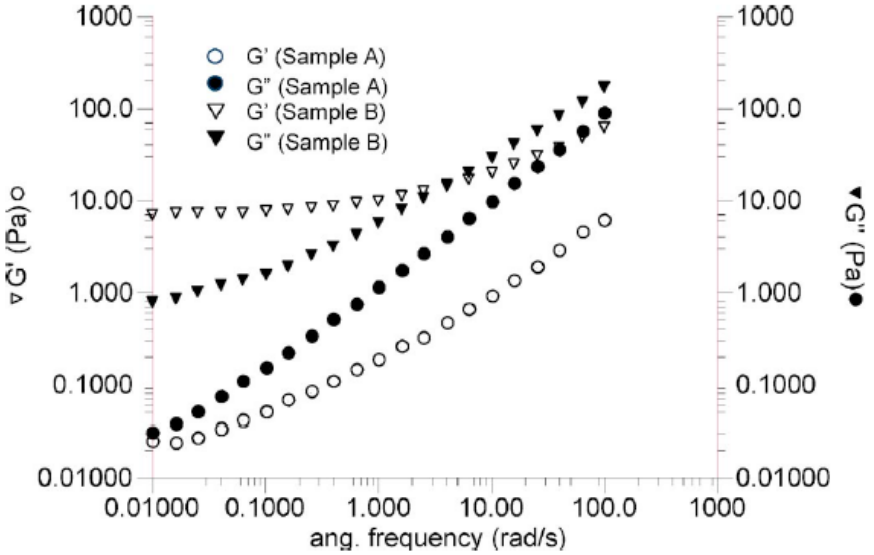


Figure 2.39: Suspensions A and B contain 0.5 wt% MWNT in epoxy. The better dispersed suspension B exhibited higher dynamic and loss modulus, especially at low frequencies [76].

longer and separated carbon nanotubes have a higher probability of interconnecting with each other and forming a more solid-like entangled network. The authors carried out some experiments on two other suspensions, suspension B and C, both samples were characterized by good dispersion. In Suspension B, MWNTs had an average aspect ratio of about 500, while in Suspension C CNTs were much shorter with an average aspect ratio of the order of 25-50. Figure 2.40 shows the frequency sweep of 0.5wt% MWNT/epoxy Suspensions B and C.

Suspension B, characterized by higher aspect ratio, exhibits higher values of storage modulus G' and loss modulus G", up to two orders of magnitude as compared to Suspension C. Indeed, larger aspect ratio samples forms an interconnecting network which increases the modules. Steady shear viscosity η for the 0,5wt% MWNT/epoxy Suspensions A-C was also analyzed, as shown in figure 2.41.

Again, well dispersed MWNT Suspension B with the high aspect ratio CNTs had the highest η values, and suspension A had the lowest values although MWNTs in Suspension A were much longer than the ones in Suspension C. Thus the quality of dispersion has a more significant effect than the aspect ratio on the viscosity of a MWNT suspension.

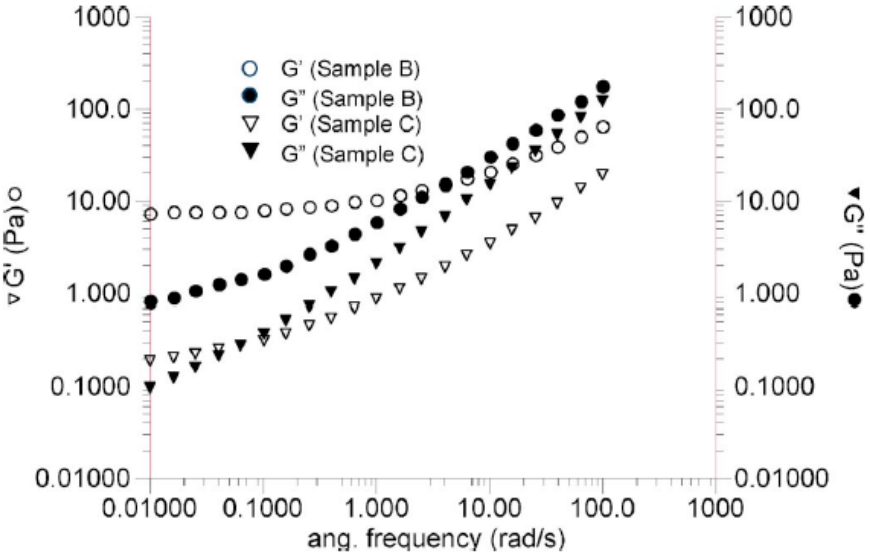


Figure 2.40: Suspensions B and C contain 0.5 wt% MWNT in epoxy. The higher the aspect ratio of MWNT in the suspension Suspension B, the higher is the dynamic modulus.[76].

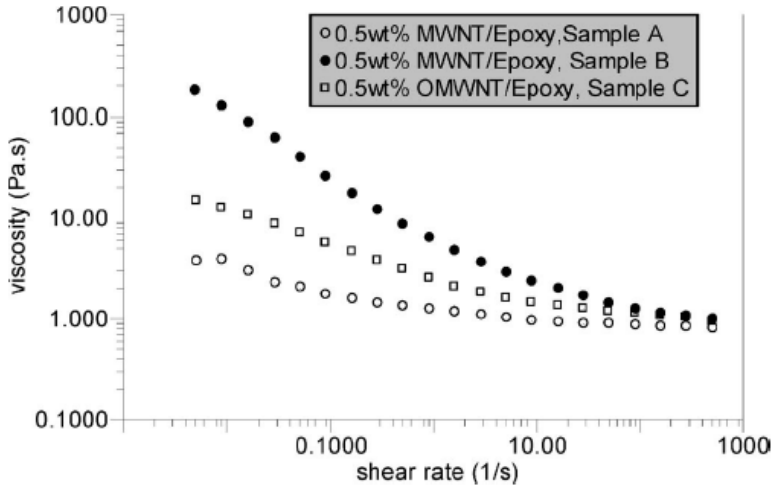


Figure 2.41: Steady shear viscosity μ of 0.5 wt% MWNT/epoxy suspensions (Suspensions A, B, and C) [76].

Chapter 3

Experimental process and method

This chapter aims to explain the experimental processes and methods used for the work on this master thesis. The mode of operation of the main tools used to prepare and characterize the samples, together with procedures used, will be explained in the following paragraphs.

3.1 CNT synthesis method: Catalytic chemical vapor deposition

The synthesis method used during the experiment is catalytic chemical vapor deposition (CVD). CVD method involves the decomposition of a gaseous or volatile compound of carbon, catalyzed by metallic nanoparticles, which also serve as nucleation sites for the initiation of carbon-nanotube growth. This method, which can be easily scaled up to industrial levels, has become the most important commercial method for CNT production. Both MWNT and SWNT synthesis have been well developed using CVD . The catalyst material may be solid, liquid, or gas and can be placed inside the furnace or fed in continuously from outside. Decomposed carbon species dissolve in the metal nanoparticles but, due to a finite solubility of carbon in the metallic particles, supersaturation will be reached followed by carbon precipitation out in the form of a fullerene dome extending into a carbon cylinder. Typical temperature range for the synthesis is 500-1,200 °C at atmospheric pressure [79, 9]. The CVD system used at the Research and Development laboratory at Nanocyl S.A. to produce carbon nanotubes is schematized in Figure 3.1.

The system consists of a horizontally positioned reaction tube, where a boat carrying the catalyst powder is inserted. The catalyst is homogeneously distributed along the boat, and the quantity of catalyst typically used is 1,9 g. The boat is inserted in the cold zone of the reactor (Figure 3.1 on the right), which is then sealed. In order to reach a inert atmosphere inside the reactor a flux of nitrogen (N_2) is first of all flown for some minutes, followed by a flux of nitrogen, hydrogen and ethylene. The mix typically contain about 70% of ethylene, 25% of hydrogen and 5% of nitrogen. After several minutes, when the composition inside the reactor is homogeneous, the boat containing the catalyst is pushed in the hot zone, previously heated up at 700°C. After 20 minutes the flux of ethylene is stopped in order to end the reaction, and the boat is moved from the hot zone to the cold zone. When the product cool down at room temperature the boat can be removed and the CNTs can be collected. Based on the weight of the product collected, the yield of reaction μ and the carbon purity (%C) is calculated as:

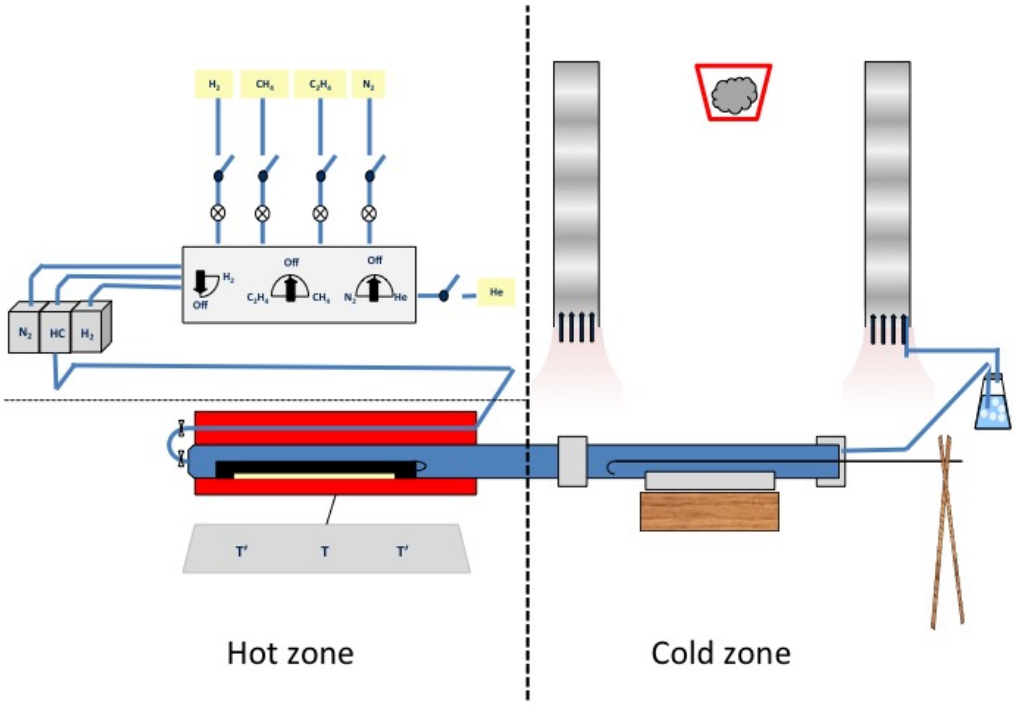


Figure 3.1: Schema of the CVD apparatus used for the synthesis of MWCNTs at Nanocyl S.A..

$$\mu = \frac{M_{NTs} - (M_{cat} \cdot 0,89)}{(M_{cat} \cdot 0,89)} \cdot 100 \tag{3.1}$$

and

$$\%C = \frac{M_{NTs} - (M_{cat} \cdot 0,89)}{M_{NTs} \cdot 100} \tag{3.2}$$

The value 0,89 is a value experimentally determined at Nanocyl S.A.. 0,11% is evaluated as the loss of mass of the catalyst that occurs during the reaction, due to an excess of water present in the catalyst. Thus, $M_{cat} \cdot 0,89$ represents the real mass of the catalyst during the synthesis process. The standard product produced at Nanocyl S.A. with the aforementioned conditions is commercialized as NC7000. Table 3.1 reports some of the specifications of the standard product.

Property	Value
Average diameter	9,0 nm
Average length	1,5 μm
Density	70-80 g/L
Carbon purity	90%
Surface area	250-300 m^2/g
Volume resistivity	$10^{-4} ohm \cdot cm$

Table 3.1: Specifications of the standard product NC7000 produced at Nanocyl S.A..

3.2 Nanocomposite processing method

The nanocomposites were produced by two different processing methods. On a small scale, using a double screw mixing (DSM) microcompounder and mini injector device and on a large scale, using a semi-industrial double twin screw extruder machine and a injection molding.

3.2.1 DSM twin screw microcompounder

A twin-screw DSM Xplore microcompounder, a small-scale laboratory compounder with a volume of 15 cm^3, was used to melt-mix the nanocomposites. It is a conical, co-rotating twin-screw microcompounder where different processing parameters, such as mixing temperature and mixing speed, can be controlled and torque values can be monitored [80]. Figure 3.2 illustrates the machine used during the experiments.



Figure 3.2: Images of twin-screw DSM Xplore microcompounder used for the compounding of the CNTs with PC and HDPE [80].

PC was predried for 4 hours at 120℃ and it was then manually mixed with the CNTs before the injection. 8 grams of mixture were inserted in the chamber at 280℃ with a speed rate of 50 rpm for 5 minutes. The process condition used were previously optimized at Nanocyl S.A..
In case of HDPE nanocomposites, HDPE was predried at 80℃ for 1 hour and then mixed with the CNTs before injection. 12 grams of mixtures were then processed at 200℃ with a speed rate of 150 rpm for 4 minutes in the microcompounder.
After the mixtures were homogenized, the melted nanocomposites were collected in the injection gun of the DSM Xplore micro injection molding machines (Figure 3.3) and injected in a specific mold for electrical measurement [81].



Figure 3.3: Images of twin-screw DSM Xplore microcompounder used for the compounding of the CNTs with PC and HDPE [81].

The only mold used during DSM experiments was the one used for obtaining specimen for electrical measurement. The mold was preheated at a specific temperature, different for each polymeric matrix used. 100℃ was used for mixture with PC and 60℃ in the case of HDPE. This mold could produce two specimens per injection, which are not enough to obtain an enough accurate average of the resistivity of the sample. Thus, two experiments for each of the mixture were done in order to obtain four specimens to be measured. Between two experiments with different concentration of MWNTs and/or different MWNTs sample, the micro compounding chamber was purged with the new mixture. All the specimens were then let in a desiccator for 24 hours before measuring.

3.2.2 Twin screw extruder and injection molding

Nanocomposites were also produced by semi-industrial twin screw extruder, to test properties of CNTs in PC and HDPE produced in a larger scale. HDPE was dried for one hour at 80℃, while PC was dried for four hours at 120℃ before being used. CNTs and the matrices were mixed in a twin screw extruder model ZSE27MX from LEISTRITZ. About three kilograms of product were mixed. In case of HDPE matrix, the process occurs under a screw speed rate of 300 rpm and the ramp of temperature along the screw increased from 190℃, where the material is added, to 220℃ at the end of the double screw. In case of mixing with PC, the ramp of temperature vary from 260℃ to 290℃, with a screw speed of 260 rpm. The screws diameter are 27 mm. The mixture is then pelletized as shown in Figure 3.4, in order to be used for injection molding.

Once the carbon nanotubes and the polymer matrix were mixed, the pellets were let dry for 1 hour at 80℃ in case of HDPE nanocomposites and for 4 hours at 120℃ in case of PC nanocomposites before being used for injection molding. Injection molding samples were done using a model Victory 80 from ENGEL



Figure 3.4: Pellets of HDPE/CNTs obtained after mixing and pelletizing with twin screw extruder[82].

(Figure 3.5).



Figure 3.5: Images of the injection molding machine used for realization of samples used for characterization [83].

For HDPE nanocomposites, the gradient of temperature along the feeding screw was 285℃ to 275℃ along the screw. The injection speed used was $10cm^3/s$. For PC nanocomposites, the gradient of temperature along the feeding screw was 300℃ to 290℃ along the screw. The injection speed used was $30cm^3/s$. For each sample, 30 specimens of dimensions according with the norm ASTM638 were produced. The specimens produced with HDPE were then used for electrical, tensile and impact tests. The specimens produced with PC were used only for electrical tests.

3.3 Characterization methods

Many different characterization methods have been used during the work of this master thesis, both to characterize the properties of the carbon nanotubes and then to study the properties of the nanocomposites produced. In the following paragraphs, the tools used to characterized the materials studied are described, together with the procedure followed.

3.3.1 Scanning electron microscopy

The scanning electron microscope (SEM) uses a focused beam of high-energy electrons to generate a variety of signals at the surface of solid specimens. The signals that derive from electron-sample interactions reveal information about the sample including external morphology (texture), chemical composition, and crystalline structure. SEM is a good choice to study the level of dispersion and the dimensions of the bundles of carbon nanotubes. The images taken during the work for this Master thesis were done using the SEM JSM-6010LV from JEOL (Figure 3.6B), in a low vacuum mode at 20Kv. The principle of SEM is shown in Figure 3.6A. An electron gun at the top of the chamber emits a beam of electrons, which passes through a series of magnetic lenses that condense the beam into an extremely fine focus. As the electron beam sweeps the surface, it excites electrons present, causing some of them to escape from the surface. These escaping electrons, known as deflected secondary electrons, have specific energies that can be measured. As they are released from each area of the sample, they are collected and counted by a detector that sends their amplified signals. The various electronic energies produced are analyzed by computer software, and the resulting image is displayed on a computer monitor [84, 85].

3.3.2 Transmission electron microscopy

The transmission electron microscope (TEM) is another very powerful tool for material science. A high energy beam of electrons is shone through a very thin sample, and the interactions between the electrons and the atoms can be used to observe features such as the structure of the materials at the nanoscopic scale. In the frame of this master thesis, TEM was a fundamental characterization tools to study the diameters of single CNTs in the different samples. To characterize the samples used during this work, TEM images were taken with a TEM TECNAI 10 with 80KV (Figure 3.7B). A schematic representation of a TEM is illustrated in Figure 3.7A. A source at the top of the microscope emits the electrons that travel through vacuum in the column of the microscope. TEM uses electromagnetic lenses to focus the electrons into a very thin beam. The beam strikes the specimen and parts of it are transmitted depending upon the thickness and nature of the specimen. This transmitted portion is focused by the objective lens into an image on phosphor screen or charge coupled device (CCD) camera. The darker areas of the image represent those areas of the sample that fewer electrons are transmitted through while the lighter areas of the image represent those areas of the sample that more electrons were transmitted through.

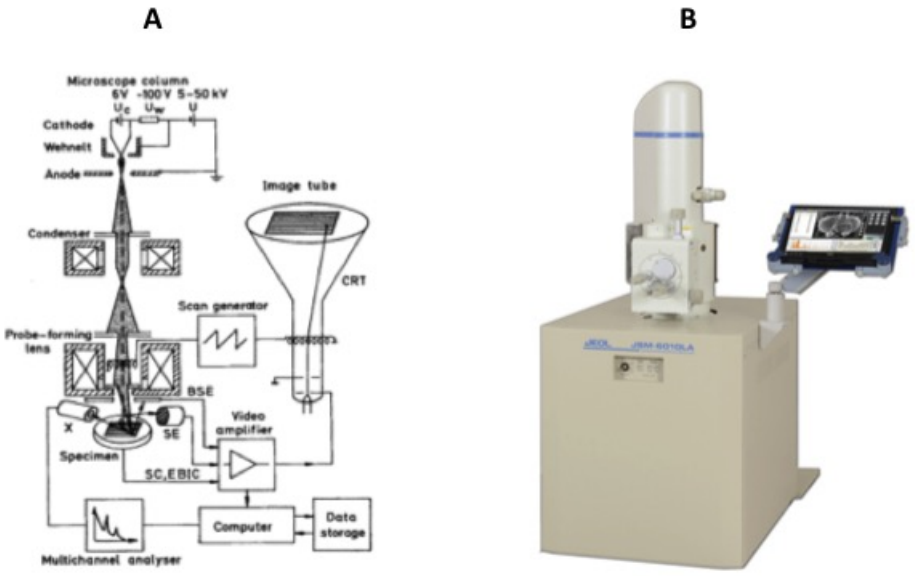


Figure 3.6: (A)Principle of the scanning electron microscope [84] (B) SEM microscope used during the work for this master thesis [85].

3.3.3 Electrical measurements

In the frame of the characterization of the nanocomposites produced, the measurement of the electrical resistivity was fundamental in order to study the electrical properties of the samples. The electrical measurement in this master thesis were done using a KEITHLEY 2700 multimeter. The tool is used to measure the electrical resistivity up to $10^7 ohm$. The electrical resistivity measurements were taken in accordance to astmD4496-87 standard. Electrical measurements were done both on the specimens produced by DSM and by injection molding. In the first case, bars 1 cm width, 0,4 cm thick and 8 cm long were injected. In case of injection molding, the bars used for electrical measurement were the same one produced for the tensile test under the norm ASTM638, and the larger extremity were successively cut. The final dimension of the bar were then 1 cm width, 0,4 cm thick and length of around 7/8 cm. The preparation of the sample and the measurement were done 24 hours after injection. In order to measure the volumetric resistivity, the extremity of the specimens to be measured were cut. Silver paint was applied on the cut extremities and then let dry for one hour.
In order to measure the surface resistivity, 1 cm of tape was put in the middle of the specimen and then silver paint was applied on the specimen, close to the

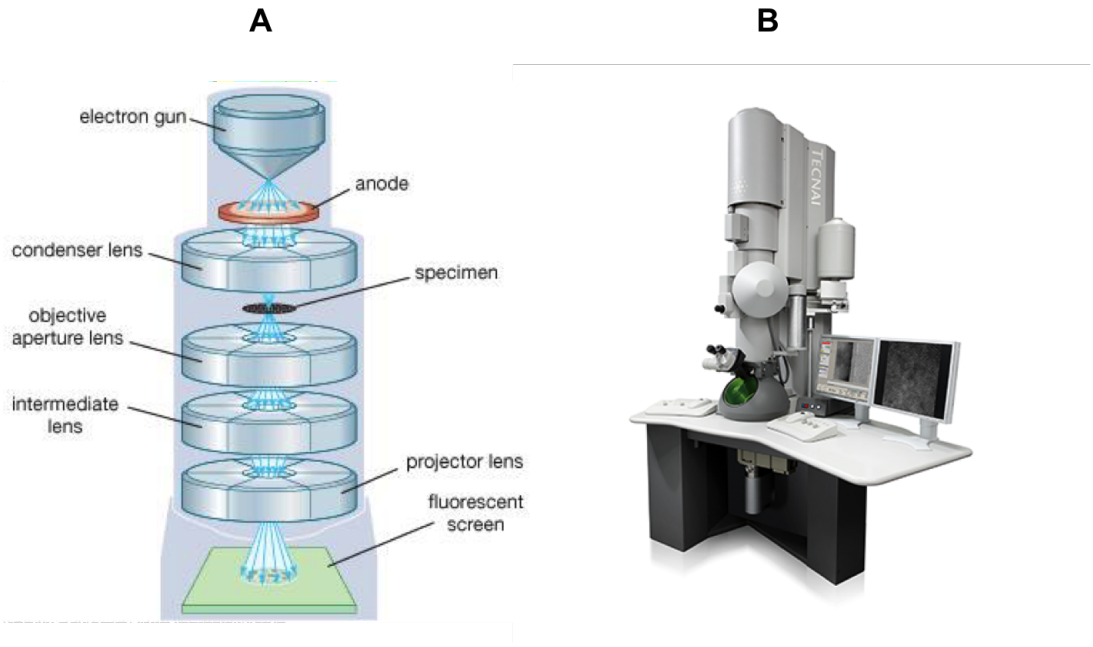


Figure 3.7: (A)Principle of the transmission electron microscope [86] (B) TEM microscope used during the work for this master thesis [87].

two edge of the tape. Once the tape was removed, the paste was let dry for one hour. Figure 3.8 schematically shows a bar ready to be measured.

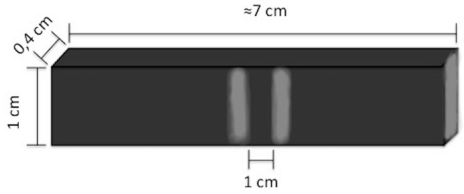


Figure 3.8: Schema of the preparation of the injected bar in order to take the electrical resistivity measurements.

After precisely measuring the dimension of the bars, the resistivity measurements were taken. The volumetric resistivity (VR) was calculated as (3.3):

$$VR = \frac{R \cdot S}{d} \tag{3.3}$$

where R = resistivity measured by the multimeter, S = the surface perpendicular to the electrodes, d = distance between the electrodes.
In order to measure the surface resistivity (SR), the following equation was used (3.4):

$$SR = \frac{R \cdot l}{d} \tag{3.4}$$

where R = resistivity measured by the multimeter, l = is the length of the line of silver paste, which correspond to the with of the bar, d = distance between the electrodes.

Both VR and SR were measured on all the samples injected, but most of the time the measurement of SR resulted to be wide and sometime not relevant, due to skin effect. Thus, in the following paragraph, only the measurement of VR will be considered to study the electrical resistivity of the samples. The main aim of measuring the electrical resistivity was to define the percolation curve of all the samples, and being able to identify the critical concentration of CNTs needed for the materials to become conductive. This concentration were shown to be highly dependent on the type of carbon nanotube as well as on the type of matrix used and the sate of dispersion. The content of CNTs needed to reach the percolation threshold is indeed significantly controlled by the affinity and interface interaction between the CNTs and the polymer used as matrix, together with the processing conditions used during the mixing. All the processing conditions used in the experiments have been previously optimized at Nanocyl S.A.. Figure 3.9 show the differences of the percolation threshold for the same CNT sample in the case of two different matrix, PC and HDPE.

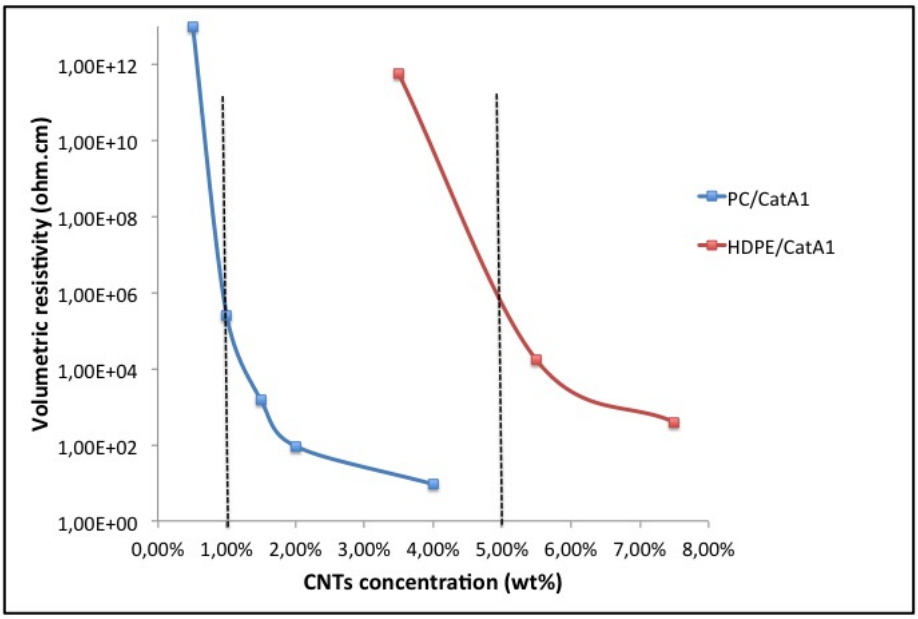


Figure 3.9: Comparison between the percolation threshold of two nanocomposites produced with PC matrix (blue) and HDPE matrix (Red) and CNTs.

From the graphs it is clear that the content of CNTs needed for a defined properties widely changes. Nanocomposites obtained by mixing CNTs with PC are already conductive with a filler content of 1wt%. In case where HDPE is used as matrix, more than 5wt% is needed to reach the percolation threshold. For this reason, in order to study the percolation curves of the two nanocomposite,

in case of PC matrix the concentration studied were ranging from 0,5% to 4% while in the case of HDPE the concentration studied varied from 3,5% to 7,5%.

3.4 Mechanical measurements

Mechanical tests were carried out on the barrels produced by injection molding. In order to have a more complete mechanical characterization of the samples, both tensile test and impact test were done. All the specimens were produced in accordance to the ASTM638 norm. The measurements were taken 48 hours after the injection. During these 48 hours, the specimens were left in the same room than the tensile test bench and the pendulum impact tester, were a constant temperature of 25°C is kept. The tensile test bench used was a model H10KT from TINIUS OLSEN equipped with an extensometer model 100S. The measurement were taken with a preload of 5kN and a speed of traction equal to 1 mm/min for the first 1% of elongation and 10mm/min after. 5 specimens for each sample were measured. The modulus was measured from the extensometer as the slope for the curve in the section between 0,05% and 0,25% of elongation. As shown in Figure 3.10, the value of the stress and strain at breakage were extremely different from one sample from the other. Thus, in the following paragraphs, only the stress and strain at yield were considered, since the properties at breakage had a too wide standard deviation, being not any more significant.

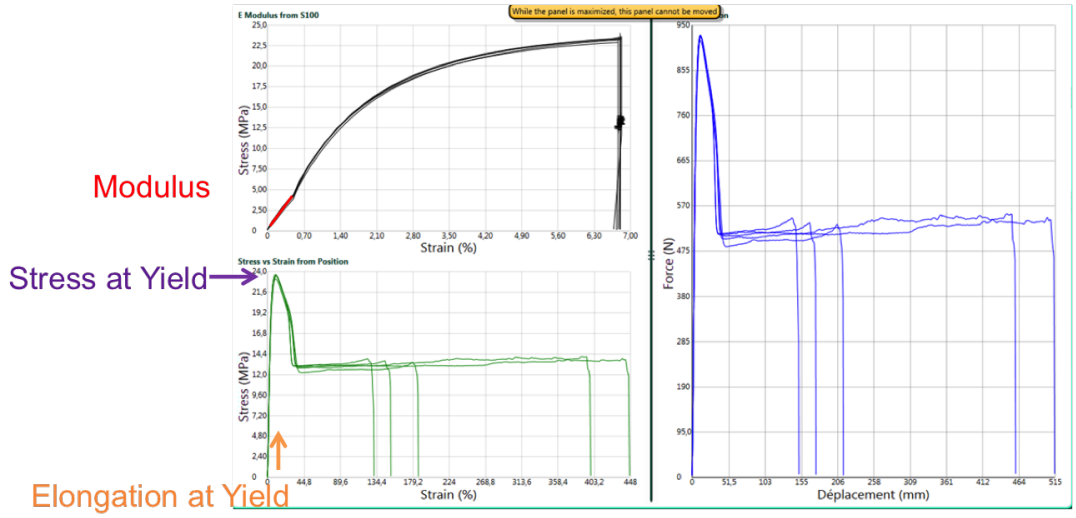


Figure 3.10: Output graphs obtained from the mechanical tests. The variation of the value at break did not allow to obtain a significant value.

In case of impact test, the same specimens used for the traction test were used, but the extremities were cut in order to obtain a bar of 8 cm long. The impact tester used was a model IT 503 from TINIUS OLSEN. The Izod testing operation procedure was followed, using a specimen of dimensions according with the ISO 180 norm. In Figure 3.11 the specifications of the specimen used are reported. For each sample, 10 specimens were measured.

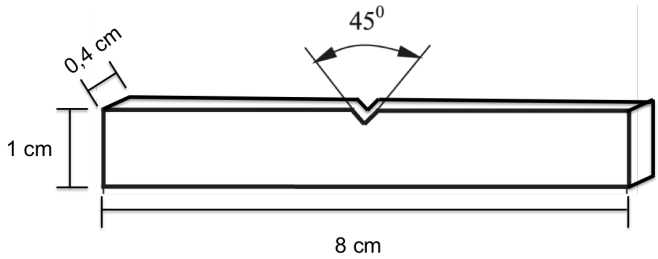


Figure 3.11: Dimension of the samples used for impact test, according to the ISO 180 norm.

3.4.1 Rheological measurements

Rheology is the study of flow and deformation of materials at specific temperature and frequency. Deformation and flow are referred to as strain or strain rate, respectively, and indicate the distance over which a body moves under the influence of an external force, or stress. A rheometer is a precision instrument that contains the material of interest in a geometric configuration, controls the environment around it, and applies and measures wide ranges of stress, strain, and strain rate. A rheometer is an interesting instrument to study the microsctructure of CNTs/polymer composite, as for example its network structure, as well as the CNT level of dispersion. In the frame of this master thesis, rheology measurements have been a very helpful instrument in order to study the variation of the viscosity and the storage and loss modulus of different nanocomposites mixed with epoxy. The rheometer used for the experiment was a Rheometer MCR301 from ANTON PAAR, illustrated in Figure 3.12.

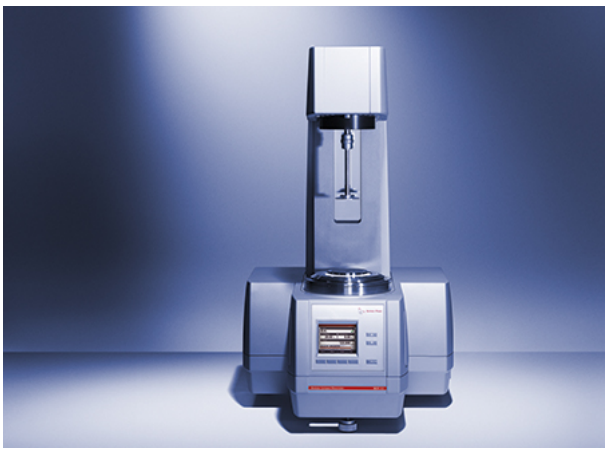


Figure 3.12: Rheometer used for measuring rheological properties [88].

Two different types of tests have been done. First of all the variation of the complex viscosity by increasing the temperature from room temperature up to 80℃ was studied. Then, the variation of the complex viscosity and the storage and loss modulus were studied at increasing frequency, from 0,1Hz to 10Hz. The experiments were done either at 0,5wt% of CNTs and at 2wt%, in order to study the variation of the level of dispersion between the different samples and at different CNTs content.

Chapter 4

Experimental results and discussion

Since the objective of this Master's thesis is to study how the morphology of CNTs can affect the final properties of the nanocomposites, as first step different synthesis conditions have been utilized in order to obtain CNTs with different characteristics. Afterwards, the CNTs have been characterized by SEM, TEM, and their dispersion state have been studied in a CNTs/epoxy mixture. The samples have then been used for producing nanocomposites in order to study their properties. The material properties were studied both by producing nanocomposites with DSM micro compounding, which allow to have a first idea of the samples having the best electrical properties. Then, experiments with a semi industrial twin screw extruder were done in order to verify the consistency of results between small and large scale production and to study the mechanical properties of the samples.

4.0.1 CNTs synthesis and characterization

CVD syntheses were carried out changing different synthesis parameters, in order to obtain carbon nanotubes with different morphologies. The variation of synthesis time, temperature, C_2H_4 concentration and catalyst were studied in order to obtain target samples either with 90% carbon purity and 85% carbon purity. The impurities present in the samples are mainly explained as catalyst particles that did not react during the experiment or amorphous carbon. Due to confidentiality issues, details concerning the catalysts cannot be provided, and the three catalysts employed during the experiments will be called from now on Catalyst A, Catalyst B, Catalyst C. The synthesis parameters were varied as follow:

- **Variation of the temperature** The time of the experiment was kept constant at 20 minutes, as well as the precursor concentration utilized during the experiment, being 100% C_2H_4. For each catalyst, the synthesis temperature was adjusted in order to obtain a final product 90% carbon purity and 85%carbon purity.
- **Variation of the precursor concentration** The precursor concentration during the experiment was modified in order to obtain a final product 90% carbon purity and 85%carbon purity, for each of the three catalyst. All the experiments were carried out at constant time, 20 minutes, and constant temperature, 700℃.
- **Variation of the time of experiment** The target temperature obtained for the synthesis of 85% carbon purity and a constant precursor concentration of 100% C_2H_4 were selected to carry out an experiment for longer time,

in order to obtain a target samples with 90% carbon purity. The target precursor concentration obtained for the synthesis of 85% carbon purity and a constant temperature of 700℃ were selected to carry out an experiment for longer time, in order to obtain a target sample with 90% carbon purity.

Being the six experiments repeated for each of the catalysts, 18 different samples were finally obtained. Table 4.0.1 summarizes the synthesis parameters used for each sample.

Sample name	Carbon purity (%)	Temperature (℃)	C_2H_4 concentration (%)	time (Min)
CatA1	90	700	64	20
CatA2	85	700	37	20
CatA3	90	640	100	20
CatA4	85	600	100	20
CatA5	90	700	37	65
CatA6	90	600	100	50
CatB1	90	700	50	20
CatB2	85	700	30	20
CatB3	90	612	100	20
CatB4	85	575	100	20
CatB5	90	700	30	48
CatB6	90	575	100	37
CatC1	90	700	55	20
CatC2	85	700	30	20
CatC3	90	640	100	20
CatC4	85	615	100	20
CatC5	90	700	30	40
CatC6	90	615	100	35

Table 4.1: Synthesis parameters for producing 18 samples that will be used for the study of this Master's thesis.

CatA, CatB, CatC stands respectively for CNTs synthesized by Catalyst A, catalyst B, Catalyst C. For each sample, around 50 grams of CNTs were needed in order to ensure enough product to undertake all the following experiments; the CVD apparatus used for the synthesis does not allow the production of more that 20 grams per experiment, thus each experiment was carried out multiple times in order to obtain 50 grams of the final product. Thus, each of the 18 final samples resulted as mixture of all the CNTs synthesized with multiple experiments keeping the same experimental conditions. As expected, higher synthesis temperature leads to an increase of carbon purity in the final product. The decrease in catalyst residues is the result of increased carbon yields at the higher synthesis temperatures, providing a dilution of the catalyst particles within the sample [89]. Noteworthy, the target conditions for the synthesis of CNTs for each catalyst are deeply different. Different types of catalyst demand different synthesis parameters, thus they had to be adjusted for each set of synthesis. Catalyst B were the one synthesized at lower temperature, when keeping constant precursor concentration and time, and at lower precursor concentration, when keeping constant temperature and time.
In order to evaluate the carbon purity, the samples out of the reactor were weighted. From equation 4.1 it was possible to determine the content of carbon present in the final product right after the synthesis:

$$\%C = \frac{M_{NTs} - (M_{cat} \cdot 0,89)}{M_{NTs} \cdot 100} \tag{4.1}$$

The value 0,89 is a value experimentally determined at Nanocyl S.A.. 0,11% is evaluated as the loss of mass of the catalyst that occurs during the reaction, due to an excess of water present in the catalyst. Thus, $M_{cat} \cdot 0,89$ represents the real mass of the catalyst during the synthesis process.

As mentioned before, the final samples utilized for the following experiments is actually a mixture of CNTs coming from experiments done at same conditions but at different times. Thus it was decided to further check the purity of the final products, and to investigate the thermal stability of the CNTs, thermogravimetric analysis (TGA) were carried out on the different samples. TGA analyses were performed on a TA Instrument, TGA Q5000, thermogravimetric analyzer. Samples were tested in a platinum pan at a heating rate of 25℃ /min up to 800℃ under oxygen and argon atmosphere. Sample masses vary from 2 to 15 mg. By TGA analysis it was possible to determine the percentage of carbon present in the different samples and the thermal stability, i.e. the temperature at which the conversion of carbon into CO_2 occurs. Controversial results were found in the literature concerning the variation of the oxidative stability with the synthesis temperature [89, 41]. Lee *et al.* reported that higher synthesis temperatures resulted in high crystalline CNTs. Their TGA plots showed significant increases in nanotube oxidative stability as the synthesis temperature was increased [41]. On the contrary, in accordance with results reported in other studies [89], strong correlation of synthesis temperature with the onset of CNT combustion was not observed, verifying that the residual catalyst particles has little or no effect on nanotube oxidative stability. TGA is a useful instrument in order to verify the CNT purity of the samples. The loss of mass of the samples after annealing corresponds to the percentage of carbon in the specimen, which reacted with oxygen and was eliminated as CO_2. Figure 4.1 and Figure 4.2 show the results obtained for two samples with respectively 85% and 90% carbon purity.

As expected and observed also in all the other TGA analyses, the value of carbon percentage is not exactly the one measured by weighting the samples. This observation does not sound new, considering that the CNTs produced are indeed a mixture of syntheses undertaken under different experiments and also considering that the yield of reaction in different zones of the reactor is not exactly the same. In this context, TGA analyses were carried out on CNTs produced in the same experiment but taken in two different zones of the reactor, at the center and at the extremities. The results demonstrated that the carbon purity may indeed vary of around 2% in purity.

As a second step, the samples were characterized in order to study the different properties of the CNTs produced at different conditions. Measurement of density were done, then morphological characterizations by TEM and SEM were carried out in order to determine respectively the diameter of all the CNTs samples and the size of their agglomerates and bundles. Finally, rheological measurement were done in order to investigate the variation of the level of dispersion of the samples in an epoxy matrix. Considering the large number of different samples synthesized, it was not possible to carry out all the tests on all the 18 samples.

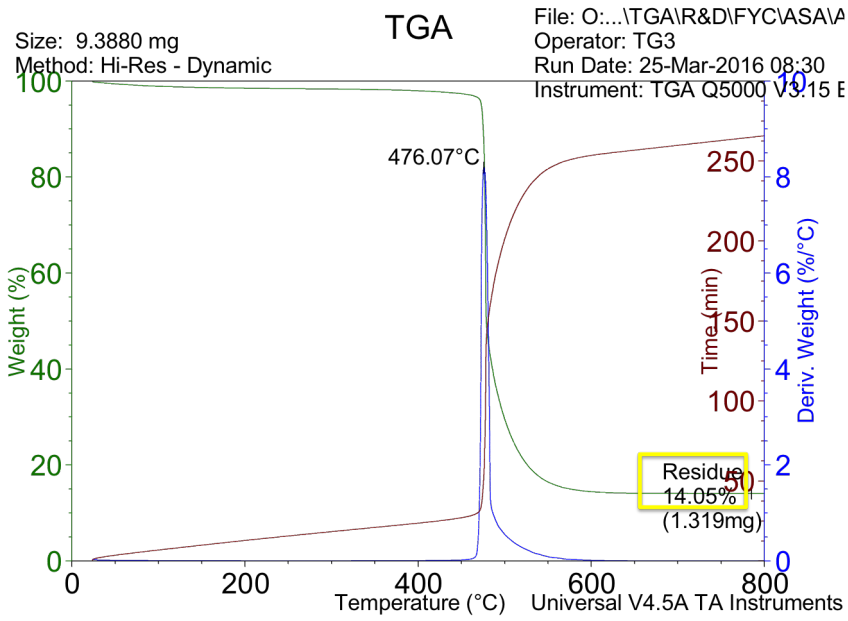


Figure 4.1: TGA analysis of a sample 85% carbon purity

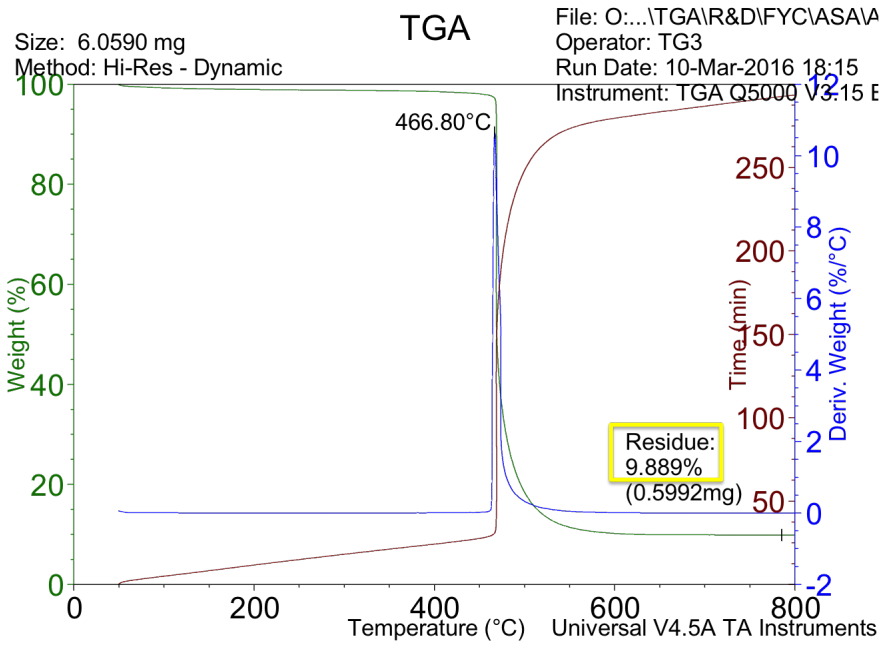


Figure 4.2: TGA analysis of a CNTs sample with 90% carbon purity

Some measurement were done on a limited number of specimen, trying to select the most significant.

4.1 Study of the variation of the carbon nanotubes diameter by TEM

TEM characterization was done in order to study the variation of the diameters on the 18 different samples. Different images of each sample, for different areas of the sample and at different magnifications were taken. Figure 4.3 shows three images at different magnification for a sample of catalyst A.

The diameter of around 200 carbon nanotubes per sample were then measured in order to get a statistic measurement of the value with the relative standard deviation. Table 4.1 recaps all the values of diameters with the relative standard deviation for each samples. The three columns highlight the differences between CNTs produced by Catalyst A (CatAx), Catalyst B (CatBx) and Catalyst C (CatCx).

Sample name	Diameter (nm)	Sample name	Diameter (d)	Sample name	Diameter (d)
CatA1	$9,2 \pm 2,5$	CatB1	$8,5 \pm 2,3$	CatC1	$8,2\pm,28$
CatA2	$9,3 \pm 2,7$	CatB2	$10,5 \pm 4$	CatC2	$9,8 \pm 2,9$
CatA3	$8,1 \pm 3,3$	CatB3	$7,1 \pm 1,6$	CatC3	$7,6 \pm 2,2$
CatA4	$7,5 \pm 2,3$	CatB4	$8,2 \pm 2,6$	CatC4	$7,9 \pm 2,2$
CatA5	$10,1 \pm 2,7$	CatB5	$10,0 \pm 2,8$	CatC5	$11,4 \pm 4,7$
CatA6	$7,4 \pm 1,5$	CatB6	$7,3 \pm 2,1$	CatC6	$7,6 \pm 2,5$

Table 4.2: Values of the diameters of all the CNTs samples.

Samples CatA(B)(C)3, CatA(B)(C)4 and CatA(B)(C)6 were produced at lower temperature. CatA(B)(C)1 and CatA(B)(C)2 were produced at higher temperature and CatA(B)(C)5 was synthesized at higher temperature for longer time. The results show a tendency towards increasing the average diameters for samples produced at higher temperatures. In particular, the effect is even increased when the synthesis is carried out for long time. The effect is reproduced in the case of the three samples. The carbon percentage does not to influence the final diameter. In agreement with what has already been observed in the literature, higher temperature syntheses facilitate sintering between catalyst nanoparticles, thus inducing an increase of the final diameters.

4.2 Density measurement

Measurement of the density of the different samples previously synthesized were done. A fluometer KARG INDUSTRIETECHNIK - Bulk Density Tester ADP was utilized to measure the bulk density of the powders. The powder is dropped in a 100 ml volume cup and is weighted. The measurement of the volume is then obtained by dividing the weight by the volume. Figure 4.4 shows the results obtained. The density as function of the different synthesis conditions and catalyst used is highlighted. In order to simplify the understanding of the graph, instead of giving the name of each sample for each point, only the synthesis parameter that is changed during the synthesis is shown in the following graph.

By changing the catalyst, a wide variation of the value of density of CNTs is observed. CNTs produced by Catalyst A resulted to have the higher value of

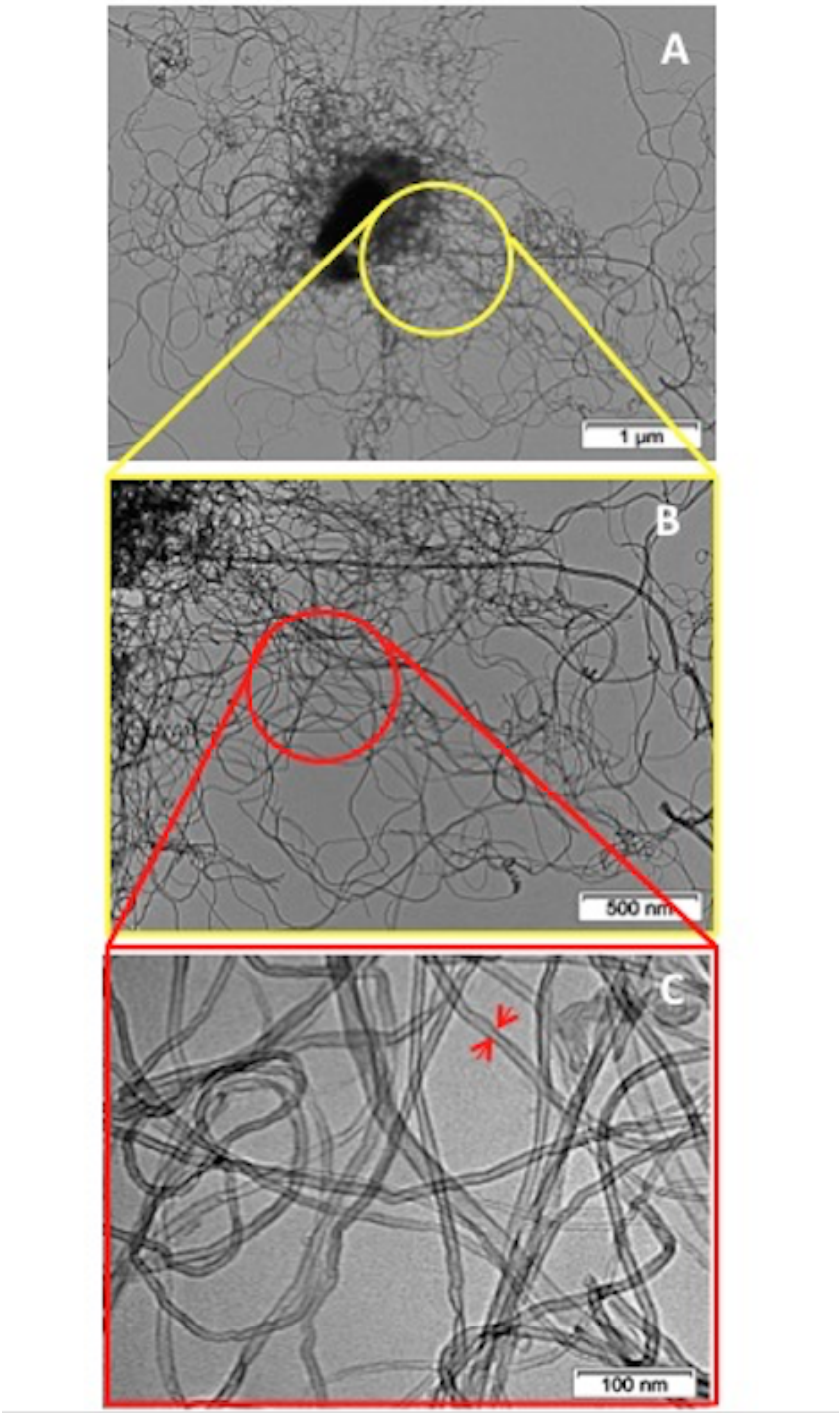


Figure 4.3: TEM images of sample CatA1 taken at different magnifications in order to measure the value of the diameters.

density, being around $60 \pm 10 g/L$; Catalyst B and C shows significantly lower values, respectively $23 \pm 10 g/L$ and $10 \pm 3 g/L$. Variation of the density of CNTs produced by different catalyst is explained by differences in the catalyst composition, whose information cannot be provided due to confidential issues. In general, no big differences are observed between CNTs 90% carbon purity

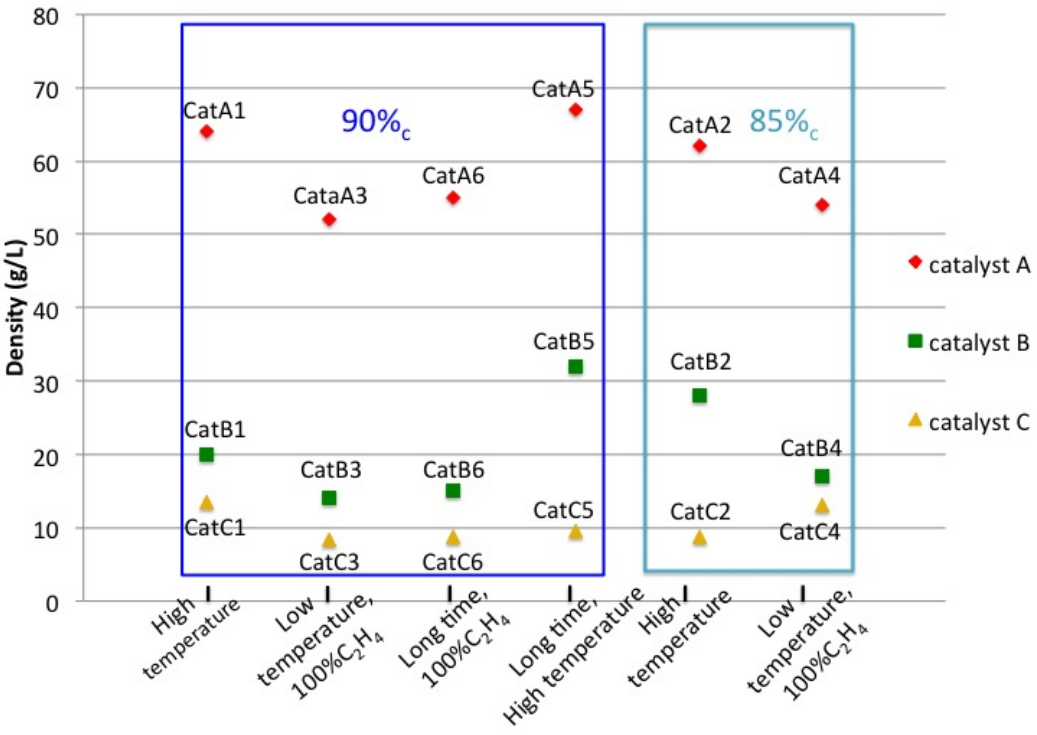


Figure 4.4: Variation of the density for the 18 samples produced. On the x-axis the synthesis conditions are indicated. Red diamonds indicate samples synthesized by catalyst A; Green squares indicate samples synthesized by catalyst C; Yellow triangles indicate samples synthesized by catalyst C.

(indicated in the graph as $90\%_c$) and 85% carbon purity (indicated in the graph as $85\%_c$) of samples produced by the same catalyst. Nonetheless, an interesting trend is noted when observing the variation of the density with the synthesis conditions. Syntheses done at high temperature lead to higher value of density of CNTs in the case of the three catalyst, and both in the case of 90% and 85% carbon percentage. The explanation of this trend can be clarified taking into consideration the results obtained by TEM analysis. At higher temperature synthesis catalyst particles tend to sinter, leading to CNTs with bigger diameters. Thus the sample containing small diameters CNTs will occupy a bigger volume compared to the one with a bigger diameters, decreasing the density of the sample.

4.3 Study of the level of dispersion: rheological measurement

In order to study the level of dispersion of CNTs, measurements of the viscosity and the storage and loss modulus were done. In particular, rheology is an interesting instrument in order to obtain more information concerning the dispersion of the filler in the matrix. As first analysis, mixtures of 2wt% CNT and epoxy were tested. All the mixtures were homogenized by four cycles of three

roll mill under standard conditions in order to assure an equal homogenization for all the samples. Only 12 CNTs over the 18 produced were studied. Tests were taken over temperature and frequency. Figure 4.5A show the variation of the complex viscosity with the temperature. CNTs/epoxy composites produced with Catalyst C are characterized by higher viscosity, almost one order of magnitude higher compared with the samples produced by Catalyst A and B. No big differences can be observed between CNTs produced by the same catalyst, as well as between CNTs produced by catalyst A and B, which all present a complex viscosity of around $10^3 Pas$. The only CNTs showing a significant lower value of complex viscosity are CatB4, CatB6 and CatA4. Both the three CNTs were syntheses at low temperature. It is interesting to observe that while for most of the samples the viscosity is constant over the temperature, in case of epoxy mixed with CatB4 and CatB6 a minimum in the curve is present. A possible explanation to this phenomena is that in these specific cases, the CNTs are not well dispersed in the matrix. Thus, when starting increasing the temperature the viscosity increases since the behavior is governed by the movement of the polymer chains. Further increasing the temperature, a strong network between CNTs and polymer is formed and the viscosity is decreased. In all other cases, a network structure is already formed and thus the viscosity is temperature independent. However, this could be due both to a good level of dispersion and to the presence of longer CNTs that eases the formation of a strong network between carbon nanotube and polymers chains.

For what concerns the variation of the complex viscosity with the frequency, again it can be observed in Figure 4.5 B a significant increase of the value of $|\eta|$ in case of samples prepared with Catalyst C. No other big differences between the different samples can be observed. The storage modulus and the loss modulus have been measured. Figure 4.6 show the plot for the variation of the storage modulus G' and the loss modulus G" with the frequency.

The biggest differences can be observed again between CNTs obtained by Catalyst C compared with the ones obtained by Catalyst A and B, difference that is even more highlighted when observing the storage modulus. Both modulus are increasing with frequency but the rate of increasing changes with the samples. The slope α of the curve $G' vs f^{\alpha}$ have been studied in order to further investigate variations in the degree of dispersion of carbon nanotubes in the matrix. The results actually showed that the variation of the slope of the different samples were not significantly changing, resulting in small value of α, further evidence of the good level of dispersion of the samples.
Considering all the samples reached a good level of dispersion in the case of a mixture 2wt% of CNTs, it was not possible to actually determine if there were some big differences in the level of dispersion between samples produced by the same catalyst.
In order to be able to better highlight the differences between samples, the mixture previously used was then diluted in epoxy in order to obtain a mixture 0,5 wt% CNTs/Epoxy. Figure 4.7 shows a comparison of the complex viscosity (Figure 4.7A) and the storage modulus (Figure 4.7B) between three samples 0,5wt% and 2wt% of CNTs.

The variation of the complex viscosity deeply varies between samples 0,5wt%

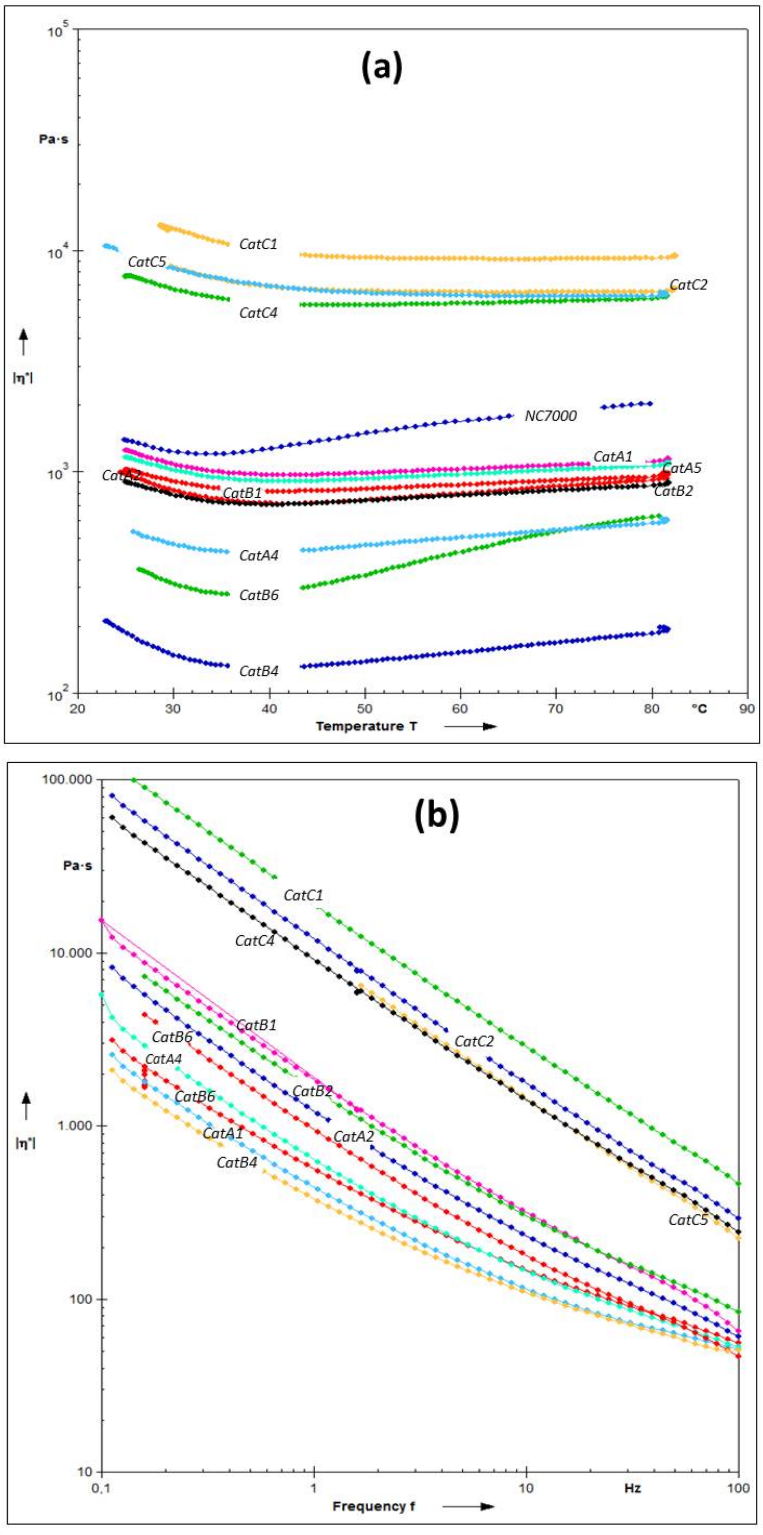


Figure 4.5: (a) complex viscosity of a mixture 2wt% CNTs/epoxy versus temperature. (b) complex viscosity of a mixture 2wt% CNTs/epoxy versus frequency (measurement taken at 25°).

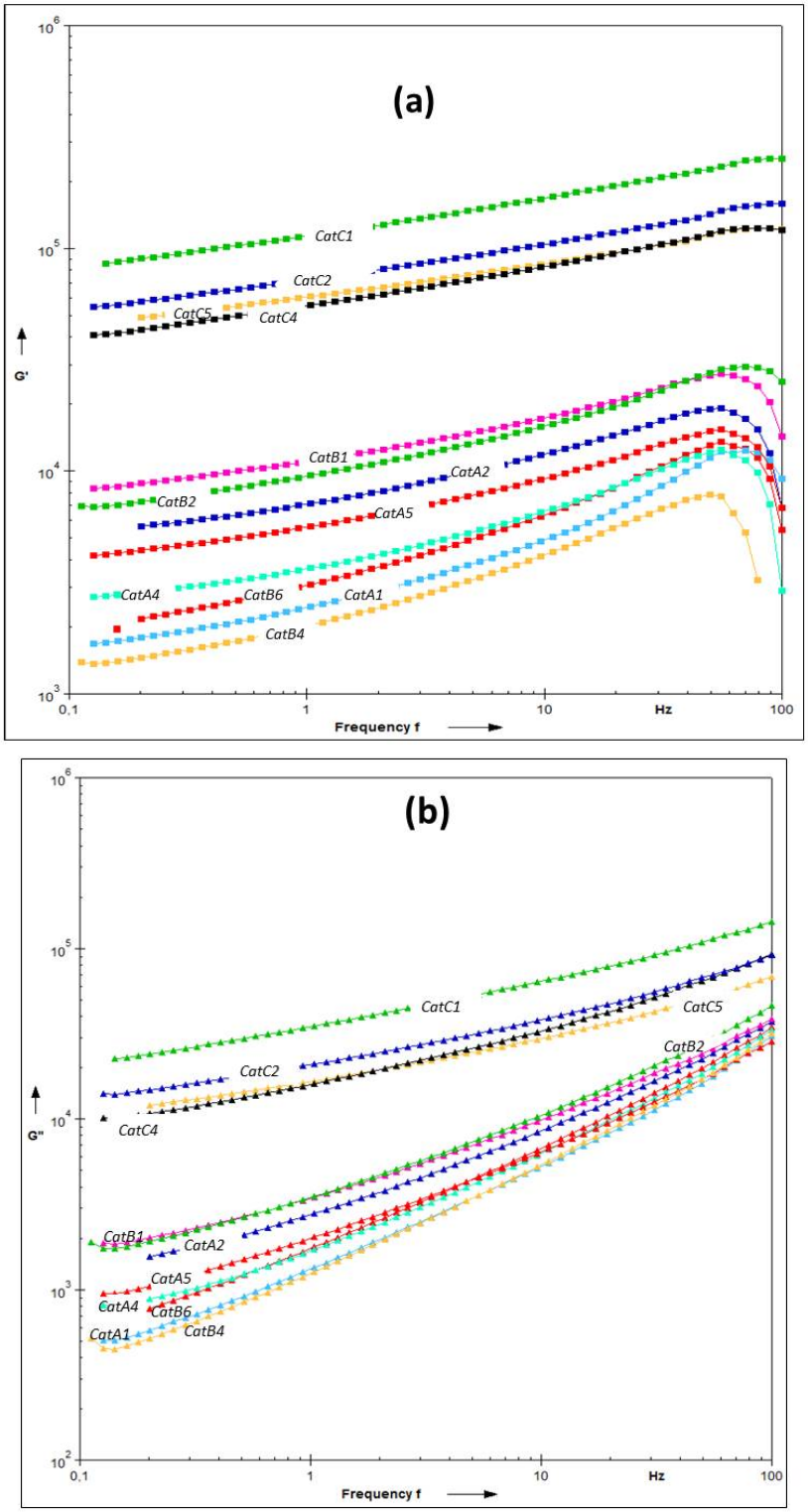


Figure 4.6: (A) Storage modulus G' of a mixture 2wt% CNTs/epoxy versus frequency (measurement taken at 25°). (B) Loss modulus G" of a mixture 2wt% CNTs/epoxy versus frequency (measurement taken at 25°)

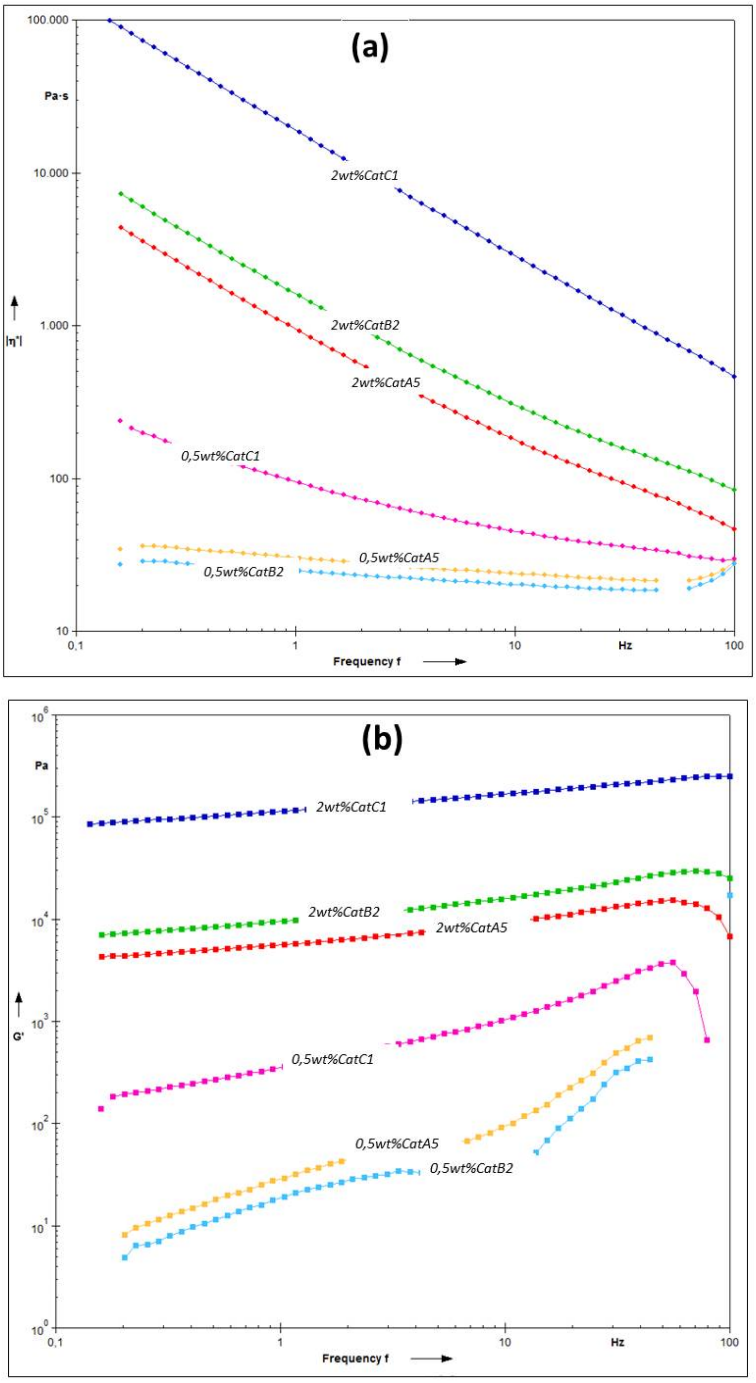


Figure 4.7: (A) Comparison of complex viscosity between three samples 0.5wt% CNTs/epoxy and 2wt% CNTs/epoxy (measurement taken at 25°) (B) Comparison of storage modulus G' between three samples 0.5wt% CNTs/epoxy and 2wt% CNTs/epoxy (measurement taken at 25°)

and 2wt%, most of all in the case of samples produced by Catalyst A and B (Figure 4.7). The rheological responses of CatA5 and CatB2 are very similar to the one of the neat polymer, characterized by a Newtonian plateau with a small frequency dependence, due to the fully relaxed polymer chain which

is not affected by the low content of CNTs, which are probably aggregated, without forming a well dispersed network with the matrix. On the other side, it is noteworthy that the sample produced by catalyst C shows a significant dependency on the viscosity with the frequency even at 0,5wt%, showing a shear thinning effect. Observing the storage modulus (Figure 4.7B) of the sample 0,5wt% CNTs, the curve are far from being flat but they show a significant variation of the value with the frequency. The slope of the curve of each sample prepared have been calculated in order to evaluate the variation of dispersion. Table 4.3 reports all the values of the slope α for each samples.

Sample name	α	Sample name	α	Sample name	α
CatA1	$0,695$	CatB1	$0,853$	CatC1	$0,378$
CatA2	$0,867$	CatB2	$0,771$	CatC2	$0,257$
CatA4	$1,285$	CatB4	$0,831$	CatC4	$0,702$
CatA5	$0,731$	CatB6	$0,744$	CatC5	$0,257$

Table 4.3: Value of the slope of the curve $G'vsf^{\alpha}$ in a mixture 0,5wt% CNTs/epoxy

The CNTs were produced by Catalyst C present a value of α significant lower compared with all the ones of CNTs produced by catalyst A or B. It is relevant to underline that for each catalyst, the samples synthesized at lower temperature (CatA4, CatB4, CatC4) are characterized by the highest value of α, showing a worst level of dispersion. In order to further investigate the level of agglomeration of the carbon nanotube, we also decided to take some SEM images of some samples to try to understand the differences in morphology between the different specimens.

4.4 Study of the level of dispersion: SEM analysis

SEM analysis was done on some of the samples produced for each of the catalyst in order to investigate differences in morphology of the CNTs, the dimension of the aggregates and the level of dispersion of the CNTs. Figure 4.8 shows the images taken from samples CatA1, CatB1 and CatC1 at different magnifications. The three CNTs have been synthesized with the same conditions but with different types of catalyst. The images show significant difference in the CNT morphology and aggregation between all the three samples. CatA1 is significantly more dense, appearing as a big agglomeration of bundles. CatB1 and CatC1 seems to have a similar morphology, characterized by bundles of thickness around $5\mu m$. The dimensions of all the bundles seems to be about the same in the case of CatB1, while in case of CatC1 significantly smaller bundles are also observed, showing a better level of dispersion. In general, CNTs observed in CatB1 and CatC1 are more aligned compared to the ones observed in CatA1. Moreover, CNTs produced by catalyst C have a very organized structure, aggregating in a less dense configuration which almost allow to identify the single nanotube in the structure, appearing with a spring-configuration-like.

TEM analysis shows a decrease of the CNTs diameters in the case of synthesis

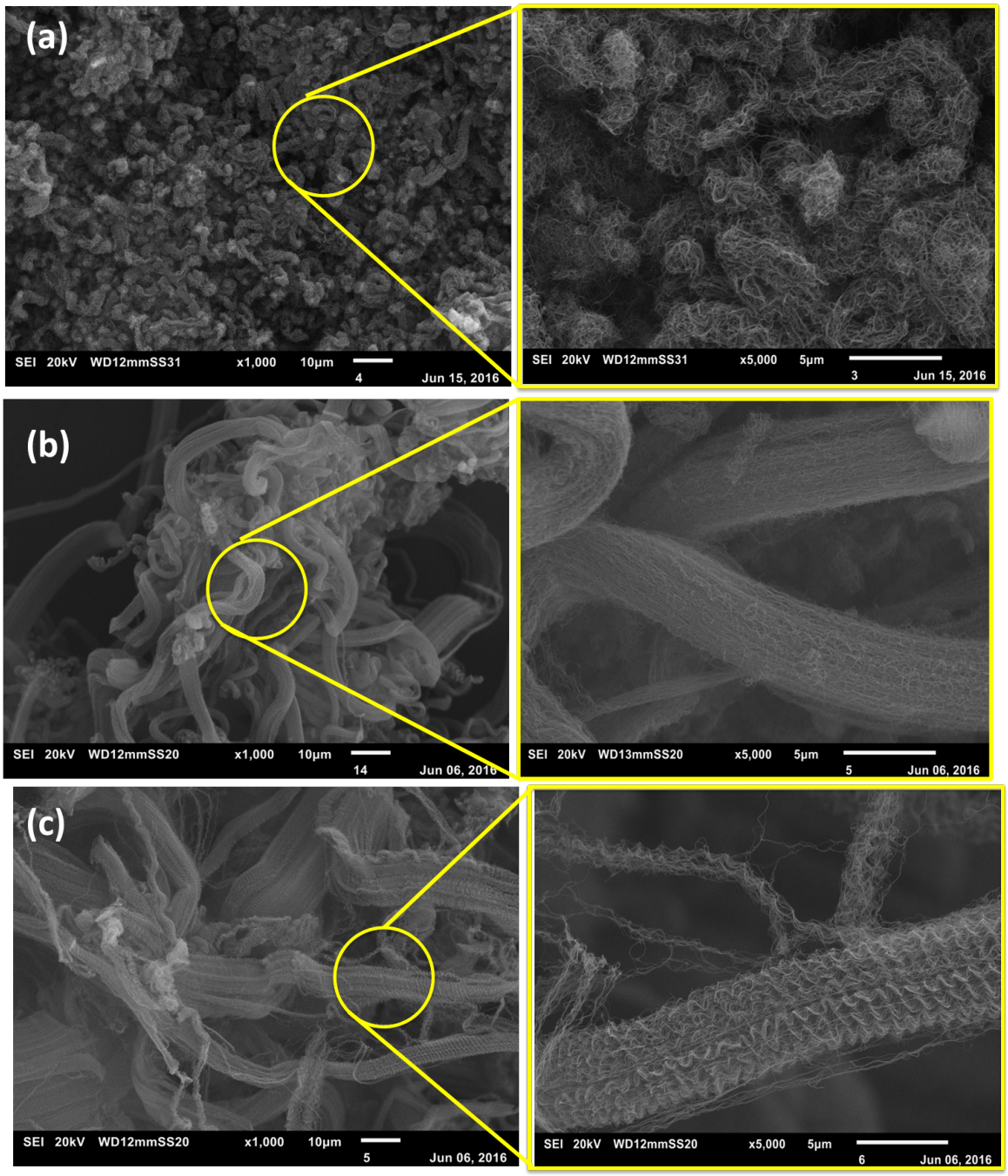


Figure 4.8: SEM analysis of samples CatA1 (a), CatB1 (b), CatC1 (c) at different magnifications.

at lower temperature; moreover, from the rheological measurements the CNTs produced at lower temperature seem to differentiate from the others, showing a worst level of dispersion. Figure 4.9 shows CNTs synthesized at low temperature with the three different catalysts. Interesting is the comparison between the images in Figure 4.8 and Figure 4.9.

Observing the differences between the samples produced at higher temperature (Figure 4.8) and low temperature (Figure 4.9) it was seen that in the three

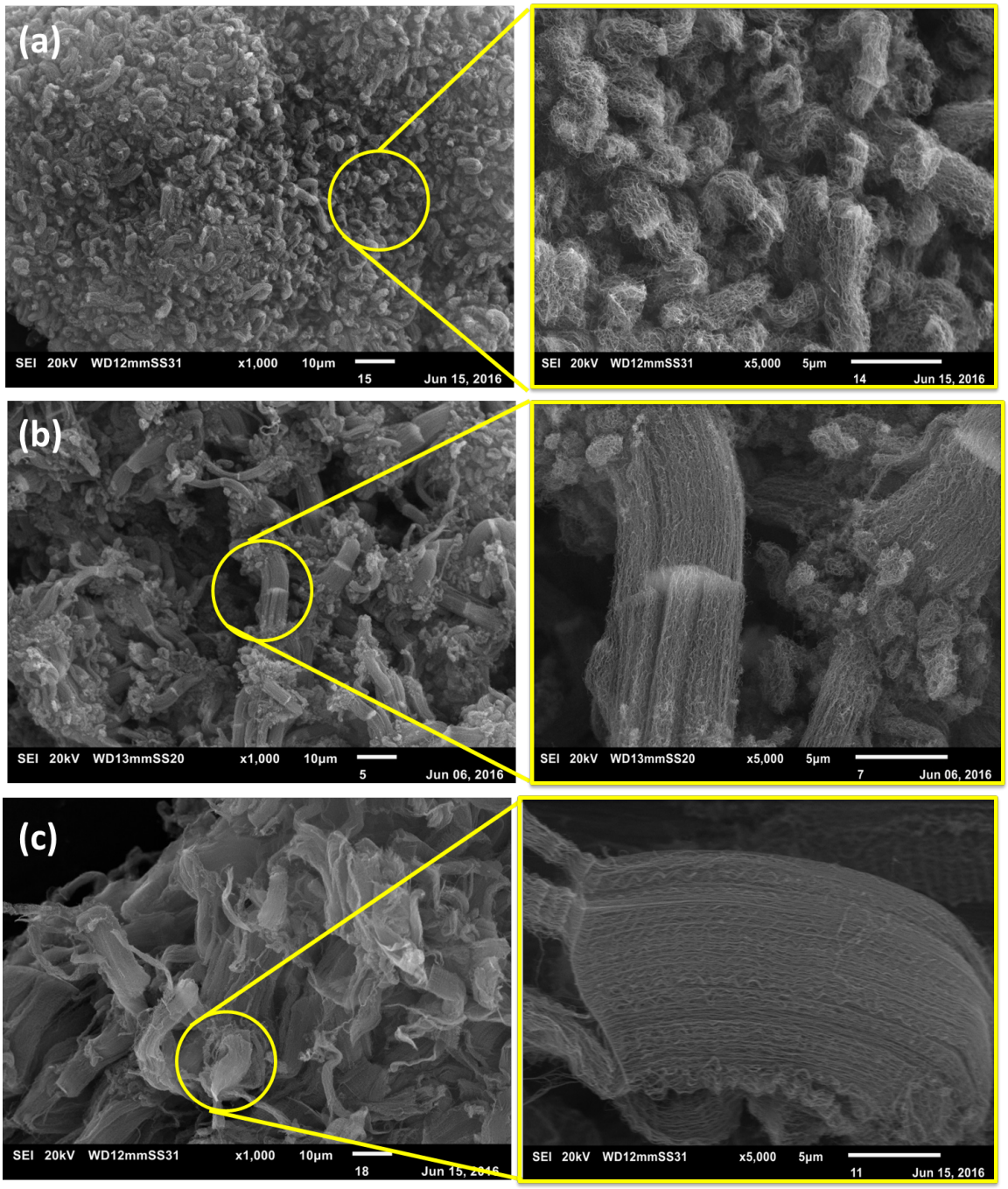


Figure 4.9: SEM analysis of CatA4 (a), CatB4 (b), CatC4 (c) at different magnifications.

cases (Catalyst A, Catalyst B and Catalyst C) the CNTs produced at lower temperature are aggregated in bigger and less dispersed bundles. Low temperature synthesis with Catalyst A (Figure 4.9A) is characterized by bundles of dimension slightly bigger compared to high temperature synthesis with Catalyst A (Figure 4.8a), but extremely more dense and compact. Figure 4.9B and C shows a significant increase of the dimension of the bundles for the samples synthesized by Catalyst B and C, compared to what was observed in Figure 4.8 B and C.

Moreover, in the low temperature synthesis samples the presence of the catalyst perpendicular to the growth of the CNTs can be easily observed.

As a second step after the production and the characterization of the CNTs, all the samples have been used to produce nanocomposite in order to study the variation of the properties with the different synthesis conditions. From the characterization and the study of the dispersion of the CNTs, a variation of the resistivity with the different catalyst were expected. The electrical properties were measured on nanocomposites produced by mixing the different CNTs both with polycarbonate (PC) and high density polyethylene (HDPE) matrices.

4.5 DSM microcompouding experiments

DSM micro-compounding experiments were carried out in order to study the electrical conductivity of nanocomposites produced using the CNTs previously analyzed. First of all polycarbonate (PC) nanocomposites were tested. Each DSM experiment produces two bars, thus two experiments were done for each CNTs samples in order to do electrical measurements on four specimens. The objective was to define a percolation curve for each CNTs nanocomposite, so samples with different concentrations starting from 0,5wt% to 4wt% were produced. The process conditions used were the one previously optimized at Nanocyl S.A.. The compound was mixed at 280℃ with an average mixing speed of 50 rpm, for 5 minutes. The materials were then extruded and injected in a mold at 100℃. The electrical measurement were taken one day after the injection and the specimens were collected in a dessicator in order to avoid absorbency of humidity and thus to invalidate the measurement. Figure 4.10 shows the percolation curves for each of the sample.

From the graph it can be observed a significant difference in resistivity between samples produced by catalyst C compared with the ones produced by catalyst A and B. Samples from Catalyst C are already conductive for concentrations above 0,5wt% while samples produced by Catalyst A and B have a percolation threshold between 1wt% and 1,5wt%. The torque applied inside the chamber was monitored for each sample during the mixing process, showing significantly different values between samples produced by Catalyst C compared with the ones produced by Catalyst A and B. During processing, mixture with Catalyst C samples required application of higher stress due to the high viscosity of the mixture, which could had further helped to better disperse the CNTs in the matrix and thus increases the conductivity of the final nanocomposite. Considering a standard deviation about one order of magnitude for each measurement, not much can be said considering differences in the resistivity between samples produced by the same catalyst. It is not possible to define a trend and a link with the synthesis conditions since for the three sets of CNTs the best performances are found in CNTs synthesized with different conditions.
Optical measurements were done with an optical microscope AXIO from Zeiss on all the nanocomposites with 2wt% CNTs, with the goal of studying the dispersion of the carbon nanotubes in the matrix at this scale. Figure 4.11 shows the images taken for all the samples. From the images, it is not possible to

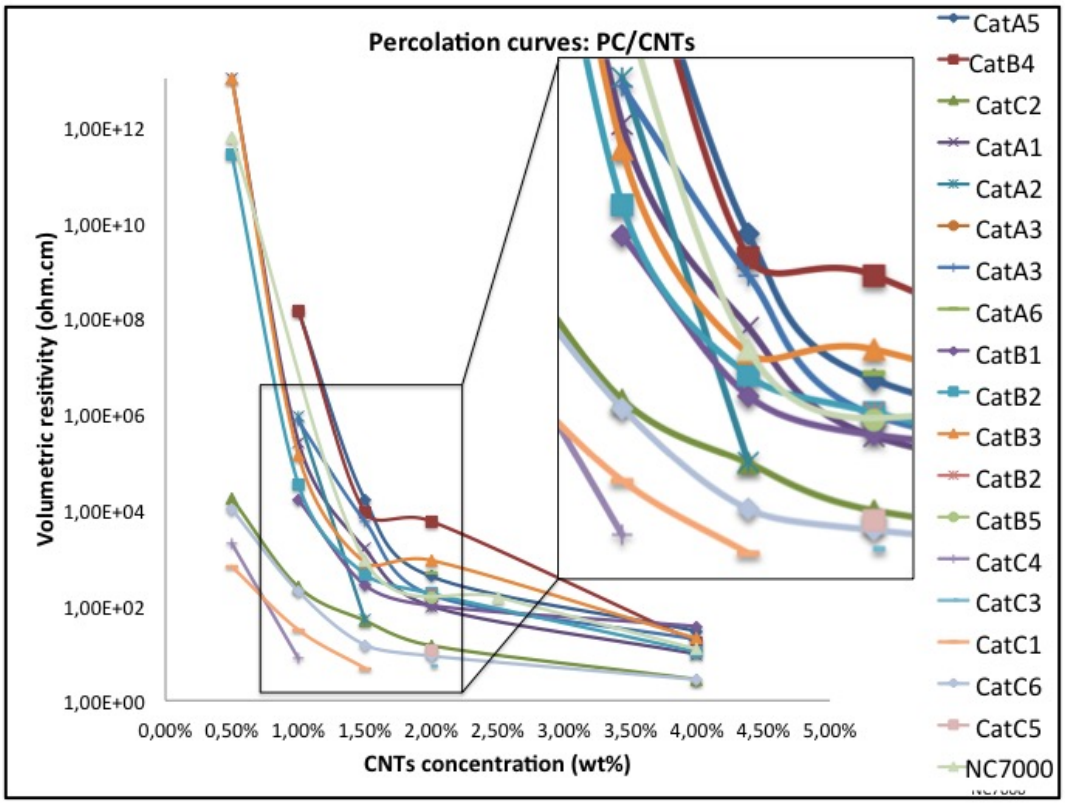


Figure 4.10: Percolation curves of the PC/CNTs produced with the nanotubes previously synthesized

define a relationship between the level of dispersion observed by optical microscope and the results obtained measuring the conductivity of the samples. It was determined that microscopic images cannot be of any help when observing the agglomeration of the CNTs in a matrix since the level of dispersion that matters for the final properties can be observed only at the nanometric scale.

From the electrical measurements taken from PC nanocomposites, it was clear that Catalyst C produces the more conductive nanocomposites but it was not possible to discriminate the best sample between the ones synthesized with the same catalyst.

The same experiments were done with a different matrix, High Density Polyethylene (HDPE), again producing 4 specimen for each nanocomposites. Not all the CNTs samples were used but the most significant ones were selected in order to see if it was possible to better highlight differences between the resistivity of the samples. The process conditions used were the one previously optimized at Nanocyl S.A., thus different from the ones used for the PC matrix. The compound was mixed at 200°C with an average mixing speed of 150 rpm, for 4 minutes. The material were then extruded and injected in a mold at 60°C. The electrical measurements were taken one day after the injection. Figure 4.12 shows the percolation curves of the samples tested.

Due to lower affinity with the matrix compared with PC, an higher loading of

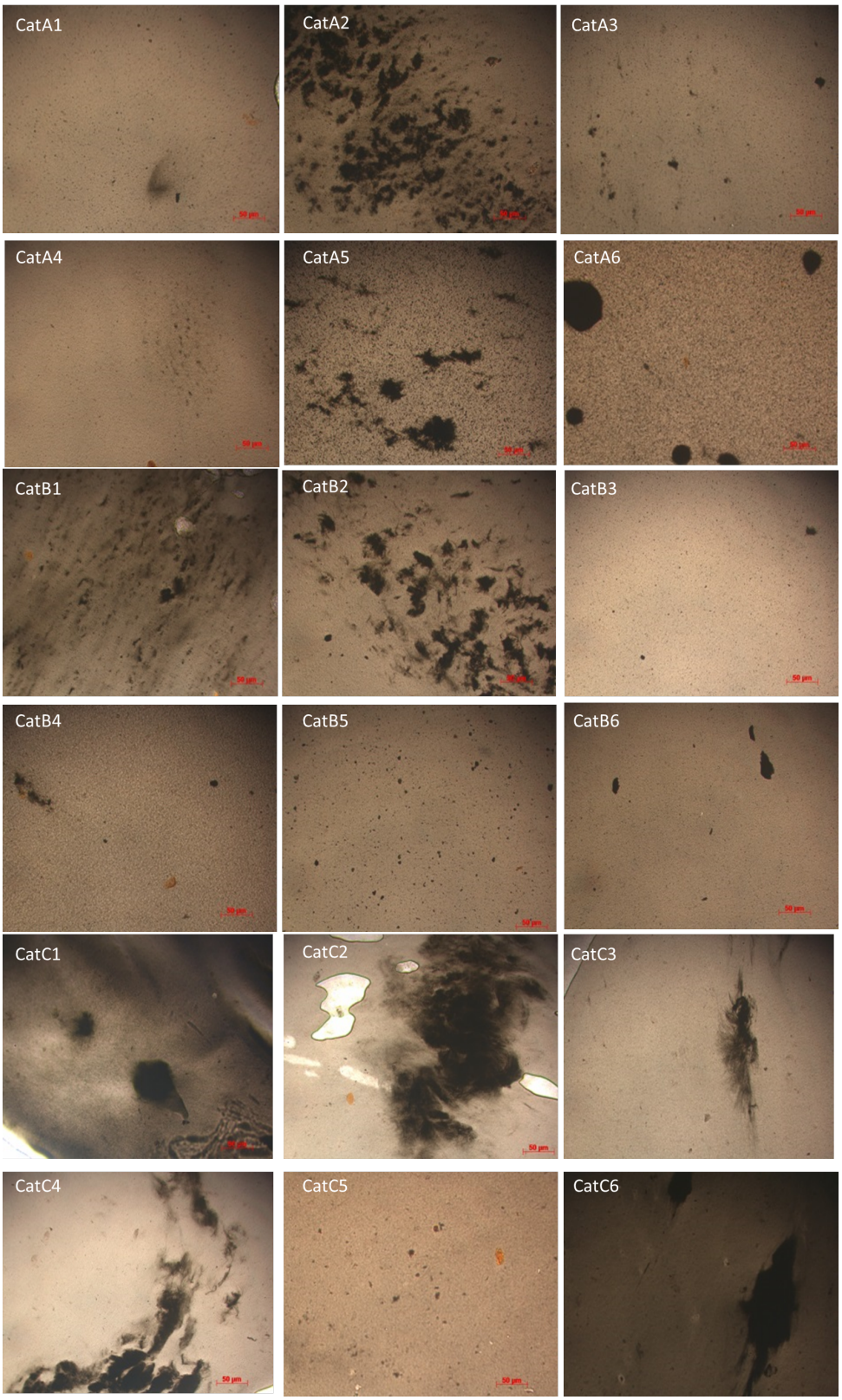


Figure 4.11: Optical images of (A)CatA5, (B) CatB4, (C) CatC3. The scale bar is $50\mu m$

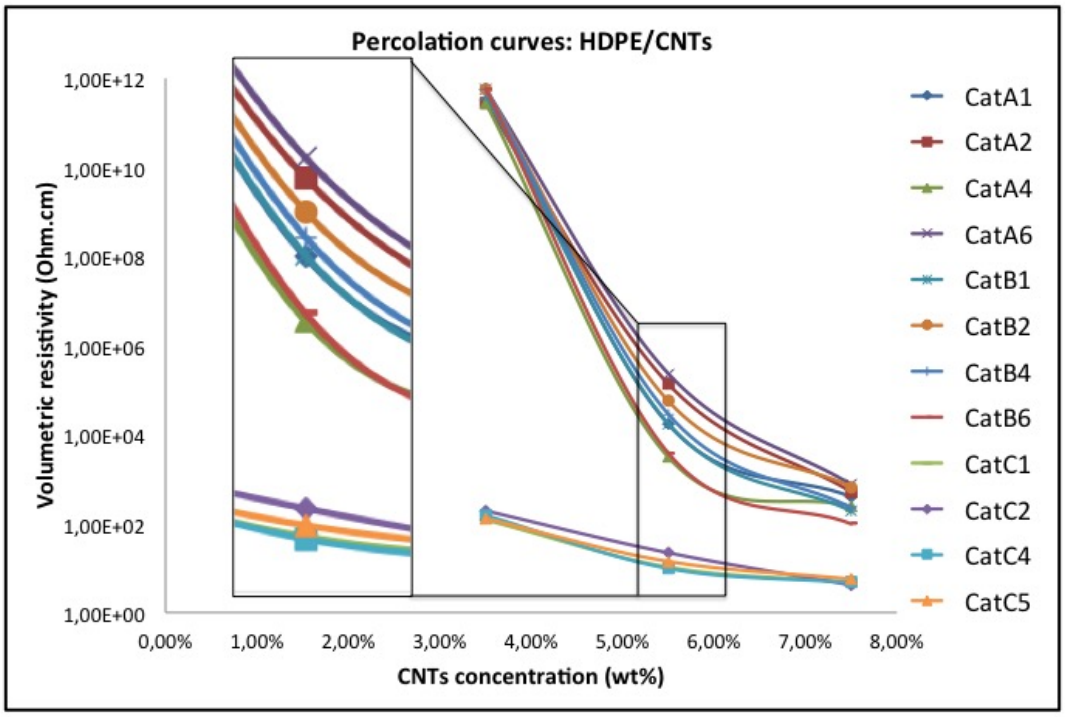


Figure 4.12: Percolation curves of the HDPE/CNTs produced with the CNTs previously synthesized

filler is necessary in order for the material to be conductive, thus the nanocomposites were tested at 3,5wt% 5,5wt% and 7,5wt%. Again, all the nanocomposites produced with CNTS synthesized by catalyst C were found to have significantly better performance, having a resistivity of only $10^2 ohm \cdot cm$ at 3,5wt% while all the other samples reach the percolation threshold at around 5wt%. Again, it was not possible to discriminate a better samples based on the synthesis conditions. The results were consistent with what was observed characterizing the CNTs.
catalyst C samples were the ones with a significant better dispersion, most of all observed by the rheological measurements, and indeed they show an increase of the conductivity in the final nanocomposites, both in the case of PC matrix and HDPE matrix. Despite a variation in the CNTs morphology and differences in dispersion level between high temperature and low temperature synthesis, these differences were not relevant enough to actually have a significant role on the final properties of the nanocomposites.
A different study was then carried out in order to understand how the processing conditions were actually affecting the final results. One sample for each catalyst was chosen in order to test the effect of the variation of the temperature, the speed of processing and the time of experiment. The nanocomposites was chosen as the one having an average electrical resistivity between the all samples for each catalyst. Table 4.5 summarized the conditions used for each experiments; all the

experiments were done using 1 wt% and 1,5 wt% CatA1, CatB2, CatC2, mixed with PC. Due to technical problems, experiment 5 and 6 could not be done with 1wt% CNTs.

Nº Experiment	speed (rpm)	Mixing temperature (°C)	Time of experiment
St. conditions	50	280	5
Exp 1	50	260	5
Exp 2	50	300	5
Exp 3	100	260	5
Exp 4	200	280	5
Exp 5	50	280	2
Exp 6	50	280	15

Table 4.4: Processing conditions used in different experiments in order to verify the effect of the parameters on CNTs produced by different catalyst.

For each sample, two experiments were done so that the electrical resistivity measurement were taken on 4 specimens. All the samples are measured one day after the injections. Figure 4.13 shows the results obtained by mixing the three mixtures with conditions as Exp 1 and Exp 2 (Table 4.5) at 1,5%wt CNTs (Figure 4.13a) and at 1,0%wt CNTs(Figure 4.13b).

It is evident that increasing the speed of mixing the volumetric resistivity significantly decreases. This effect is further highlighted when carrying out the experiment with 1wt% CNTs (Figure 4.13B). By increasing the speed of mixing also a significant increase of the force applied to compound occurs. Increasing the speed up to 200 rpm, probably leads to break the CNTs in shorter CNTs, hindering the conductivity of the final nanocomposite and thus increasing the resistivity of several order of magnitude. The effect is highlighted close to the percolation threshold, being a concentration particularly sensitive to the variation of the synthesis conditions. This effect is not observed in the case of CatA1 sample. A jump is observed when increasing the speed from 50rpm to 100rpm, but no significant variation of the resistivity is seen when increasing up to 200 rpm. If this particular behavior was due to strongest carbon nanotube, we should not observe a decrease of resistivity at 100 rpm. The constant resistivity while increasing the speed up to 200 rpm is probably due to a difference in the length of the carbon nanotubes. Being probably the CNTs of CatA1 shorter, a speed of 100 rpm is probably enough to break the longest carbon nanotubes. It is not possible to observe any variation when further increasing the speed, since most of the CNTs are too short to actually "feel" the effect of a higher speed of mixing. The second experimental condition tested is the variation of the temperature during the mixing. Figure 4.14 shows the results obtained by mixing the three samples with conditions as Exp 3 and Exp 4 (Table 4.5) at 1,5wt% CNTs (Figure 4.14a) and 1,0wt% CNTs (Figure 4.14b).

CatB2 and CatC2 show the same behavior in the case of mixture with 1wt% and 1,5wt%. No big differences are observed while decreasing the temperature from 300°C to 280°C but a sharp increase of resistivity is seen when decreasing down to 260°C. Increasing the viscosity should normally help for increasing the

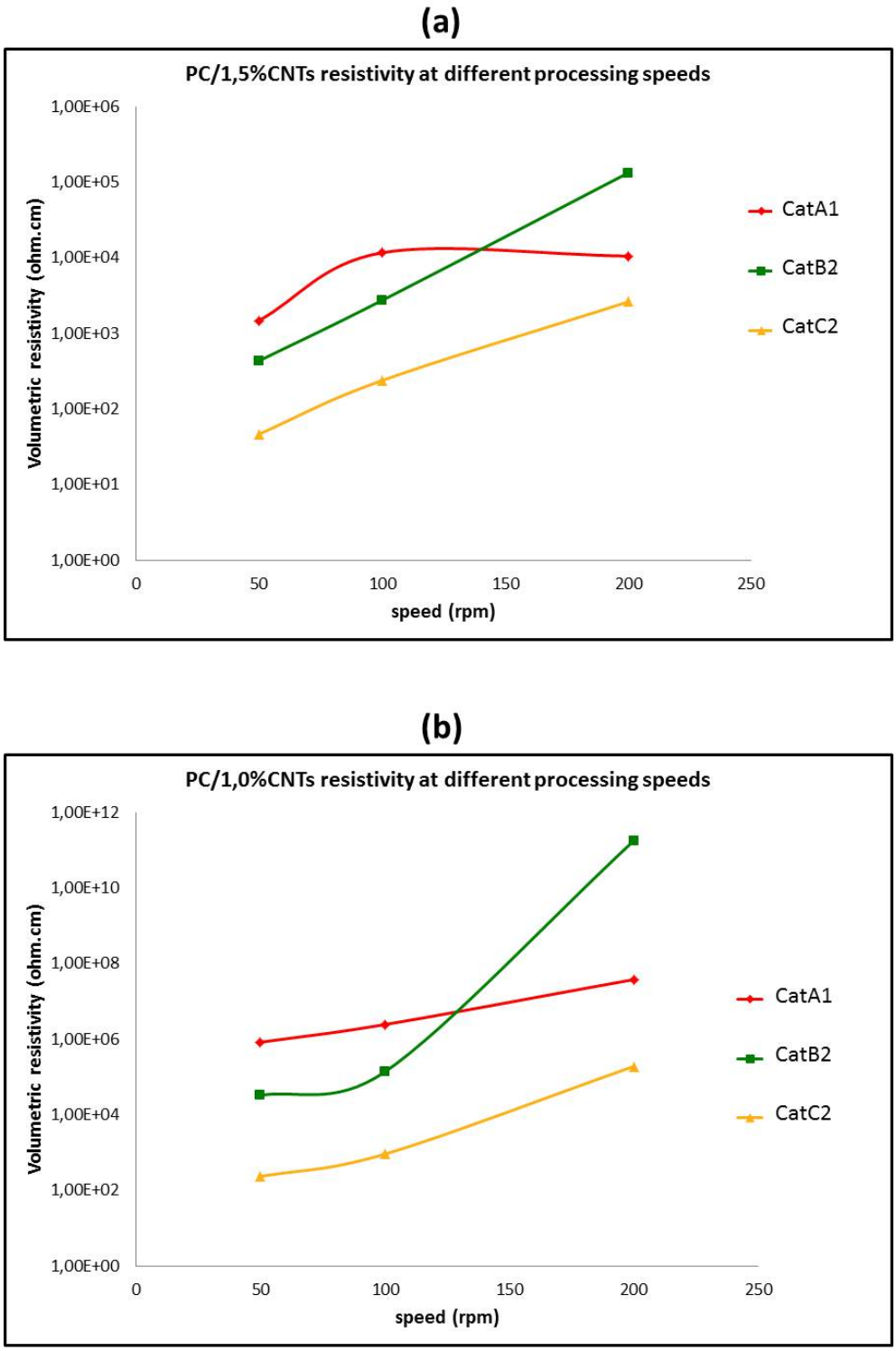


Figure 4.13: Electrical resistivity of nanocomposites PC/CNTs at different mixing speed for (A) 1,5wt% CNTs and (B) 1,0wt% CNTs.

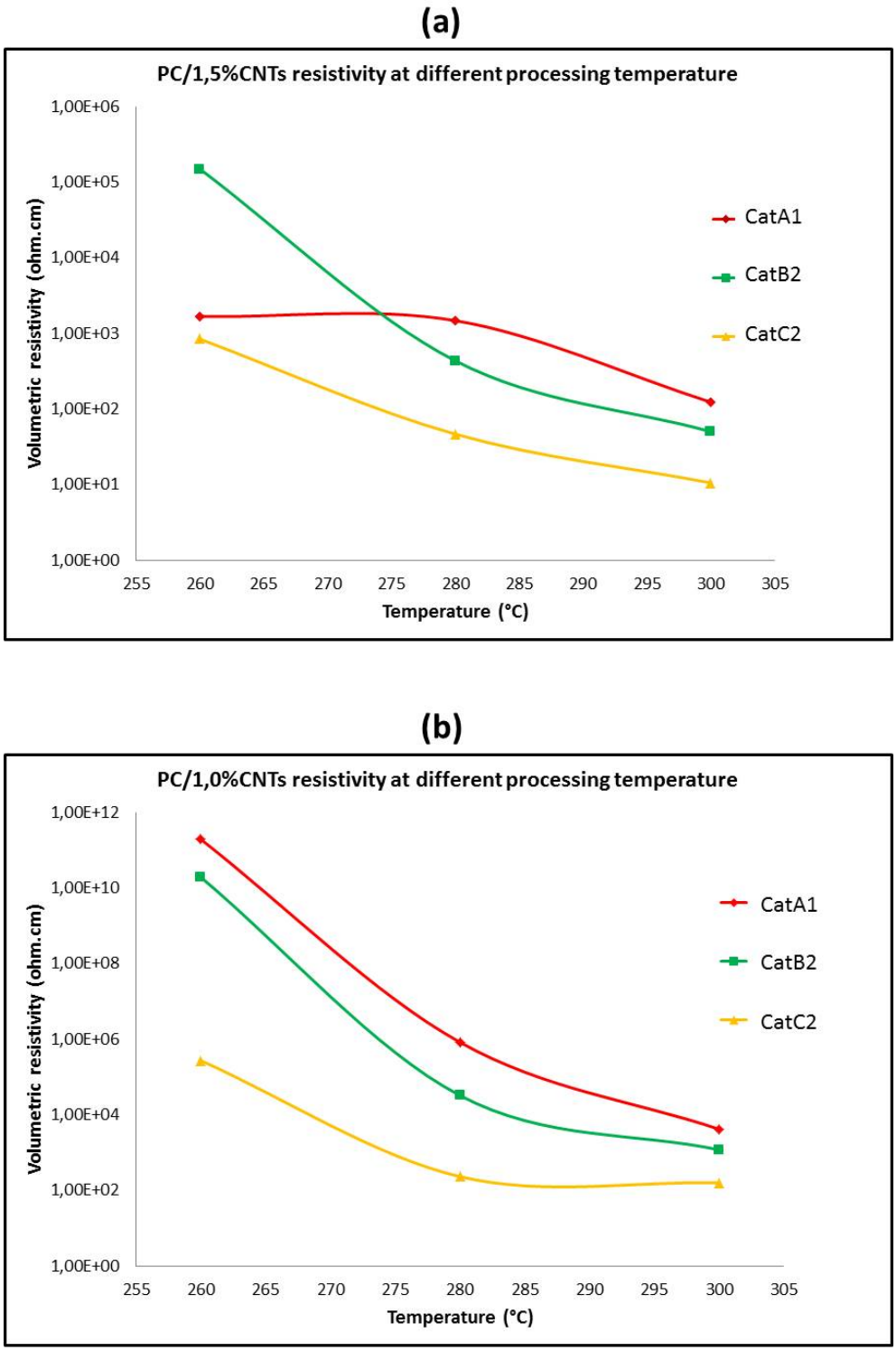


Figure 4.14: Electrical resistivity of nanocomposites PC/CNTs at different processing temperature for (A) 1,5wt% CNTs and (B) 1,0wt% CNTs.

dispersion of the carbon nanotube in the matrix but in this case, it probably leads to an excess of stress applied and thus a break of the CNTs leading to an increase of resistivity. Different results are obtained in case of CatA1 which behave differently in the case of nanocomposites 1,5wt% (Figure 4.14A) and 1wt% (Figure 4.14B) of CNTs. In case of 1,5wt% CNT (Figure 4.14A) we observe a slight decrease in electrical resistivity from 300℃ to 280 ℃ and no differences when further decreasing the mixing temperature down to 260℃. The reason is probably again the length of the CNTs in the samples. Being shorter than the CNTs produced by CatB and CatC, even further increasing the viscosity and thus increasing the shear stress, this does not cause any variation on the final length of the CNTs and then no variation in electrical resistivity. Differently, a significant decrease of the electrical resistivity is observe at 1wt% CNTs nanocomposites. In this case the experiment is done on a concentration very close to the percolation threshold, so probably breaking even just few CNTs could significantly affect the final property of the material.
The last experimental condition tested is the variation of the mixing time. Figure 4.15 show the results obtained by mixing the three samples with conditions as Exp 5 and Exp 6 (Table 4.5). In this case, due to technical problems with the tools used for the experiments, it was not possible to carry out the experiment also for 1wt% CNT filling.

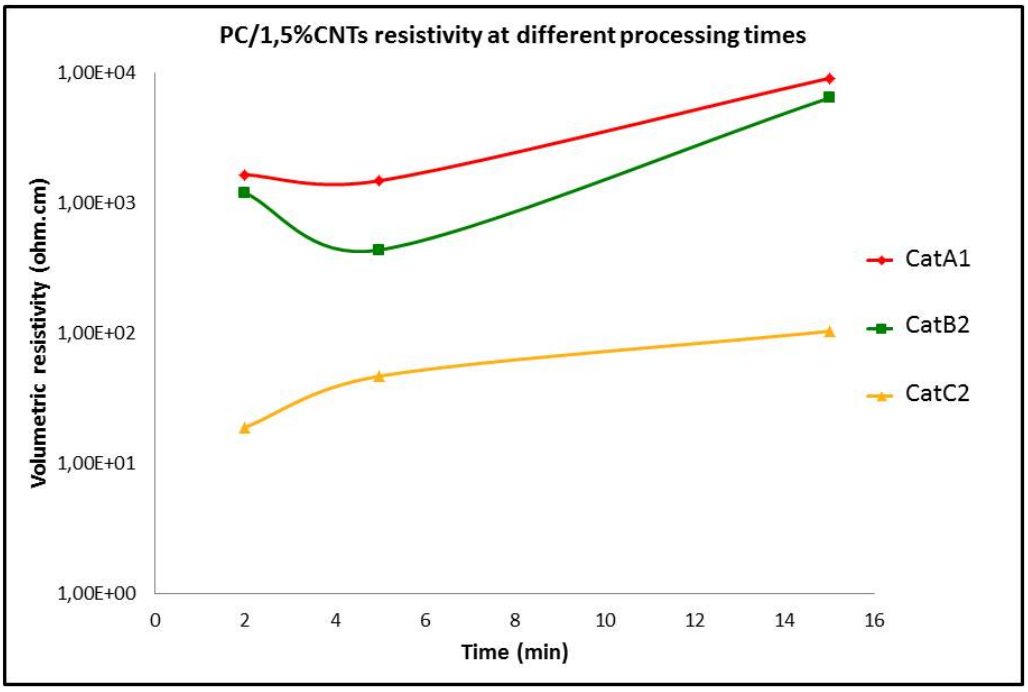


Figure 4.15: Electrical resistivity of nanocomposites PC/1,5wt%CNTs at different processing time

In this case, no big differences where observed by changing the duration of

experiment. As common trend, it can be said that the resistivity tends to increase by increasing the time of experiment in all the three cases. An explanation could be either a decrease of viscosity after long time processing, which hinders a good dispersion in the matrix or again a tendency in breaking the CNTs due to the long stress applied on the samples.

4.6 Injection molding experiments

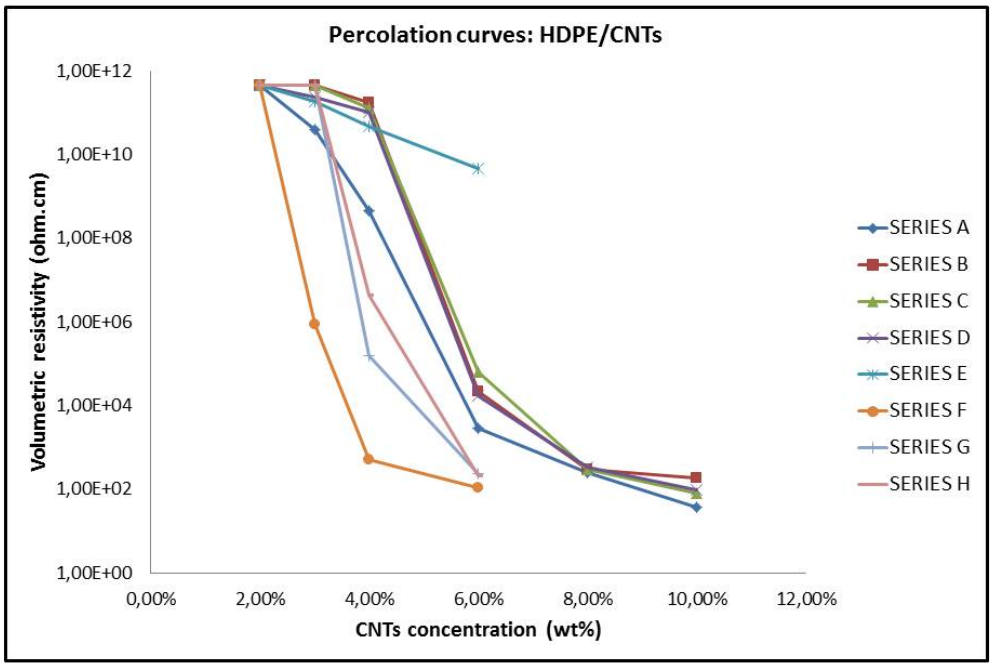
In order to verify the consistency of results between nanocomposites produced at the small scale and at large scale, injection molding experiments were carried out. It was not possible to use the same CNTs previously prepared since the excessive quantity of CNTs needed to produce nanocomposites with the injection molding. Thus, the different batches of CNTs tested were produced in the production site of Nanocyl S.A.. Different series of CNTs produced with catalyst A and catalyst C were synthesized. The aim was to verify the better performances of catalyst C even when produced in large scale, and to compare the mechanical properties. Then, different treatments were also tested to see how this affected the final electrical and mechanical properties of the final nanocomposites. Table 4.6 describes the different conditions used to produce the samples. Series A and B were produced in the same conditions but in two different batches.

Sample name	catalyst	Carbon purity (%)	Treatment
Series A	Catalyst A	90	/
Series B	Catalyst A	90	/
Series C	Catalyst A	90	Densified 3 bar
Series D	Catalyst A	90	Densified 5 bar
Series E	Catalyst A	90	Purified
Series F	Catalyst C	90	/
Series G	Catalyst C	85	Densified 1 bar
Series H	Catalyst C	85	Densified 3 bar

Table 4.5: Process conditions used for producing the CNTs series used for injection molding experiments

CNTs were compounded into HDPE and PC with a twin screw extruder under proprietary conditions and the compounds were molded by injection in an injection molding machine. Electrical measurements were done on all the samples to evaluate the variation of the conductivity both between CNTs produced with the same catalyst and processed with different treatments and to verify the differences between catalyst A and C observed in the previous experiments. Figure 4.16 shows the results obtained by mixing the CNTs with HDPE (top graph) and by mixing CNTs with PC (bottom graph).

From the results obtained by HDPE nanocomposites (Figure 4.16 top), some differences between Series A and B, CNTs produces with the same conditions but in different batches, are observed. An increase of conductivity in case of Series A



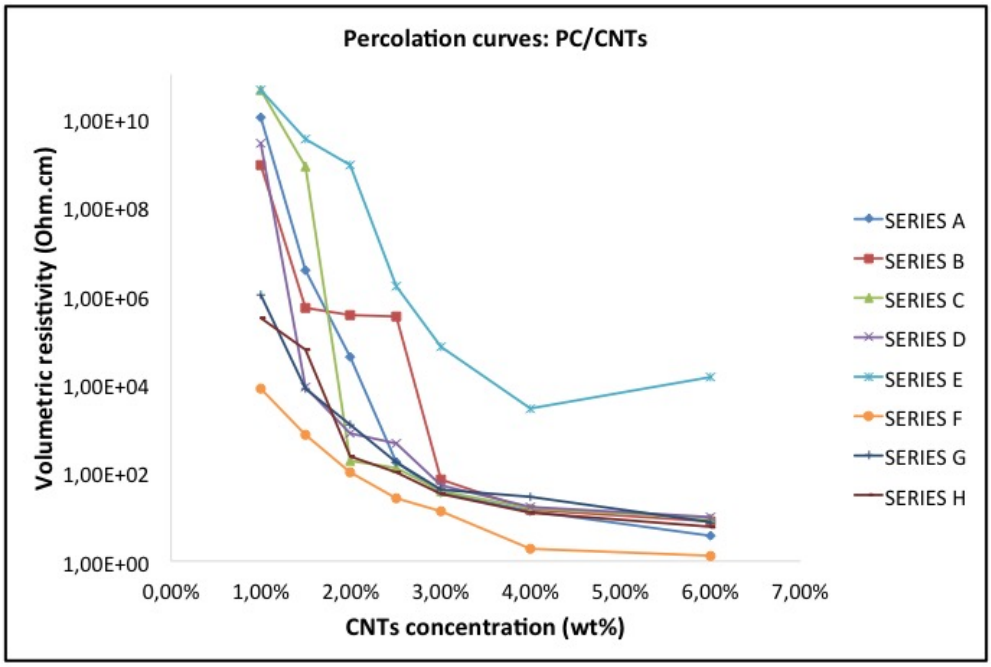


Figure 4.16: Electrical resistivity of nanocomposites HDPE/CNTs (top) and PC/CNTs (bottom) produced by injection molding at different conditions.

is observed, which is anyway not so crucial to lead to significant variation in the value of percolation threshold. Series E shows the highest resistivity. The CNTs have been purified, leading to a breakage of the tubes due to the specific process, which decrease their length and is thus destructive for the final properties of the nanocomposite. Series C and D shows no variation in conductivity compared with Series B, being the same product but densified respectively at 3 and 5 bar. The process of densification does not effect at all the product synthesized with Catalyst A, while seems to have a significant effect on product synthesized with Catalyst C.
Series F, G and H results in different conductivity, leading to a significant variation of the percolation threshold. Series F can be considered conductive for concentrations higher then 2wt%, while for Series G and H the percolation threshold is closer to 4wt%. A contribution to the conductivity of CNTs produced by catalyst C is probably given by the very low density, which makes the product considerably dependent on densification processes, already appreciable when densified 1 bar (Series G). Noteworthy, the differences in conductivity observed in nanocomposites filled with CNTs synthesized with Catalyst C and A and produced by injection molding are consistent with the results observed in case of experiments carried out at a smaller scale, with DSM microcompounder. All the series containing CNTs produced with Catalyst C show better performances even in case of densified samples.
More significant variations in the electrical resistivity are observed in PC nanocomposites (Figure 4.16 bottom). In this case, slight differences are observed between Series produced with CNTS synthesized by Catalyst A (Series A,B,C,D,E). As in case of HDPE nanocomposites, Series E shows the worst performances and a small variation of the percolation threshold is observed between series C and D. Anyway, being the difference only 0,5wt%, this could be attributed to standard error in the measurement. For what concern nanocomposites produced with CNTS synthesized by Catalyst C (Series F,G,H), again Series F shows the best performances, while a small increase of the resistivity is observed in case of Series G and H.
In general, the conclusion drawn in case of HDPE nanocomposites are confirmed by results obtained by PC nanocomposites. Moreover, the significant variation of the percolation threshold between PC and HDPE nanocomposite produced by microcompounder are also observed in case of large scale production.

Mechanical test were done on the nanocomposites produced with HDPE matrix, in order to evaluate the variation of the mechanical properties in the different Series of nanocomposites. Due to impossibility in producing samples for mechanical test with microcompounder, it was not relevant to compare the results with the small scale production. Tensile test and impact test were used to measure the modulus, the stress and strain at yield and the notched impact of the different samples. The value of stress and strain at break could not be measured due to the huge standard deviation of the values, making the results not anymore significant. Figure 4.17 shows the variation of the modulus with the content of CNTs for the different series studied.

For most of the nanocomposites with small content of CNTs analyzed, a slight

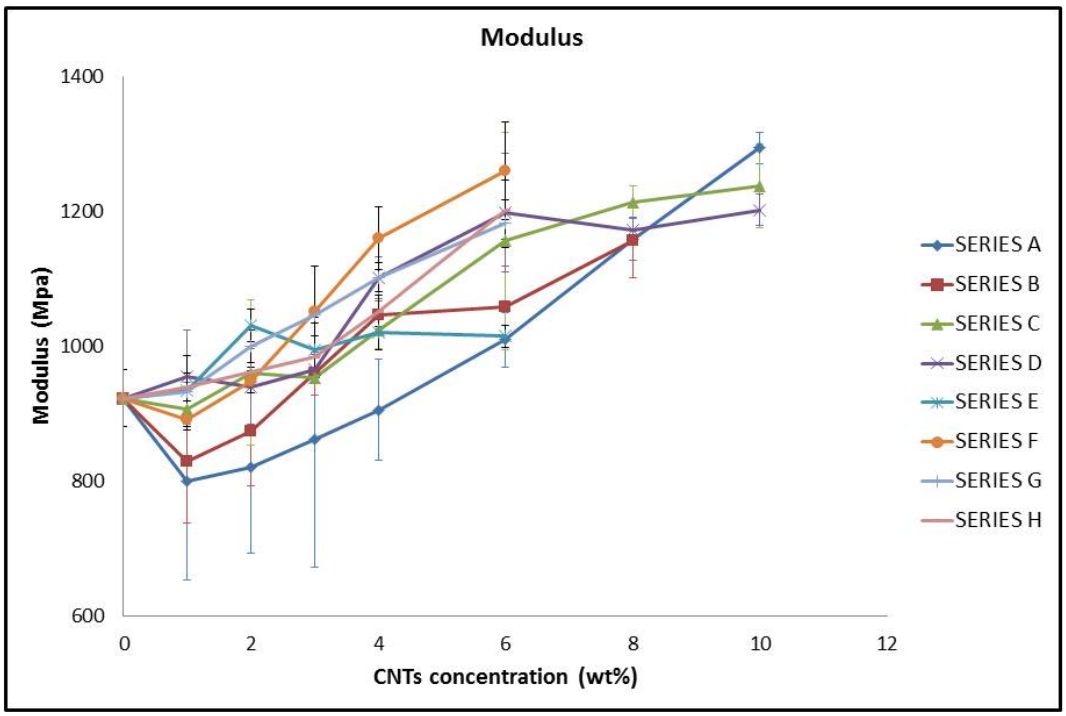


Figure 4.17: Elastic modulus of nanocomposites HDPE/CNTs produced by injection molding in different conditions.

decrease of value of modulus and a high standard deviation are observed. These results are in accordance with the fact that for small content of CNTs in the matrix, the filler does not create a real network which can help increasing the mechanical properties. On the contrary, the low content of filler might results as agglomeration of CNTs dispersed in the matrix acting as defect and thus focusing the stress at the interface CNTs/matrix. For nanocomposites containing more that 2wt% CNTs, the stiffness starts to increase, reaching a significant improvement of the mechanical property. At high content of CNTs, no important differences are observed between the samples filled with CNTs produced by the same catalyst. Interesting differences are observed between samples containing catalyst A and Catalyst C nanotubes. At 6wt% CNTs, Series F shows a significant increase of stiffness compared with any other series.
In Figure 4.18, the variation of the stress (Figure 4.18A) and the elongation (Figure 4.18B) is observed.

A real increase of the stiffness (Figure 4.18A) is again observed when the content of CNTs is higher than 4wt%. In accord with the results obtained for the value of the modulus, a slight difference in the value between CNTs produced by Catalyst C not treated (Series F) and densified (Series G and H) can be seen at 4wt% and 6wt%, which are anyway the samples with the best performances. For what concerns the variation of the elongation at yield (Figure 4.18B), no signif-

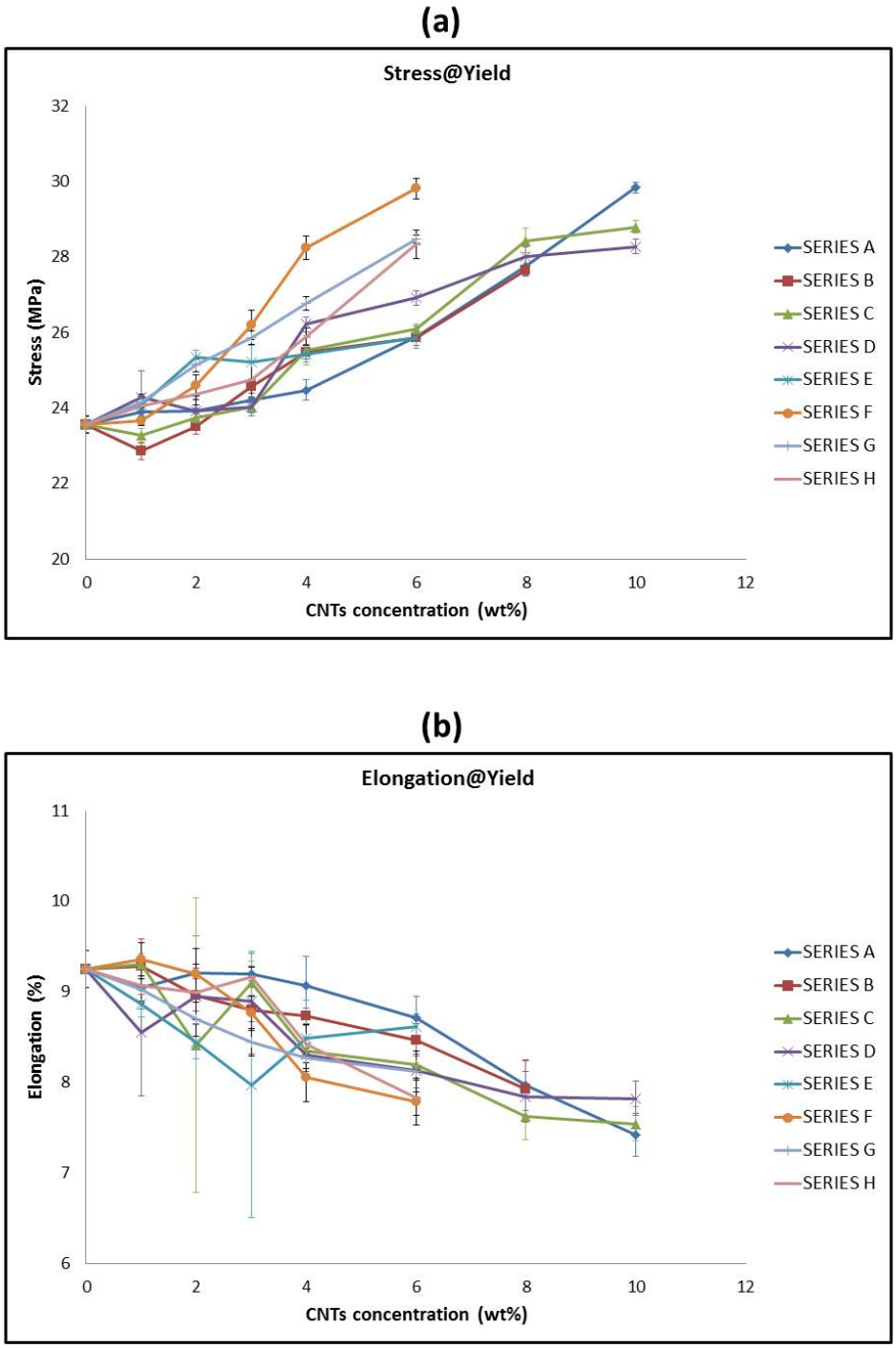


Figure 4.18: (A) Stress at yield and (B) Elongation at yield of nanocomposites HDPE/CNTs produced by injection molding at different conditions.

icant differences are observed between all the samples. Increasing the content of CNTs a slight decrease of the elongation is identified for high content of fillers. Figure 4.19 shows the results obtained by impact test.

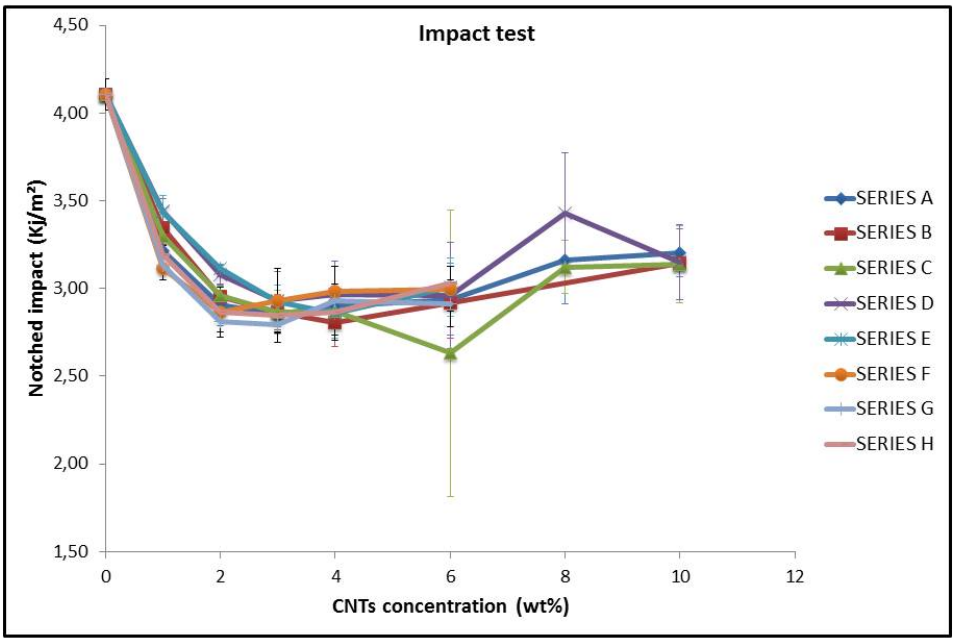


Figure 4.19: Notched impact of nanocomposites HDPE/CNTs produced by injection molding at different conditions

A slight decrease of the absorbed energy is observed from the neat polymer and the filled one. Anyway, there are no differences between the value of the notched impact between the different series, as well as between the different loading the value remain more or less constant.

Chapter 5

Conclusions and prospective

Carbon nanotubes polymer nanocomposites are one of the most promising material to be used for electrical and structural application. Their unique properties make CNTs a perfect candidate in many different field, ranging from electronic devices, energetic or structural application as well as for biotechnologies. The peculiarity of CNTs is their high aspect ratio, combined with its extraordinary conductivity and mechanical properties. The high aspect ratio offers the big advantage of providing high performance even at a small content of filler. On the other side, this generate big Van der Waals forces between the CNTs which lead them to agglomerate in bundles which significantly decrease the final properties of the nanocomposites. One of the biggest challenge nowadays is to find an effective way to increase the dispersion of the CNTs inside the matrix in order to be able to take advantage of the synergy between every disentangled nanotube present in the matrix.

The objective of the master thesis is to study the influence of the CNTs morphology on the dispersion state and on the final properties of polymer nanocomposites. For this purpose, different synthesis conditions are tested to produce different CNTs, whose properties are studied in PC and HDPE matrices. Dispersion level is characterized by electronic microscopes and in epoxy/CNTs mixtures.

Different synthesis conditions are tested on a lab scale CVD apparatus, among which the most interesting are the variation of the synthesis temperature and the variation of the catalyst used for the experiments. Three different catalysts, named Catalyst A, Catalyst B and Catalyst C are studied. From TEM analysis, CNTs produced at higher temperature are characterized by bigger diameters, thanks to a sintering effect occurring between the nanoparticles of the catalysts during the synthesis. For means of dispersion characterization, SEM images of the CNTs are taken. CNTs produced by catalyst A are significantly more dense, appearing as big agglomeration of bundles, while CNTs produced by Catalysts B and C present well dispersed and aligned nanotubes. Moreover, images taken from CNTs produced at high temperature show a better level of dispersion. Rheological measurement are taken on epoxy/CNTs mixture, in order to further study the variation of dispersion state of the different CNTs. Mixtures containing CNTs produced by Catalyst C show a wide increase of the level of dispersion.

Electrical properties of nanocomposites produced with DSM microcompounder are studied. The influence of the dispersion state of the CNTs on the final properties of the nanocomposites are verified. Nanocomposites containing CNTs pro-

duced by Catalyst C are indeed the ones showing the lower resistivity, while nanocomposites containing CNTs produced by Catalyst A and B show a higher resistivity. The results are confirmed both when testing PC nanocomposites and HDPE nanocomposites. No significant variation of the resistivity is observed between CNTs produced by the same catalyst but with different synthesis conditions.

As a last study, CNTs produced on industrial scale with Catalyst A and Catalyst C are mixed in a twin screw extruder and HDPE and PC nanocomposites are studied. The aim is to check that the differences observed on small scale production are verified on nanocomposites produced on semi-industrial level. Different series of CNTs are produced, also applying different treatment on the CNTs. The electrical measurement are in accordance with what observed on previous measurements. Catalyst C CNTs are confirmed to be the product with the best performances. Mechanical measurement are done on HDPE nanocomposites, showing that nanocomposites containing Catalyst C CNTs have better mechanical properties, which are anyway not so far from results obtained by Catalyst A CNTs nanocomposites.

Concluding, it can be stated that the choice of the catalyst is the most important parameter leading to biggest differences in the final level of dispersion and performances. Synthesis parameters definitely affect the final morphology of the CNTs and a slight increase of the dispersion level was observed in synthesis at higher temperature. Anyway, it was not possible to define a link between CNTs synthesis conditions and properties of the final nanocomposites. Results obtain on a lab scale were confirmed by measurement taken on nanocomposites produced on a semi industrial scale.

Further investigations on the effect of the synthesis parameters on the final properties should be done. It could be interesting to produce CNTs with bigger variations in the synthesis conditions in order to obtain more defined differences in the morphology of the CNTs. A specific study concerning the length of the CNTs could be helpful in order to verify the differences in the aspect ratio between the nanotubes. The good performances obtained by nanocomposites containing Catalyst C CNTs suggest that these products could be used in a future generation of CNTs nanocomposites for electronic packaging applications. In order to confirm the quality of the samples produced, it would be interesting to carry out cleanliness test on the nanocomposites. Cleanliness refers to the absence of particles in the component which might negatively affect the final properties of the product. This is one of the most important parameter that has to be controlled in order to assure optimal performance in electronic packaging applications, and would be the last proof of the good level of product obtained.

Bibliography

[1] Jacob M Wernik and Shaker A Meguid. Recent developments in multifunctional nanocomposites using carbon nanotubes. *Applied Mechanics Reviews*, 63(5):050801, 2010.

[2] Sumio Iijima et al. Helical microtubules of graphitic carbon. *nature*, 354(6348):56–58, 1991.

[3] Muthuraman Harish. *Processing and study of carbon nanotube/polymer nanocomposites and polymer electrolyte materials*, 2005.

[4] Ernesto Joselevich, Hongjie Dai, Jie Liu, Kenji Hata, and Alan H Windle. Carbon nanotube synthesis and organization. In *Carbon nanotubes*, pages 101–165. Springer, 2007.

[5] C Journet and P Bernier. Production of carbon nanotubes. *Applied physics A: Materials science & processing*, 67(1):1–9, 1998.

[6] Meyya Meyyappan, Lance Delzeit, Alan Cassell, and David Hash. Carbon nanotube growth by pecvd: a review. *Plasma Sources Science and Technology*, 12(2):205, 2003.

[7] Richard E Smalley, Mildred S Dresselhaus, Gene Dresselhaus, and Phaedon Avouris. *Carbon nanotubes: synthesis, structure, properties, and applications*, volume 80. Springer Science & Business Media, 2003.

[8] Andrea Szabó, Caterina Perri, Anita Csató, Girolamo Giordano, Danilo Vuono, and János B Nagy. Synthesis methods of carbon nanotubes and related materials. *Materials*, 3(5):3092–3140, 2010.

[9] Krzysztof Koziol, Bojan Obrad Boskovic, and Noorhana Yahya. Synthesis of carbon nanostructures by cvd method. In *Carbon and Oxide Nanostructures*, pages 23–49. Springer, 2010.

[10] Mukul Kumar and Yoshinori Ando. Chemical vapor deposition of carbon nanotubes: a review on growth mechanism and mass production. *Journal of nanoscience and nanotechnology*, 10(6):3739–3758, 2010.

[11] Jay P Gore and Anup Sane. Flame synthesis of carbon nanotubes. *Carbon Nanotubes-Synthesis, Characterization, Applications*, (1):16801, 2011.

[12] Alexei Matyushov. Growth of carbon nanotubes via chemical vapor deposition. *SUNFEST*, page 81.

[13] Rupesh Khare and Suryasarathi Bose. Carbon nanotube based composites-a review. *Journal of minerals and Materials Characterization and Engineering*, 4(01):31, 2005.

[14] Carole E Baddour and Cedric Briens. Carbon nanotube synthesis: a review. *International Journal of Chemical Reactor Engineering*, 3(1), 2005.

[15] Mukul Kumar and Yoshinori Ando. *Carbon nanotube synthesis and growth mechanism*. INTECH Open Access Publisher, 2011.

[16] Çınar Öncel and Yuda Yürüm. Carbon nanotube synthesis via the catalytic cvd method: a review on the effect of reaction parameters. *Fullerenes, Nanotubes, and Carbon Nonstructures*, 14(1):17–37, 2006.

[17] GL Hornyak, L Grigorian, AC Dillon, PA Parilla, KM Jones, and MJ Heben. A temperature window for chemical vapor decomposition growth of single-wall carbon nanotubes. *The Journal of Physical Chemistry B*, 106(11):2821–2825, 2002.

[18] Jing Kong, Alan M Cassell, and Hongjie Dai. Chemical vapor deposition of methane for single-walled carbon nanotubes. *Chemical Physics Letters*, 292(4):567–574, 1998.

[19] Jing Kong, Hyongsok T Soh, Alan M Cassell, Calvin F Quate, and Hongjie Dai. Synthesis of individual single-walled carbon nanotubes on patterned silicon wafers. *Nature*, 395(6705):878–881, 1998.

[20] Alan M Cassell, Jeffrey A Raymakers, Jing Kong, and Hongjie Dai. Large scale cvd synthesis of single-walled carbon nanotubes. *The Journal of Physical Chemistry B*, 103(31):6484–6492, 1999.

[21] Christophe Laurent, Emmanuel Flahaut, Alain Peigney, and Abel Rousset. Metal nanoparticles for the catalytic synthesis of carbon nanotubes. *New Journal of Chemistry*, 22(11):1229–1237, 1998.

[22] Anna Moisala, Albert G Nasibulin, and Esko I Kauppinen. The role of metal nanoparticles in the catalytic production of single-walled carbon nanotubes—a review. *Journal of Physics: condensed matter*, 15(42):S3011, 2003.

[23] SB Sinnott, R Andrews, D Qian, Apparao M Rao, Z Mao, EC Dickey, and F Derbyshire. Model of carbon nanotube growth through chemical vapor deposition. *Chemical Physics Letters*, 315(1):25–30, 1999.

[24] Arnaud Magrez, Jin Won Seo, Rita Smajda, Marijana Mionić, and László Forró. Catalytic cvd synthesis of carbon nanotubes: towards high yield and low temperature growth. *Materials*, 3(11):4871–4891, 2010.

[25] Qingwen Li, Hao Yan, Jin Zhang, and Zhongfan Liu. Effect of hydrocarbons precursors on the formation of carbon nanotubes in chemical vapor deposition. *Carbon*, 42(4):829–835, 2004.

[26] Giuseppe Gulino, Ricardo Vieira, Julien Amadou, Patrick Nguyen, Marc J Ledoux, Signorino Galvagno, Gabriele Centi, and Cuong Pham-Huu. C 2 h 6 as an active carbon source for a large scale synthesis of carbon nanotubes by chemical vapour deposition. *Applied Catalysis A: General*, 279(1):89–97, 2005.

[27] Hongtao Cui, Gyula Eres, Jane Y Howe, A Puretkzy, M Varela, David B Geohegan, and Douglas H Lowndes. Growth behavior of carbon nanotubes on multilayered metal catalyst film in chemical vapor deposition. *Chemical Physics Letters*, 374(3):222–228, 2003.

[28] Th Dikonimos Makris, L Giorgi, R Giorgi, N Lisi, and E Salernitano. Cnt growth on alumina supported nickel catalyst by thermal cvd. *Diamond and related materials*, 14(3):815–819, 2005.

[29] Hiroki Ago, Shingo Imamura, Toshiya Okazaki, Takeshi Saito, Motoo Yumura, and Masaharu Tsuji. Cvd growth of single-walled carbon nanotubes with narrow diameter distribution over fe/mgo catalyst and their fluorescence spectroscopy. *The Journal of Physical Chemistry B*, 109(20):10035–10041, 2005.

[30] Rodney Andrews, David Jacques, Dali Qian, and Terry Rantell. Multiwall carbon nanotubes: synthesis and application. *Accounts of Chemical Research*, 35(12):1008–1017, 2002.

[31] Lijie Ci, Sishen Xie, Dongsheng Tang, Xiaoqin Yan, Yubao Li, Zuqin Liu, Xiaoping Zou, Weiya Zhou, and Gang Wang. Controllable growth of single wall carbon nanotubes by pyrolizing acetylene on the floating iron catalysts. *Chemical physics letters*, 349(3):191–195, 2001.

[32] Teresa de los Arcos, Michael Gunnar Garnier, Jin Won Seo, Peter Oelhafen, Verena Thommen, and Daniel Mathys. The influence of catalyst chemical state and morphology on carbon nanotube growth. *The Journal of Physical Chemistry B*, 108(23):7728–7734, 2004.

[33] Cheol Jin Lee, Jeunghee Park, and A Yu Jeong. Catalyst effect on carbon nanotubes synthesized by thermal chemical vapor deposition. *Chemical Physics Letters*, 360(3):250–255, 2002.

[34] I Willems, Z Konya, J-F Colomer, G Van Tendeloo, N Nagaraju, A Fonseca, and JB Nagy. Control of the outer diameter of thin carbon nanotubes synthesized by catalytic decomposition of hydrocarbons. *Chemical Physics Letters*, 317(1):71–76, 2000.

[35] Chin Li Cheung, Andrea Kurtz, Hongkun Park, and Charles M Lieber. Diameter-controlled synthesis of carbon nanotubes. *The Journal of Physical Chemistry B*, 106(10):2429–2433, 2002.

[36] N Nagaraju, A Fonseca, Z Konya, and JB Nagy. Alumina and silica supported metal catalysts for the production of carbon nanotubes. *Journal of molecular catalysis A: Chemical*, 181(1):57–62, 2002.

[37] JW Ward, BQ Wei, and PM Ajayan. Substrate effects on the growth of carbon nanotubes by thermal decomposition of methane. *Chemical Physics Letters*, 376(5):717–725, 2003.

[38] Hongjie Dai. Carbon nanotubes: synthesis, integration, and properties. *Accounts of chemical research*, 35(12):1035–1044, 2002.

[39] MP Siegal, DL Overmyer, and PP Provencio. Precise control of multiwall carbon nanotube diameters using thermal chemical vapor deposition. *Applied physics letters*, 80(12):2171–2173, 2002.

[40] AM Benito, Y Maniette, E Munoz, and MT Martinez. Carbon nanotubes production by catalytic pyrolysis of benzene. *Carbon*, 36(5):681–683, 1998.

[41] Cheol Jin Lee, Jeunghee Park, Yoon Huh, and Jeong Yong Lee. Temperature effect on the growth of carbon nanotubes using thermal chemical vapor deposition. *Chemical Physics Letters*, 343(1):33–38, 2001.

[42] Padmakar D Kichambare, Dali Qian, Elizabeth C Dickey, and Craig A Grimes. Thin film metallic catalyst coatings for the growth of multiwalled carbon nanotubes by pyrolysis of xylene. *Carbon*, 40(11):1903–1909, 2002.

[43] Jason H Hafner, Michael J Bronikowski, Bobak R Azamian, Pavel Nikolaev, Andrew G Rinzler, Daniel T Colbert, Ken A Smith, and Richard E Smalley. Catalytic growth of single-wall carbon nanotubes from metal particles. *Chemical Physics Letters*, 296(1):195–202, 1998.

[44] http://www.grandviewresearch.com/industry-analysis/carbon-nanotubes-cnt market.

[45] PM Ajayan, O Stephan, C Colliex, D Trauth, et al. Aligned carbon nanotube arrays formed by cutting a polymer resin-nanotube composite. *SCIENCE-NEW YORK THEN WASHINGTON-*, pages 1212–1212, 1994.

[46] Zdenko Spitalsky, Dimitrios Tasis, Konstantinos Papagelis, and Costas Galiotis. Carbon nanotube–polymer composites: chemistry, processing, mechanical and electrical properties. *Progress in polymer science*, 35(3):357–401, 2010.

[47] Mohammad Moniruzzaman and Karen I Winey. Polymer nanocomposites containing carbon nanotubes. *Macromolecules*, 39(16):5194–5205, 2006.

[48] Jonathan N Coleman, Umar Khan, Werner J Blau, and Yurii K Gun'ko. Small but strong: a review of the mechanical properties of carbon nanotube–polymer composites. *Carbon*, 44(9):1624–1652, 2006.

[49] Hiroaki Miyagawa, Manjusri Misra, and Amar K Mohanty. Mechanical properties of carbon nanotubes and their polymer nanocomposites. *Journal of Nanoscience and Nanotechnology*, 5(10):1593–1615, 2005.

[50] AV Desai and MA Haque. Mechanics of the interface for carbon nanotube–polymer composites. *Thin-walled structures*, 43(11):1787–1803, 2005.

[51] Erik T Thostenson and Tsu-Wei Chou. Processing-structure-multi-functional property relationship in carbon nanotube/epoxy composites. *Carbon*, 44(14):3022–3029, 2006.

[52] Petra Pötschke, Mahmoud Abdel-Goad, Ingo Alig, Sergej Dudkin, and Dirk Lellinger. Rheological and dielectrical characterization of melt mixed polycarbonate-multiwalled carbon nanotube composites. *Polymer*, 45(26):8863–8870, 2004.

[53] Florian H Gojny, Malte HG Wichmann, Bodo Fiedler, and Karl Schulte. Influence of different carbon nanotubes on the mechanical properties of epoxy matrix composites–a comparative study. *Composites Science and Technology*, 65(15):2300–2313, 2005.

[54] YY Huang, SV Ahir, and EM Terentjev. Dispersion rheology of carbon nanotubes in a polymer matrix. *Physical Review B*, 73(12):125422, 2006.

[55] Peng-Cheng Ma, Naveed A Siddiqui, Gad Marom, and Jang-Kyo Kim. Dispersion and functionalization of carbon nanotubes for polymer-based nanocomposites: a review. *Composites Part A: Applied Science and Manufacturing*, 41(10):1345–1367, 2010.

[56] Xiao-Lin Xie, Yiu-Wing Mai, and Xing-Ping Zhou. Dispersion and alignment of carbon nanotubes in polymer matrix: a review. *Materials Science and Engineering: R: Reports*, 49(4):89–112, 2005.

[57] JB Bai and Aïssa Allaoui. Effect of the length and the aggregate size of mwnts on the improvement efficiency of the mechanical and electrical properties of nanocomposites—experimental investigation. *Composites Part A: applied science and manufacturing*, 34(8):689–694, 2003.

[58] O Breuer and Uttandaraman Sundararaj. Big returns from small fibers: a review of polymer/carbon nanotube composites. *Polymer composites*, 25(6):630–645, 2004.

[59] Petra Pötschke, Arup R Bhattacharyya, Andreas Janke, Sven Pegel, Albrecht Leonhardt, Christine Täschner, Manfred Ritschel, Siegmar Roth, Björn Hornbostel, and Jiri Cech. Melt mixing as method to disperse carbon nanotubes into thermoplastic polymers. *Fullerenes, nanotubes, and carbon nanostructures*, 13(S1):211–224, 2005.

[60] Petra Pötschke, Arup R Bhattacharyya, and Andreas Janke. Melt mixing of polycarbonate with multiwalled carbon nanotubes: microscopic studies on the state of dispersion. *European Polymer Journal*, 40(1):137–148, 2004.

[61] G Gkikas, N-M Barkoula, and AS Paipetis. Effect of dispersion conditions on the thermo-mechanical and toughness properties of multi walled carbon nanotubes-reinforced epoxy. *Composites Part B: Engineering*, 43(6):2697–2705, 2012.

[62] S Bal and SS Samal. Carbon nanotube reinforced polymer composites—a state of the art. *Bulletin of Materials Science*, 30(4):379–386, 2007.

[63] Chunyu Li and Tsu-Wei Chou. Elastic moduli of multi-walled carbon nanotubes and the effect of van der waals forces. *Composites Science and Technology*, 63(11):1517–1524, 2003.

[64] Erik T Thostenson and Tsu-Wei Chou. On the elastic properties of carbon nanotube-based composites: modelling and characterization. *Journal of Physics D: Applied Physics*, 36(5):573, 2003.

[65] Jiaxi Guo, Yanjun Liu, Ricardo Prada-Silvy, Yongqiang Tan, Samina Azad, Beate Krause, Petra Pötschke, and Brian P Grady. Aspect ratio effects of multi-walled carbon nanotubes on electrical, mechanical, and thermal properties of polycarbonate/mwcnt composites. *Journal of Polymer Science Part B: Polymer Physics*, 52(1):73–83, 2014.

[66] Frank Yepez Castillo, Robert Socher, Beate Krause, Robert Headrick, Brian P Grady, Ricardo Prada-Silvy, and Petra Pötschke. Electrical, mechanical, and glass transition behavior of polycarbonate-based nanocomposites with different multi-walled carbon nanotubes. *Polymer*, 52(17):3835–3845, 2011.

[67] JH Du, Jinbo Bai, HM Cheng, et al. The present status and key problems of carbon nanotube based polymer composites. *Express Polymer Letters*, 1(5):253–273, 2007.

[68] Petra Pötschke, TD Fornes, and DR Paul. Rheological behavior of multiwalled carbon nanotube/polycarbonate composites. *Polymer*, 43(11):3247–3255, 2002.

[69] Wolfgang Bauhofer and Josef Z Kovacs. A review and analysis of electrical percolation in carbon nanotube polymer composites. *Composites Science and Technology*, 69(10):1486–1498, 2009.

[70] Jing Li, Peng Cheng Ma, Wing Sze Chow, Chi Kai To, Ben Zhong Tang, and J-K Kim. Correlations between percolation threshold, dispersion state, and aspect ratio of carbon nanotubes. *Advanced Functional Materials*, 17(16):3207–3215, 2007.

[71] Olga Valentino, Maria Sarno, Nicola G Rainone, Maria Rossella Nobile, Paolo Ciambelli, Heinz C Neitzert, and George P Simon. Influence of the polymer structure and nanotube concentration on the conductivity and rheological properties of polyethylene/cnt composites. *Physica E: Low-dimensional systems and nanostructures*, 40(7):2440–2445, 2008.

[72] Fangming Du, John E Fischer, and Karen I Winey. Effect of nanotube alignment on percolation conductivity in carbon nanotube/polymer composites. *Physical Review B*, 72(12):121404, 2005.

[73] Ashkan Behnam, Jing Guo, and Ant Ural. Effects of nanotube alignment and measurement direction on percolation resistivity in single-walled carbon nanotube films. *Journal of Applied Physics*, 102(4):044313, 2007.

[74] Gaurav Kasaliwal, Andreas Göldel, and Petra Pötschke. Influence of processing conditions in small-scale melt mixing and compression molding on the resistivity and morphology of polycarbonate–mwnt composites. *Journal of Applied Polymer Science*, 112(6):3494–3509, 2009.

[75] Robert Socher, Beate Krause, Michael T Müller, Regine Boldt, and Petra Pötschke. The influence of matrix viscosity on mwcnt dispersion and electrical properties in different thermoplastic nanocomposites. *Polymer*, 53(2):495–504, 2012.

[76] Zhihang Fan and Suresh G Advani. Rheology of multiwall carbon nanotube suspensions. *Journal of Rheology (1978-present)*, 51(4):585–604, 2007.

[77] Fangming Du, Robert C Scogna, Wei Zhou, Stijn Brand, John E Fischer, and Karen I Winey. Nanotube networks in polymer nanocomposites: rheology and electrical conductivity. *Macromolecules*, 37(24):9048–9055, 2004.

[78] Samaneh Abbasi, Pierre J Carreau, Abdessalem Derdouri, and Michel Moan. Rheological properties and percolation in suspensions of multiwalled carbon nanotubes in polycarbonate. *Rheologica acta*, 48(9):943–959, 2009.

[79] JC Charlier, PC Eklund, J Zhu, and AC Ferrari. Carbon nanotubes: Advanced topics in the synthesis, structure, properties and applications. *Jorio, A*, 2008.

[80] http://www.xplore-together.com/products/micro-compounders.

[81] http://www.xplore-together.com/products/injection-moulders.

[82] http://www.nanocyl.com.

[83] https://www.engelglobal.com/en/us/solutions/injection-moulding-machines/victory-1.html.

[84] Ludwig Reimer. *Transmission electron microscopy: physics of image formation and microanalysis*, volume 36. Springer, 2013.

[85] http://www.encyclopedia.com/topic/electron-microscopy.aspx.

[86] https://www.britannica.com/technology/transmission-electron-microscope.

[87] https://www.fei.com/products/tem/tecnai/.

[88] http://www.anton-paar.com/ca-en/products/details/mcr-rheometer-series/.

[89] David Bom, Rodney Andrews, David Jacques, John Anthony, Bailin Chen, Mark S Meier, and John P Selegue. Thermogravimetric analysis of the oxidation of multiwalled carbon nanotubes: evidence for the role of defect sites in carbon nanotube chemistry. *Nano Letters*, 2(6):615–619, 2002.